Bioinspired Ion Pairs Transforming Poorly Water-soluble Compounds into Protic Ionic Liquids

and

Deep Eutectic Solvents

Dissertation zur Erlangung des naturwissenschaftlichen Doktorgrades der

Julius-Maximilians-Universität Würzburg

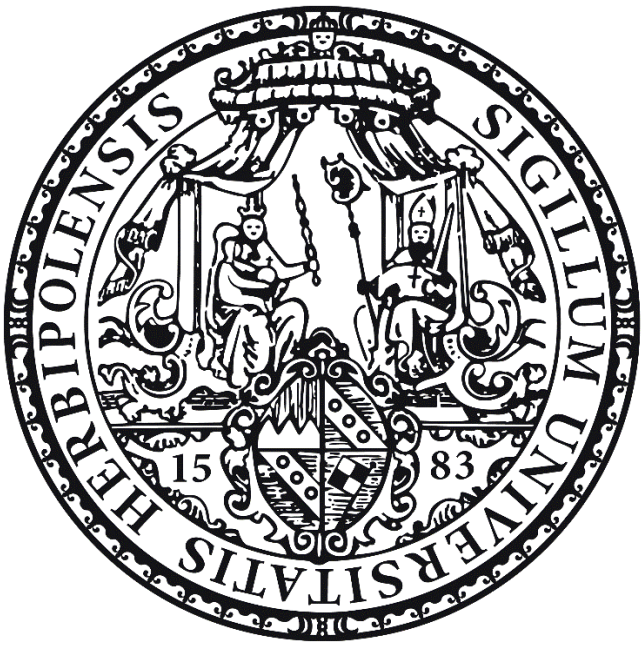

vorgelegt von

Paul Mathias Güntzel

aus

Bad Rodach

Würzburg 2020

Bioinspired Ion Pairs Transforming Poorly Water-soluble Compounds into Protic Ionic Liquids

and

Deep Eutectic Solvents

Dissertation zur Erlangung des naturwissenschaftlichen Doktorgrades der

Julius-Maximilians-Universität Würzburg

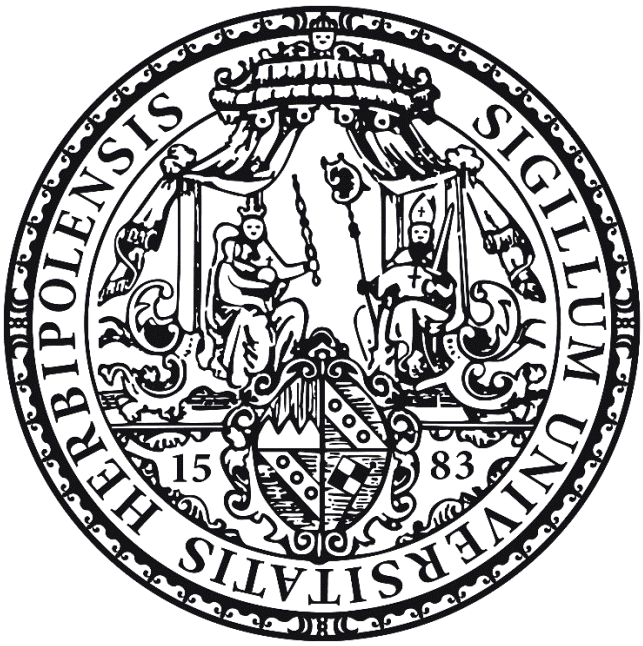

vorgelegt von

Paul Mathias Güntzel

aus

Bad Rodach

Würzburg 2020

Eingereicht bei der Fakultät für Chemie und Pharmazie am

_____

Gutachter der schriftlichen Arbeit

1. Gutachter: _____

2. Gutachter: _____

Prüfer des öffentlichen Promotionskolloquiums

1. Prüfer: _____

2. Prüfer: _____

3. Prüfer: _____

Datum des öffentlichen Promotionskolloquiums _____

Doktorurkunde ausgehändigt am _____

„*Sobald jemand in einer Sache Meister geworden ist, sollte er in einer neuen Sache Schüler werden*“

--Gerhart Johann Robert Hauptmann--

Die vorliegende Arbeit wurde in der Zeit von April 2016 bis Januar 2020 am Institut für Pharmazie und Lebensmittelchemie der Bayrischen Julius-Maximilians-Universität Würzburg unter der Anleitung von Frau Prof. Dr. Ulrike Holzgrabe angefertigt.

Danksagung

Mein besonderer Dank gilt Frau Prof. Dr. Ulrike Holzgrabe für die Möglichkeit diese Arbeit in Ihrer Arbeitsgruppe anfertigen zu können. Ebenfalls danke ich Ihr für das Vertrauen in mich und meine Arbeit, die spannenden Projekte sowie die helfenden Gespräche und Anregungen in jeder Phase der Promotion.

Weiterhin möchte ich mich bei Herrn Prof. Dr. Dr. Lorenz Meinel für die fachliche Hilfe sowie die Ideen und Anregungen bei technologischen Fragen bedanken. Auch bin ich Ihm für die Nutzung der Räumlichkeiten und Gerätschaften in der Pharmazeutischen Technologie zu großem Dank verpflichtet.

Ebenfalls möchte ich mich bei Prof. Dr. Dr. h. c. mult. Gerhard Bringmann und Dr. Shaimaa Seaf für die ausgesprochen gute Zusammenarbeit bedanken.

Mein herzlicher Dank gilt auch allen Kolleginnen und Kollegen des AK Holzgrabe und des AK Meinel für das stets angenehme Arbeitsklima, die netten Gespräche und der fachlichen Hilfe bei der Lösung von Problemen.

Bedanken möchte ich mich auch bei Dr. Johannes Wiest, Dr. Andreas Hartung und Dr. Daniela Brünnert für das vertrauensvolle Verhältnis und die fruchtbaren Gespräche während der gemeinsamen Arbeit.

An dieser Stelle möchte ich mich auch bei meinen Praktikantinnen und Praktikanten bedanken, die mich während meiner Promotion begleitet und tatkräftig unterstützt haben: Hannah, Leonard, Sebastian, Corinna, Adriana, Pavel und Annelie.

Auch möchte ich mich bei Herrn Prof. Dr. Christoph Sotriffer für das Anvertrauen der Aufgaben im Rahmen des Studentenpraktikums „Allgemeine, anorganische Chemie der Arznei-, Hilfsstoffe und Schadstoffe“ und meinen Kolleginnen und Kollegen aus dem AK Sotriffer für die stets angenehme Arbeitsatmosphäre bedanken.

Ein ganz besonderes Dankeschön gilt meinen Eltern, Herbert und Friderike, die mich immer unterstützt und stets gefordert und gefördert haben. Weiterhin danke ich meiner Familie und meinen Freunden, die immer da waren, wenn ich sie brauchte und somit einen großen Beitrag zum Gelingen dieser Arbeit geleistet haben.

Table of Contents

TABLE OF CONTENTS

List of abbreviations

AHA	α-Hydroxycarboxylic acid
AIL	Aprotic ionic liquid
API	Active pharmaceutical ingredients
BHA	β-Hydroxycarboxylic acid
CA	Carboxylic acid
DES	Deep eutectic solvent
DLS	Dynamic light scattering
DSC	Differential scanning calorimetry
GS	Glass solution
HBA	Hydrogen-bond acceptor
HBD	Hydrogen-bond donor
HPLC	High performance liquid chromatography
HSP70	Heat shock protein70
HSP90	Heat shock protein90
IL	Ionic liquid
IR	Infrared spectroscopy
MM	Multiple myeloma
MP	Melting point
m/z	Mass-to-charge ratio
NADES	Natural deep eutectic solvents
NMR	Nuclear magnetic resonance
OA	Organic acid

LIST OF ABBREVIATIONS

OIL	Oligomeric ionic liquid
PDI	Polydispersity index
PIL	Protic ionic liquid
RTIL	Room temperature ionic liquid
SD	Solid dispersion
SM	Secondary metabolite
T_g	Glass transition temperature
XRPD	X-ray powder diffraction

1 Introduction

The diversity of organic compounds in plants represents the products of primary and secondary plant metabolism. Primary metabolites, like carbohydrates, amino acids, and organic acids (OAs) are involved in many vital processes, including plant growth and development, respiration and photosynthesis, and hormone and protein synthesis and occur in all types within broad phylogenetic groups. However, secondary metabolites (SMs) including alkaloids, flavonoids, carotenoids, sterols, phenolic acids, and glucosinolates have many different tasks; among others, they protect plants against herbivores and microorganisms and are also responsible for the color of vegetables and fruits [1]. Due to the fact that many SMs are toxic to the plant itself, several mechanisms for detoxification and/or compartmentation are indispensable, which may avoid harmful effects in the cells as well as improve the efficiency of their production. Once SMs have been transported to their storage sites, they may form longer-lasting structures by interaction with chemicals, e.g. by salt formation, or proteins or undergo chemical reactions for recycling in other metabolic pathways [2]. In higher plants the cell vacuole has been shown in many instances to be the storage compartment for SMs as well as for primary metabolites like sugars, amino acids, and OAs. Since the primary metabolites are present in very large quantities, researchers suspected that in addition to water and lipid, a third type of liquid consists of these compounds and forms a so-called natural deep eutectic solvent (NADES) in living organisms. These NADES can play a role in all types of cellular processes and help to understand difficult-to-understand phenomena such as the biosynthesis and storage of water-insoluble SMs, macromolecules, and biopolymers such as cellulose and amylose. For example, researchers found that the solubility of the flavonoid rutin was 50 to 100 times higher in various NADES than in water, and that enzymes completely dissolved in NADES were inactive but became active after water was added. This observation, and the fact that the combination of ubiquitous natural compounds forms liquids with very low melting points, obviously enables living cells to withstand extreme environmental conditions such as drought, salt stress, and high and low temperatures. For example, living cells can survive the drought by forming NADES, in which the membranes, enzymes, and metabolites remain stable [3, 4].

Since around 40% of the approved drugs and almost 90% of the molecules in the discovery pipeline are poorly water-soluble, research in pharmaceutics focuses on

improving the solubility and increasing the dissolution rate of active pharmaceutical ingredients (APIs) [5]. For this reason, various methods, including amorphization and salt formation, are used to manipulate the physical properties of the APIs, in particular their crystallinity and consequently their bioavailability [6-8].

In the early 19th century, Sertürner isolated morphine as its meconate salt, an early indication of the importance of salt formation in nature in order to overcome the problem of poor water solubility of water-insoluble compounds. In addition, the isolation of the morphine meconate shows the beneficial behavior of sterically sophisticated counterions compared to the small size halides, which are the counterions for the morphine salts on the market [9-10]. Carboxylic acid (CA) salts of basic drugs have higher aqueous solubilities since they lower the crystal lattice forces because of their size and their reduced charge density as well as their ability of forming hydrogen bonds between acids' hydroxyl groups in aqueous environment [11, 12]. Nowadays, half of the drug molecules are administered as a salt, mainly as a halide salt, but the number of reported examples of cationic or anionic APIs in combination with non-toxic, naturally occurring counterions is increasing steadily [13, 14]. These bioinspired salts, consisting of APIs and naturally occurring counterions, may offer several beneficial physical properties compared with the correspondent original neutral formulations in terms of melting point, crystallinity, hygroscopicity, and dissolution rate, as well as pharmaceutical properties, including bioavailability, permeability, and drug delivery [15, 16].

1.1 Ionic Liquids (ILs)

ILs are generally defined as organic salts with melting points below 100 °C. They are comprised only of ions and some of them are liquid at ambient temperature, so called room temperature ionic liquids (RTILs) [17-19]. These liquid organic salts have interesting properties, including improved thermal stability and viscosity as shown for various imidazolium salts used as absorbent [20], vanishingly low vapor pressures as shown for 1-butyl-3-methylimidazolium hexafluorophosphate [C_4-mim]-[PF_6] [21, 22] and not-flammable properties, as shown for ILs, which consist of ring-shaped ammonium cations and imide anions [23]. The beneficial properties of ILs make them to benign industrial alternatives to conventional volatile organic solvents [24, 25]. In addition, due to their beneficial physicochemical properties such as improved water

solubility and dissolution rate, ILs have caught the attention of pharmaceutical researchers as a potential drug formulation [8, 26, 27]. For example, ILs are a powerful class of cationic hydrotropes for the increased water solubility of vanillin and gallic acid based ILs as shown by Claudio et al. [28]. So-called “hydrotropes” are a class of highly water-soluble salts or molecules characterized by an amphiphilic structure and are used to increase the concentration of hydrophobic solutes in aqueous solutions by two major driving forces: the first is the solute-hydrotrope binding, the second is the water activity depression [28, 29]. The water activity itself is affected by ionic dissociation, which increases the water activity depression, and the self-aggregation of the hydrotropes, which reduces the water activity depression [29].

ILs can be subdivided into comparatively less studied protic ionic liquids (PILs), which are prepared by proton transfer reactions of Brønsted bases (e.g. triethylamine) and Brønsted acids (e.g. *p*-toluenesulfonic acid), as well as well-characterized aprotic ionic liquids (AILs) such as imidazolium salts, which are generally prepared by quaternization (alkylation) of amines and subsequent anion exchange [30, 31]. Most AILs are based on polyhalide counter-anions, such as hexafluorophosphate [PF_6^-] [32] and tetrafluoroborate [BF_4^-] [33], which have a reduced charge density due to the electron-withdrawing effect of the halogens. This charge delocalization leads to a reduced electrostatic interaction with the cation, resulting in a weakening of the crystal lattice and consequently in a reduction of the melting temperature [12]. However, the pharmaceutical applications of AILs based on polyhalide counter-anions are severely restricted due to their toxicological and ecological issues [34].

An alternative approach to overcome these drawbacks is to follow nature’s blueprint and develop ILs that consist of natural components that have well-characterized biodegradable and toxicological properties. Hence, Fukaya et al. [35] developed ILs that consist solely of biomaterials such as choline chloride and naturally occurring OAs, so called Bio-ILs (**Fig. 1**), as well as Abbott et al. [36] introduced low-melting deep eutectic liquid systems, that are also based on choline chloride.

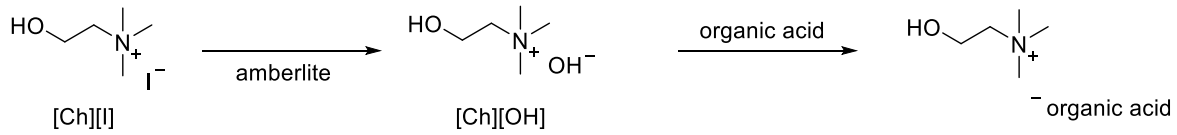

Figure 1: Choline based Bio-ILs [35].

Several APIs as well as most naturally occurring alkaloids are nitrogen-containing heterocycles with low symmetry and diffuse charge distribution [37, 38]. Because most of them are not permanently charged ions, the formation PILs, by an acid (HA) – base (B) neutralization reaction, seems to be an attractive strategy to improve their pharmaceutical properties such as solubility, bioavailability, and drug delivery [39-41]. Protic oligomeric ILs (OILs), a subdomain of PILs, have been explored recently by Stoimenovski et al. [40] and are H-bonded acid-oligomer based ILs, consisting of several equivalents of acid and one equivalent of base. The excess of acid leads to the formation of oligomeric hydrogen-bonded acid complexes, which has been shown by Johansson et al. [42] for ILs composed of glacial acetic acid and *N*-methylpyrrolidine in various molar ratios (1 : 1, 2 : 1, 3 : 1; moles of acid to moles of base). The oligomeric species are stronger acids than the monomeric species and therefore form weaker conjugate bases, which leads to a shift in the proton transfer equilibrium towards the ionized species. In addition, H-bonded acid-oligomer based pharmaceutically active ILs, namely lidocainium salicylate (in different molar ratios) were presented by Bica et al. [43], to improve the properties of the salts, including modification of stoichiometry for dosage options and in liquefaction for drug delivery.

1.2 Solid dispersions (SDs)

SDs can be classified according to their physical state as well as their number of solid-state phases and they can be very diverse, including eutectic mixtures, solid solutions, glass solutions and glass suspensions (**Fig. 2**) [7]. In the 1970th, Chiou and Riegelman have defined them as “a dispersion of one or more active ingredients in an inert carrier at the solid state prepared by melting (fusion), solvent, or melting-solvent method” [44]. So far, many SD approaches have been carried out, for example Soni et al. [45] prepared SDs of furosemide and the carriers PVPK30 and PEG 6000 by

solvent evaporation methods, or Siahi-Shadbad et al. [46] prepared SDs of furosemide, PVP and microcrystalline cellulose according to the cogrinding process using a ball mill.

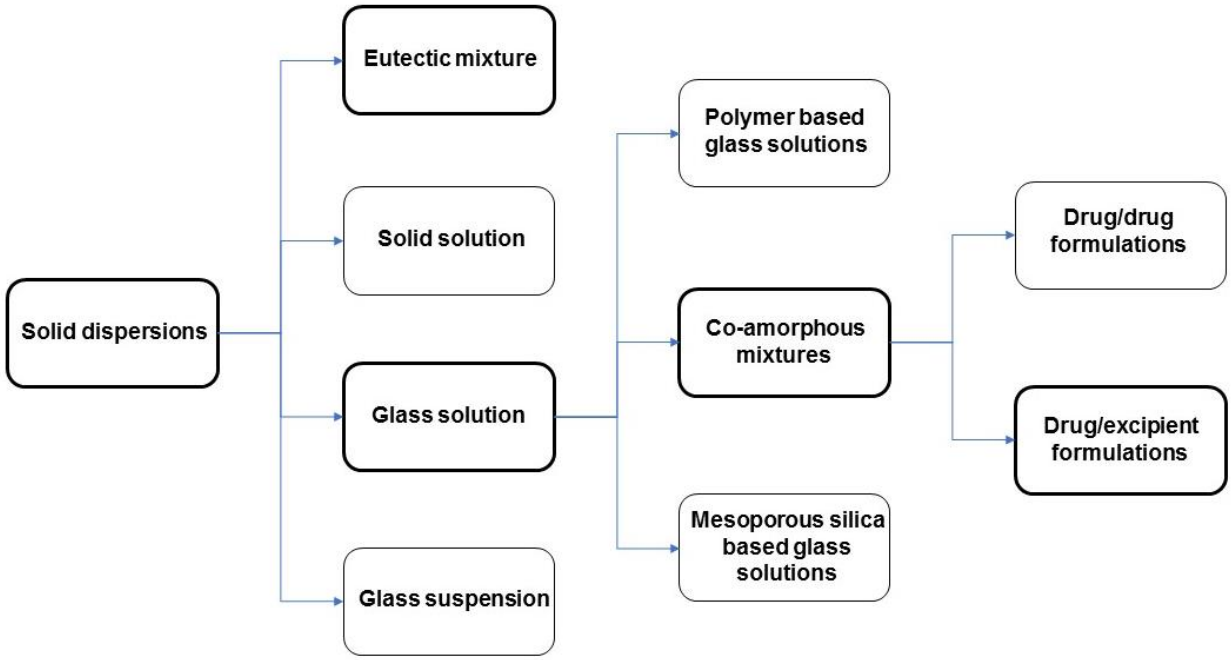

Figure 2: SDs overview [7].

SDs are of interest in the pharmaceutical field because of their potential to improve oral bioavailability of poorly water-soluble drugs through drug dissolution enhancement because of their amorphous nature. Many studies showed that SDs, e.g. co-amorphous systems, exhibit a higher physical stability in solid state than the pure amorphous drugs. The increased stability is attributed to several factors, including intermolecular interactions like hydrogen bonding and π-π-interactions between mixtures' components. Whereas the homodimers of pure amorphous APIs recrystallize usually at a rather high rate, the heterodimers of amorphous SDs show a time-delayed recrystallization behavior. A suggested explanation for the delay is, that the intermolecular bonds of the heterodimer must be broken first, followed by the formation of homodimers and a subsequent establishment of a long-range order within the solid [7, 47-49]. In addition, SDs prevent the recrystallization process of a solute by hydrotropic solubilization, which was demonstrated by Kamble et al. [50] for aqueous norfloxacin-SD solutions.

Deep eutectic solvents (DES), a subunit of SDs, and ILs have similar physical properties and share many characteristics, including low vapor pressure, relatively wide liquid range, and non-flammability [51-53]. The term “deep eutectic solvent” was introduced in the early 2000th by Abbott et al. [36] and represents a new type of solvent, consisting of large, nonsymmetric ions that have low lattice energy and hence low melting points. DES are usually obtained by mixing two components, a hydrogen-bond donor (HBD), i.e. OAs, sugars or amino acids, and a hydrogen-bond acceptor (HBA), i.e. quaternary ammonium salts that crystallize simultaneously when the temperature is lowered [36, 54]. Hydrogen bonding between the HBD and the HBA leads to charge delocalization, which is responsible for the low melting point of the mixture relative to the melting points of the individual components (**Fig. 3**) [55, 56].

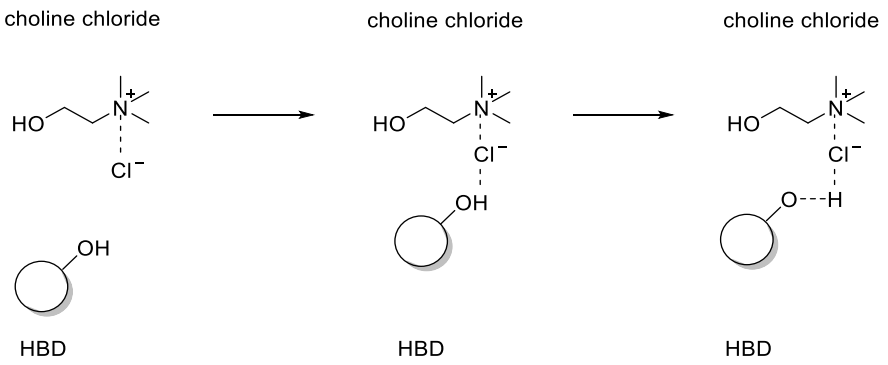

Figure 3: Interaction of an HBD with the quaternary ammonium salt choline chloride [55].

The wide range of HBD and HBA candidates enables a new family of tailor-made designer solvents, which may be used as carrier system for poorly water-soluble biomolecules [52]. In addition, DES are very promising for applications in the pharmaceutical field, since they offer low manufacturing costs and easy manufacturing processes, e.g. the heating method described by Abbott et. al. [36], in which the components are mixed, heated and stirred until a homogeneous liquid is formed [56-59].

Another type of SDs are glass solutions (GSs), in which the solute is molecularly dispersed in the amorphous carrier. GSs are homogeneous single-phase systems that consist of API, OAs, carbohydrates, and/or organic polymers such as poly(vinylpyrrolidone) (PVP) and cellulose derivatives. GSs have a much higher

viscosity than comparable liquid solutions and are used to improve the solubility of a solute in water and to improve the dissolution rate of an API, as shown for a GS made from griseofulvin and citric acid by Chiou and Riegelmann [54].

1.3 Multiple myeloma (MM)

MM is a neoplastic plasma cell disorder that is characterized by clonal proliferation of malignant plasma cells in the bone marrow microenvironment, monoclonal protein in the blood or urine, and associated organ dysfunction. It accounts for approximately 1% of neoplastic diseases and 13% of hematologic cancers [60-62]. The incidences are about 20,000 per year in the United States [63-65]. Despite recent therapeutic advances, including autologous hematopoietic stem cell transplantation, the use of various proteasome inhibitors alone or in combination with an immunmodulatory agent (IMiD) and a corticosteroid, or the use of the histone deacetylase inhibitor panobinostat in combination with bortezomib and dexamethasone, MM remains a mostly incurable disease with an average survival rate between 3 and 6 years [66-68].

A promising new strategy for the treatment in the MM is a dual depletion of heat shock protein90 (HSP90) and the heat shock factor-1/heat shock protein70 (HSF-1/HSP70) system. Researchers have already developed different potent HSP90 inhibitors, like geldanamycin derivatives 17-AAG and 17-DMAG or Isoxazole NVP-AUY922, but clinical cell studies revealed an upregulation of HSP70 during HSP90 inhibition, which diminished the efficacy of the HSP90 inhibition approach (**Fig. 4**) [69-71].

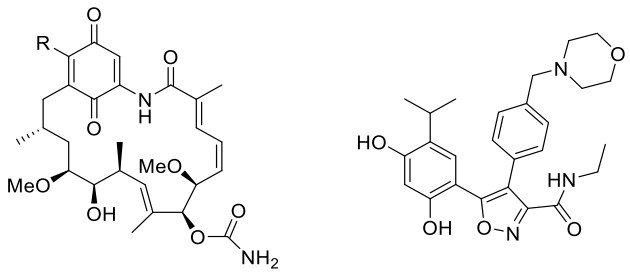

Figure 4: HSP90 inhibitors 17-AAG, 17-DMAG and NVP-AUY922 [70].

Hence, a simultaneously application of HSP90 and HSP70 inhibitors was aimed and potent isoquinolone-type HSP70 inhibitors were already developed (**Fig. 5**). Unfortunately, these potent agents suffer from poor water solubility, which diminishes the application for *in vitro* and consequently *in vivo* studies [72].

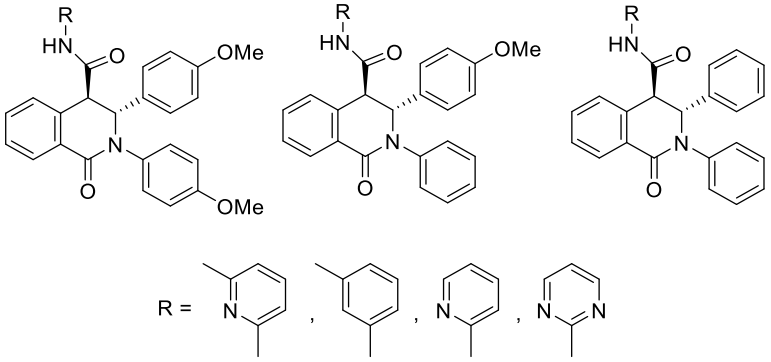

Figure 5: Isoquinolone-type HSP70 inhibitors [72].

1.4 References

[1] Hounsome, N.; Hounsome, B.; Tomos, D.; Edwards-Jones, G. *J. Food Sci.* **2008,** *73*, R48-65.

[2] Roytrakul, S.; Verpoorte, R. *Phytochem. Rev.* **2007,** *6*, 383-396.

[3] Roberts, M. F.; Homeyer, B. C.; Pham, T. D. T. *Z. Naturforsch.* **1991,** *46c*, 377-388.

[4] Choi, Y. H.; van Spronsen, J.; Dai, Y.; Verberne, M.; Hollmann, F.; Arends, I. W.; Witkamp, G. J.; Verpoorte, R. *Plant Physiol.* **2011,** *156*, 1701-1705.

[5] Bhakay, A.; Rahman, M.; Dave, R. N.; Bilgili, E. *Pharmaceutics* **2018,** *10*.

[6] Domingos, S.; Andre, V.; Quaresma, S.; Martins, I. C.; Minas da Piedade, M. F.; Duarte, M. T. *J. Pharm. Pharmacol.* **2015,** *67*, 830-846.

[7] Dengale, S. J.; Grohganz, H.; Rades, T.; Lobmann, K. *Adv. Drug Deliv. Rev.* **2016,** *100*, 116-125.

[8] Marrucho, I. M.; Branco, L. C.; Rebelo, L. P. *Annu. Rev. Chem. Biomol. Eng.* **2014,** *5*, 527-546.

[9] Hamilton, G. R.; Baskett, T. F. *Can J Anaesth* **2000,** *47*, 367-374.

[10] Sertürner, F. W. *Trommsdorff's Journal der Pharmazie für Aerzte, Apotheker und Chemisten* **1805,** *13*.

[11] Agharkar, S.; Lindenbaum, S.; Higuchi, T. *J. Pharm. Sci.* **1976,** *65*, 747-749.

[12] Naert, P.; Rabaey, K.; Stevens, C. V. *Green Chem.* **2018,** *20*, 4277-4286.

[13] Sekhon, B. S. *Asian J. Pharm. Biol. Res.* **2011,** *1*, 395-411.

[14] Stahl, P. H.; Wermuth, C. G. *Weinheim, Wiley-VCH* **2011**.

[15] Petkovic, M.; Ferguson, J. L.; Nimal Gunaratne, H. Q.; Rui Ferreira; Leitao, M. C.; Seddon, K. R.; Rebelo, L. P. N.; Pereira, C. S. *Green Chem.* **2010,** *12*, 643-649.

[16] Petkovic, M.; Seddon, K. R.; Rebelo, L. P.; Silva Pereira, C. *Chem. Soc. Rev.* **2011,** *40*, 1383-1403.

[17] Ferraz, R.; Branco, L. C.; Prudencio, C.; Noronha, J. P.; Petrovski, Z. *ChemMedChem* **2011,** *6*, 975-985.

[18] MacFarlane, D. R.; Seddon, K. R. *Aust J. Chem.* **2007,** *60*, 3.

[19] Welton, T. *Chem. Rev.* **1999,** *99*, 2071-2084.

[20] Villanueva, M.; Coronas, A.; García, J.; Salgado, J. *Ind. Eng. Chem. Res.* **2013,** *52*, 15718-15727.

[21] Bier, M.; Dietrich, S. *Mol. Phys.* **2010,** *108*, 211-214.

[22] Paulechka, Y. U.; Kabo, G. J.; Blokhin, A. V.; Vydrov, O. A.; Magee, J. W.; Frenkel, M. *J. Chem. Eng. Data* **2003,** *48*, 457-462.

[23] Salem, N.; Abu-Lebdeh, Y. *J. Electrochem. Soc.* **2014,** *161*, A1593-A1601.

[24] Lei, Z.; Chen, B.; Koo, Y. M.; MacFarlane, D. R. *Chem. Rev.* **2017,** *117*, 6633-6635.

[25] Docherty, K. M.; Kulpa, J. C. F. *Green Chem.* **2005,** *7*, 185.

[26] Egorova, K. S.; Gordeev, E. G.; Ananikov, V. P. *Chem. Rev.* **2017,** *117*, 7132-7189.

[27] Shamshina, J. L.; Barber, P. S.; Rogers, R. D. *Expert Opin. Drug Deliv.* **2013,** *10*, 1367-1381.

[28] Claudio, A. F.; Neves, M. C.; Shimizu, K.; Canongia Lopes, J. N.; Freire, M. G.; Coutinho, J. A. *Green Chem.* **2015,** *17*, 3948-3963.

[29] Booth, J. J.; Abbott, S.; Shimizu, S. *J. Phys. Chem. B* **2012,** *116*, 14915-14921.

[30] Shmukler, L. E.; Gruzdev, M. S.; Kudryakova, N. O.; Fadeeva, Y. A.; Kolker, A. M.; Safonova, L. P. *RSC Adv.* **2016,** *6*, 109664-109671.

[31] Greaves, T. L.; Drummond, C. J. *Chem. Rev.* **2015,** *115*, 11379-11448.

[32] Holloczki, O.; Macchiagodena, M.; Weber, H.; Thomas, M.; Brehm, M.; Stark, A.; Russina, O.; Triolo, A.; Kirchner, B. *Chemphyschem* **2015,** *16*, 3325-3333.

[33] Anderson, J. L.; Armstrong, D. W.; Wei, G. T. *Anal. Chem.* **2007,** *79*, 4247-4247.

[34] Stolte, S.; Arning, J. r.; Bottin-Weber, U.; Matzke, M.; Stock, F.; Thiele, K.; Uerdingen, M.; Welz-Biermann, U.; Jastorff, B.; Ranke, J. *Green Chem.* **2006,** *8*, 621.

[35] Fukaya, Y.; Iizuka, I.; Sekikawa, K.; Ohno, H. *Green Chem.* **2007,** *9*, 1155-1157.

[36] Abbott, A. P.; Capper, G.; Davies, D. L.; Rasheed, R. K.; Tambyrajah, V. *Chem. Commun.* **2003**, 70-71.

[37] Carter, E. B.; Culver, S. L.; Fox, P. A.; Goode, R. D.; Ntai, I.; Tickell, M. D.; Traylor, R. K.; Hoffman, N. W.; Davis, J. H., Jr. *Chem. Commun.* **2004**, 630-631.

[38] Higasio, Y. S.; Shoji, T. *Appl. Catal. A-Gen.* **2001,** *221*, 197-207.

[39] Pernak, J.; Goc, I.; Mirska, I. *Green Chem.* **2004,** *6*, 323.

[40] Stoimenovski, J.; Dean, P. M.; Izgorodina, E. I.; MacFarlane, D. R. *Faraday Discuss.* **2012,** *154*, 335-52; discussion 439-64, 465-471.

[41] Easton, M. E.; Li, K.; Titi, H. M.; Kelley, S. P.; Rogers, R. D. *Cryst. Growth Des.* **2020,** *20*, 2608-2616.

[42] Johansson, K. M.; Izgorodina, E. I.; Forsyth, M.; MacFarlane, D. R.; Seddon, K. R. *Phys. Chem. Chem. Phys.* **2008,** *10*, 2972-2978.

[43] Bica, K.; Rogers, R. D. *Chem. Commun.* **2010,** *46*, 1215-1217.

[44] Chiou, W. L.; Riegelman, S. *J. Pharm. Sci.* **1971,** *60*, 1281-302.

[45] Soni, L.; Ansari, M.; Thakre, N.; Singh, A.; Bhowmick, M.; Rathi, J. *Int. J. Res. Dev. Pharm .Life Sci.* **2017,** *6*, 2571-2575.

[46] Siahi-Shadbad, M. R.; Ghanbarzadeh, S.; Barzegar-Jalali, M.; Valizadeh, H.; Taherpoor, A.; Mohammadi, G.; Barzegar-Jalali, A.; Adibkia, K. *Adv. Pharm. Bull.* **2014,** *4*, 391-399.

[47] Laitinen, R.; Lobmann, K.; Strachan, C. J.; Grohganz, H.; Rades, T. *Int. J. Pharm.* **2013,** *453*, 65-79.

[48] Löbmann, K.; Jensen, K. T.; Laitinen, R.; Rades, T.; Strachan, C. J.; Grohganz, H. In *Amorphous Solid Dispersions: Theory and Practice;* Shah, N.; Sandhu, H.; Choi, D.

S.; Chokshi, H.; Malick, A. W. Eds.; Springer New York: New York, NY, 2014; pp. 613-636.

[49] Jensen, K. T.; Larsen, F. H.; Cornett, C.; Lobmann, K.; Grohganz, H.; Rades, T. *Mol. Pharm.* **2015,** *12*, 2484-2492.

[50] Kamble, R.; Sharma, S.; Mehta, P. *J. Taibah Univ. Sci.* **2018,** *11*, 512-522.

[51] Wasserscheid, P.; Keim, W. *Angew. Chem.* **2000,** *112*, 3926-3945.

[52] Dai, Y.; van Spronsen, J.; Witkamp, G. J.; Verpoorte, R.; Choi, Y. H. *Anal. Chim. Acta* **2013,** *766*, 61-68.

[53] Cherukuvada, S.; Nangia, A. *Chem. Commun.* **2014,** *50*, 906-923.

[54] Laitinen, R.; Priemel, P. A.; Surwase, S.; Graeser, K.; Strachan, C. J.; Grohganz, H.; Rades, T. **2014**, 35-90.

[55] Harris, R. C. *Ph.d. Thesis, University of Leicester* **2009**.

[56] Smith, E. L.; Abbott, A. P.; Ryder, K. S. *Chem. Rev.* **2014,** *114*, 11060-11082.

[57] Dai, Y.; van Spronsen, J.; Witkamp, G. J.; Verpoorte, R.; Choi, Y. H. *J. Nat. Prod.* **2013,** *76*, 2162-2173.

[58] Faggian, M.; Sut, S.; Perissutti, B.; Baldan, V.; Grabnar, I.; Dall'Acqua, S. *Molecules* **2016,** *21*.

[59] Morrison, H. G.; Sun, C. C.; Neervannan, S. *Int. J. Pharm.* **2009,** *378*, 136-139.

[60] Palumbo, A.; Anderson, K. *N. Engl. J. Med.* **2011,** *364*, 1046-1060.

[61] Angtuaco, E. J.; Fassas, A. B.; Walker, R.; Sethi, R.; Barlogie, B. *Radiology* **2004,** *231*, 11-23.

[62] Kuppers, R. *Nat. Rev. Cancer* **2005,** *5*, 251-262.

[63] Kuehl, W. M.; Bergsagel, P. L. *Nat. Rev. Cancer.* **2002,** *2*, 175-187.

[64] Kuehl, W. M.; Bergsagel, P. L. *J. Clin. Invest.* **2012,** *122*, 3456-3463.

[65] Siegel, R.; Naishadham, D.; Jemal, A. *CA Cancer J. Clin.* **2012,** *62*, 283-298.

[66] Kumar, S. K.; Rajkumar, V.; Kyle, R. A.; van Duin, M.; Sonneveld, P.; Mateos, M. V.; Gay, F.; Anderson, K. C. *Nat. Rev. Dis. Primers* **2017,** *3*, 17046.

[67] Usmani, S. Z.; Hoering, A.; Cavo, M.; Miguel, J. S.; Goldschimdt, H.; Hajek, R.; Turesson, I.; Lahuerta, J. J.; Attal, M.; Barlogie, B.; Lee, J. H.; Kumar, S.; Lenhoff, S.; Morgan, G.; Rajkumar, S. V.; Durie, B. G. M.; Moreau, P. *Blood Cancer J.* **2018,** *8*, 123.

[68] Paramore, A.; Frantz, S. *Nat. Rev. Drug Discov.* **2003,** *2*, 611-612.

[69] Powers, M. V.; Clarke, P. A.; Workman, P. *Cancer Cell* **2008,** *14*, 250-262.

[70] Neckers, L.; Workman, P. *Clin. Cancer Res.* **2012,** *18*, 64-76.

[71] Workman, P. *Cancer Lett.* **2004,** *206*, 149-157.

[72] Chatterjee, M.; Hartung, A.; Holzgrabe, U.; Mueller, E.; Peinz, U.; Sotriffer, C.; Zilian, D. *Patent US9975853B2* **2018**.

2 Aim of the thesis

Since large counterions are able to prevent the formation of strong lattice forces within the crystals of an API, attempts have been made to follow nature's blueprint and to use natural organic acids (OAs) for salt formation of basic, poorly water-soluble compounds, in order to enhance their water solubility. The aim was to use a salt screening program to show whether the mostly large carboxylates form soluble PILs with basic natural products, such as papaverine, morphine and berberine as well as the API dextromethorphan (**Fig. 1**).

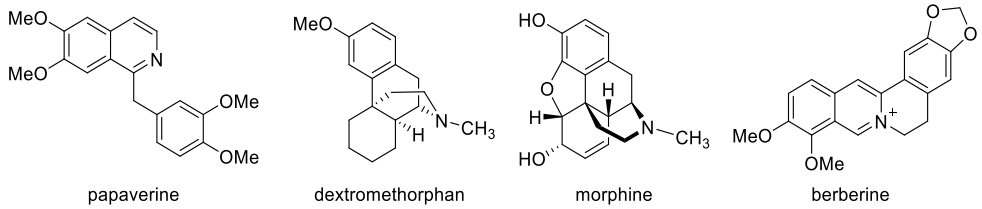

Figure 1: Different alkaloids/APIs used in a salt screening program.

Various types of naturally occurring OAs such as mono-, di- and tricarboxylic acids, α-hydroxycarboxylic acids (AHAs), β-hydroxycarboxylic acids (BHAs), benzoic acid derivatives, and hydroxycinnamic acid derivatives were used as counterions (**Fig. 2**). The obtained salts were characterized physically in their solid state and the identified PILs were examined regarding their supramolecular behavior.

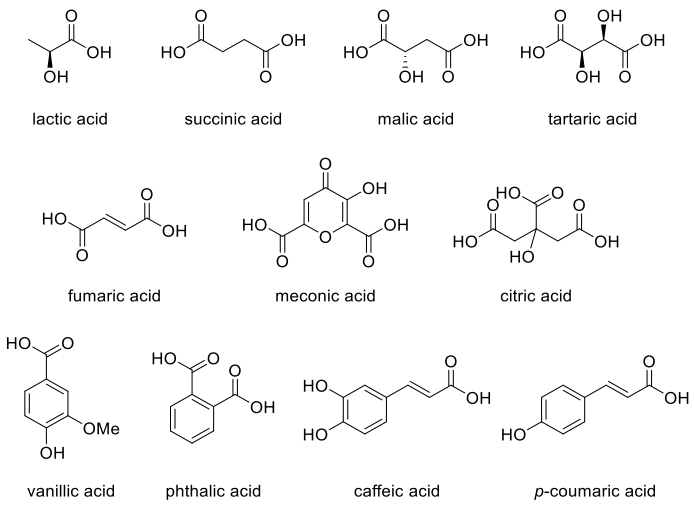

Figure 2: OAs used in a salt screening program.

Since the isoquinolone-type HSP70 inhibitors suffer from poor water solubility and high melting points, single crystal X-ray structures should be obtained to understand this phenomenon (**Fig. 3**). In addition, a DES approach was used to improve the supramolecular pattern of these compounds facilitating *in vitro* activity studies.

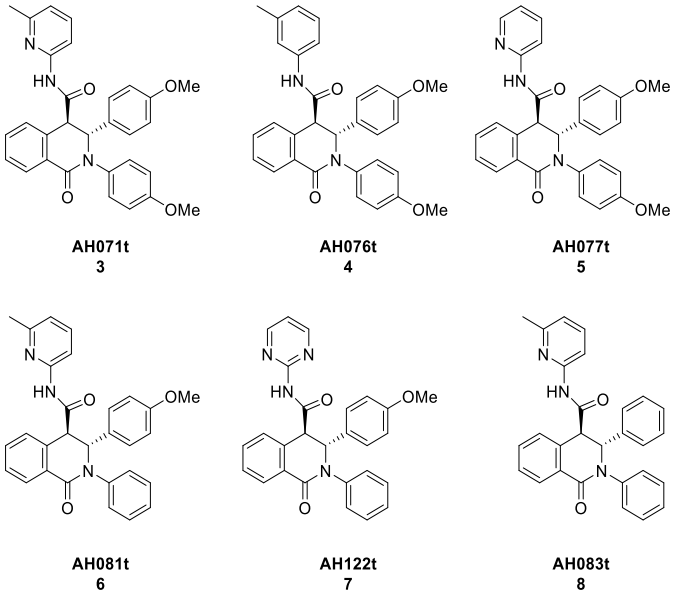

Figure 3: Singe crystal structures of various HSP70 inhibitors.

Furthermore, it was aimed to separate the racemates (**Fig. 4**) of the HSP70 inhibitor **7** by means of preparative HPLC and to determine the enantiospecific activity by EDC measurements and *in vitro* activity studies.

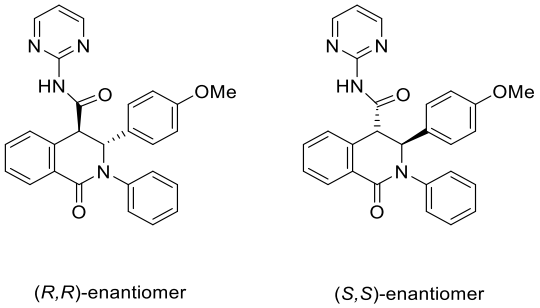

Figure 4: Enantiomers of 7.

3 Results

Since salt screening programs of several naturally occurring organic acids (OAs) and basic compounds were aimed, the β-hydroxycarboxylic acid meconic acid must be synthesized first, as described in chapter 3.1. Subsequently the results of the salt screenings were presented and discussed in chapter 3.2 as well as in chapter 3.3.

The crystal structures of several isoquinolone-type HSP70 inhibitors and a deep eutectic solvent (DES) approach to improve the water solubility of these inhibitors were presented in chapter 3.4. Accordingly, the enantiomers of the inhibitors were separated by preparative HPLC and the results of the bioactivity studies were presented in chapter 3.5.

3.1 A Convenient Preparation of Carboxy-γ-pyrone Derivatives: Meconic Acid and Comenic Acid

Paul Güntzel, Leonard Forster, Curd Schollmayer, and Ulrike Holzgrabe*

Department of Pharmaceutical and Medicinal Chemistry, Institute of Pharmacy, University of Würzburg, Am Hubland, DE-97074 Würzburg, Germany

*Corresponding author. Tel.: +49 931 3185461

E-Mail address: *ulrike.holzgrabe@uni-wuerzburg.de*

Reprinted with permission from Organic Preparations and Procedures International, 50:512-516, 2018.

The dried milky sap from *Papaver somniferum*, known as opium, contains several alkaloids with pharmacological activity. The major alkaloidal components are morphine (about 10% by weight), noscapine (about 6%) and papaverine (about 1%); the major non-alkaloidal constituents are water and organic acids (OAs), including lactic acid and

meconic acid (**1**, 3-hydroxy-2,6-dicarboxy-*γ*-pyrone) (5%) [1-8]. In the 19th century Sertürner isolated morphine as its meconate salt from opium, an early indication of the importance of OA salts [9, 10].

Salt formation of poorly water-soluble organic bases with acids leads to increased solubility in an aqueous environment compared to the non-associated form, and this explains the high concentration of acids in opium [1-3]. Since large counterions are able to prevent strong lattice forces within the crystals, it was desired to use those large natural acids, within a comprehensive screening program, for salt formation of basic, poorly water-soluble active pharmaceutical ingredients (APIs), in order to enhance their solubility [11, 12]. Here, it was intended to use the natural OAs meconic acid (**1**) and comenic acid (**2**, 5-hydroxy-2-carboxy-*γ*-pyrone) for salt formation with alkaloids. Hence, a transition-metal free short and simple synthesis of **1** and **2** was developed (**Scheme 1**), as the known procedures were unable to produce these compounds on substantial scale [13, 14]. As well, development of new methods would permit further structural modifications of both acids.

For the oxidation of the alcohol functions in **4** the procedure described by Lovell et al. was applied first [13]. However, in our hands the direct oxidation of the benzylic alcohol in **4** to the corresponding carboxylic acid (CA) in **1** by means of palladium failed. Using stronger oxidants such as chromate instead of palladium, similarly failed. A selective procedure described by Pace et al. recommends the protection of the enolic function before oxidation of the benzylic alcohols with manganese dioxide, but again, in our hands, no product was obtained [14].

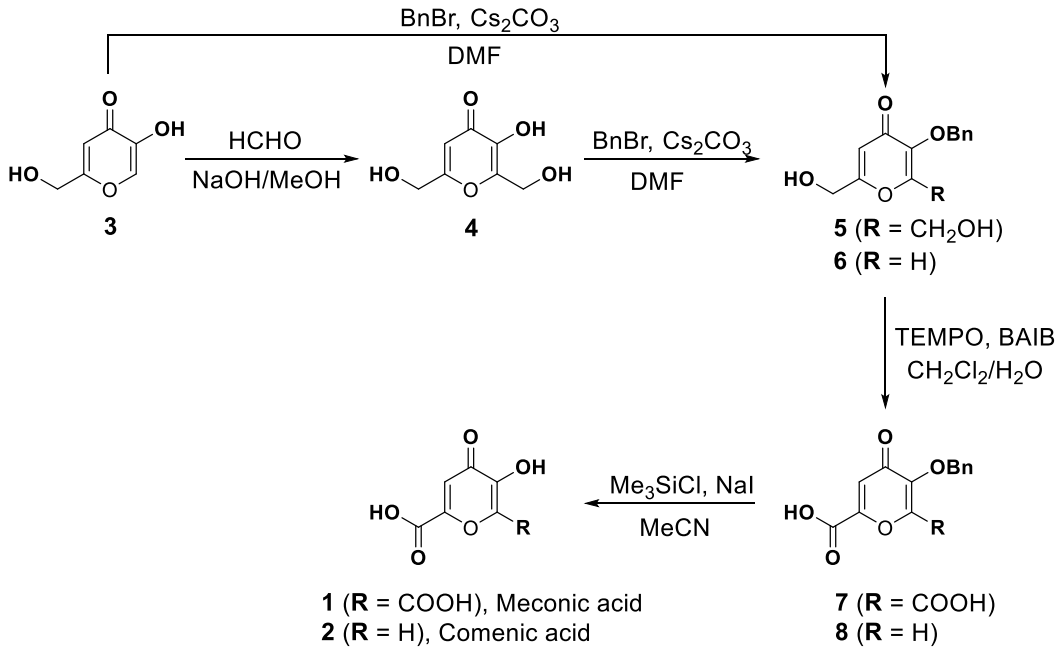

Scheme 1: Synthetic route for meconic acid and comenic acid.

Compounds **1** and **2** had been prepared starting from kojic acid **3** as depicted in Scheme 1. For the synthesis of meconic acid, the introduction of a second hydroxymethyl group in position 6 via reaction of **3** with formaldehyde in basic methanol to **4** was performed as previously described [13]. Next protection of the enolic function of **4** and **3** with benzyl bromide was required in order to achieve **5** and **6**, respectively [14]. For the oxidation of **5** and **6** to the corresponding CAs **7** and **8** the radical 2,2,6,6-tetramethylpiperidine-1-oxyl (TEMPO) in the presence of bis(acetoxy)iodobenzene (BAIB) was used, following the protocol described by Epp et al. for similar reactions [15, 16]. Subsequent deprotection of the enolic group with Me_3SiCl and sodium iodide gave **1** and **2** in almost quantitative yields.

Salt formation is indeed an attractive concept to improve the aqueous solubility of poorly water-soluble APIs [17, 18]. Nature often uses OAs as counterions for basic substances to obtain salts [1]. Accordingly, in this work the natural OAs meconic acid and comenic acid were synthesized for salt formation with alkaloids. As the well-known synthetic procedure did not lead to **1**, a new 4-step synthesis was developed, applying a transition-metal free oxidation with protection of the enolic function as the crucial step. Further advantages are the low costs and ready availability of the starting materials as well as the easy synthetic procedure. In a similar way, a novel total

synthesis of **2** was realized with a satisfactory yield. This opens a potential avenue for the synthesis of further derivatives of both acids for subsequent studies, as well.

Experimental Section

Chemicals were purchased from Sigma-Aldrich (Schnelldorf, Germany) or TCI Chemicals (Eschborn, Germany) and were used without further purification. Anhydrous solvents were purified and/or dried by standard techniques prior to being used. Melting points were measured with an MPM-H2 melting point meter from Coesfeld GmbH & Co. KG (Dortmund, Germany). ^{1}H (400.132 MHz) and ^{13}C (100.613 MHz) nuclear magnetic resonance (NMR) spectra were recorded on a Bruker AV 400 instrument (Bruker Biopsin). As an internal standard, the signals of the deuterated solvents were used (DMSO-*d*$_6$: ^{1}H 2.5 ppm, ^{13}C 39.52 ppm; $CDCl_3$: ^{1}H 7.26 ppm, ^{13}C 77.16 ppm). IR measurements were conducted on a Jasco FT/IR-6100 spectrometer (Gross-Umstadt, Germany) with a diamond total reflection unit. ASAP mass spectra were recorded on an Exactive Plus instrument (Therma Scientific) with an Orbitrap mass analyzer at the Institute of Inorganic Chemistry of the University of Würzburg. Complete characterization data are available from the authors upon request.

3-Hydroxy-2,6-dihydroxymethyl-*γ*-pyrone (4). Compound **4** was prepared as described by Lovell et al. All characterization data matched the literature [13].

3-Benzyloxy-2,6-dihydroxymethyl-*γ*-pyrone (5). Cs_2CO_3 (13.85 g, 42.52 mmol) and **4** (7.32 g, 42.52 mmol) were dissolved in DMF (130 mL) and treated with *α*-bromotoluene (5.05 mL, 42.52 mmol). The reaction mixture was heated to 70°C and stirred for 1.5 h. Then, a saturated solution of sodium chloride (150 mL) was added and the mixture was extracted with $CHCl_3$ (8 x 50 mL). The organic layer was dried over anhydrous $MgSO_4$ and evaporated under reduced pressure. After drying *in vacuo* **5** was collected as a brownish solid (8.07 g, 72% yield) and used without further purification. MP 97°C; IR (ATR, cm^{-1}): 3319, 3104, 2875, 1642, 1604, 1581, 1239, 1195, 1151, 1074, 1041, 1017, 964, 915, 876, 748, 699; ^{1}H NMR ($CDCl_3$): *δ* (ppm) = 4.31 (s, 2H, C*H*$_2$OH), 4.41 (s, 2H, C*H*$_2$OH), 5.12 (s, 2H, C*H*$_2$Ph), 6.41 (s, 1H, *H*5), 7.34 (m, 5H, C_6H_5); ^{13}C NMR ($CDCl_3$): *δ* (ppm) = 56.9 (CH_2), 60.7 (CH_2), 74.3 (CH_2), 112.6 (*C*5), 127.1 (*C*2), 128.7 – 142.3 (6*C*, (phe)), 159.5 (*C*3), 167.5 (*C*6), 176.9 (*C*4). All characterization data matched the literature [19].

3-Benzyloxy-2,6-dicarboxy-*γ*-pyrone (7). Compound **5** (8.07 g, 30.77 mmol), BAIB (29.73 g, 92.31 mmol), $NaHCO_3$ (2.59 g, 30.77 mmol), and TEMPO (2.40 g, 15.38 mmol) were dissolved in a mixture of H_2O (100 mL) and CH_2Cl_2 (100 mL) and stirred at 0°C for 24 h. After phase separation, the aqueous layer was washed with CH_2Cl_2 (2 x 40 mL) and reduced by three-quarters *in vacuo*. The pH of the solution was adjusted to 0.5 by adding concentrated HCl. The resulting colorless precipitate was filtered, washed with cold H_2O and dried under vacuum to give **7** as a solvate (5.21 g, 58%). MP 175°C; IR (ATR, cm^{-1}): 3558, 1717, 1660, 1619, 1591, 1415, 1293, 1261, 1223, 1182, 1009, 972, 914, 891, 729, 693; ^{1}H NMR (DMSO-*d*$_6$): *δ* (ppm) = 5.14 (s, 2H, C*H*$_2$Ph), 7.05 (s, 1H, *H*5), 7.33 - 7.46 (m, 5H, C_6H_5); ^{13}C NMR (DMSO-*d*$_6$): *δ* (ppm) = 73.7 (CH_2), 118.3 (*C*5), 128.2 – 136.4 (6*C*, (phe)), 147.0 (*C*2), 147.8 (*C*3), 152.3 (*C*6), 160.4 (*C*OOH), 160.5 (*C*OOH), 176.2 (*C*4).

Anal. Calcd for $C_{14}H_{10}O_7$x1.6H_2O: C, 52.70; H, 4.17. Found: C, 52.54; H, 3.93.

3-Hydroxy-2,6-dicarboxy-*γ*-pyrone (1). Compound **7** (1.00 g, 3.45 mmol) and sodium iodide (0.775 g, 5.17 mmol) were dissolved in dry MeCN (50 mL) under argon, trimethylsilyl chloride (880 µL, 6.90 mmol) was added. The solution was first stirred at 70°C for 4 h. Then, H_2O (120 mL) was added and the mixture was extracted with methyl *tert*-butyl ether (MTBE) (3 x 50 mL) and then with $CHCl_3$ (3 x 50 mL). The aqueous layer was concentrated by three-quarters under reduced pressure and the pH of the solution was adjusted to 0.5 with concentrated HCl. The solution was left at room temperature until crystals were formed. The brownish crystals were collected, recrystallized from 50% aqueous ethanol and dried *in vacuo* to give compound **1** (0.527 g, 76%). MP 290°C; IR (ATR, cm^{-1}): 3344, 2974, 1727, 1629, 1482, 1217, 910, 775; ^{1}H NMR (DMSO-*d*$_6$): *δ* (ppm) = 6.98 (s, 1H, *H*5); ^{13}C NMR (DMSO-*d*$_6$): *δ* (ppm) = 115.2 (*C*5), 135.9 (*C*3), 150.6 (*C*2), 151.9 (*C*6), 160.7 (*C*OOH), 163.4 (*C*OOH), 174.8 (*C*4); ASAP (neg.) mass spectrum *m/z* 198.9877 (calculated for $C_7H_4O_7$ 198.9873). All characterization data matched the literature [13].

5-Benzyloxy-2-hydroxymethyl-*γ*-pyrone (6). Kojic acid (**3**) (5.00 g, 35.18 mmol) and Cs_2CO_3 (11.46 g, 35.18 mmol) were dissolved in DMF (150 mL), *α*-bromotoluene (4.2 mL, 35.18 mmol) was added and the reaction mixture heated to 70°C and stirred for 0.5 h. Then, a saturated solution of sodium chloride (100 mL) was added and the mixture extracted with $CHCl_3$ (10 x 50 mL). The combined organic layers were dried over anhydrous $MgSO_4$ and evaporated under reduced pressure.

6 was collected as a brownish solid (7.37 g, 90% yield) and used without further purification. MP 137°C; IR (ATR, cm^{-1}): 3302, 3261, 1643, 1601, 1586, 1455, 1442, 1256, 1233, 1197, 1147, 1077, 1017, 946, 865, 740, 694; ^{1}H NMR ($CDCl_3$): *δ* (ppm) = 4.44 (d, 2H, ^{4}J = 0.97 Hz, C*H*$_2$OH), 5.05 (s, 2H, C*H*$_2$Ph), 6.53 (t, 1H, ^{4}J = 0.79 Hz, *H*5), 7.31 - 7.34 (m, 5H, C_6H_5), 7.53 (s, 1H, *H*2); ^{13}C NMR ($CDCl_3$): *δ* (ppm) = 61.1 (CH_2), 72.2 (CH_2), 112.5 (*C*3), 128.0 (*C*6), 128.6 – 142.0 (6*C*, (phe)), 147.1 (*C*5), 167.2 (*C*2), 175.1 (*C*4). All characterization data matched the literature [19, 20].

5-Benzyloxy-2-carboxy-*γ*-pyrone (8). In a mixture of H_2O (50 mL) and CH_2Cl_2 (50 mL), **6** (4.51 g, 19.42 mmol), BAIB (12.51 g, 38.84 mmol), $NaHCO_3$ (1.63 g, 19.42 mmol) and TEMPO (1.52 g, 9.71 mmol) were dissolved and stirred at 0°C for 2 h. After phase separation, the aqueous layer was washed with CH_2Cl_2 (2 x 40 mL) and concentrated by three-quarters under reduced pressure. The pH of the solution was adjusted to 0.5 by adding concentrated HCl. The obtained slightly orange precipitate was filtered, washed with cold H_2O and dried *in vacuo* to give **8** (2.48 g, 52%). MP 200°C; IR (ATR, cm^{-1}): 3542, 3179, 3003, 1734, 1645, 1603, 1577, 1249, 1206, 996, 940, 882, 741, 698; ^{1}H NMR (DMSO-d_6): *δ* (ppm) = 4.98 (s, 2H, C*H*$_2$Ph), 6.94 (s, 1H, *H*5), 7.34 - 7.46 (m, 5H, C_6H_5), 8.36 (s, 1H, *H*2); ^{13}C NMR (DMSO-d_6): *δ* (ppm) = 70.7 (CH_2), 117.1 (*C*3), 128.2 – 135.8 (6*C*, (phe)), 141.5 (*C*6), 148.2 (*C*5), 152.6 (*C*2), 160.8 (*C*OOH), 173.0 (*C*4). All characterization data matched the literature [20].

5-Hydroxy-2-carboxy-*γ*-pyrone (2). Compound **8** (0.50 g, 2.03 mmol) and sodium iodide (0.457 g, 3.05 mmol) were dissolved in dry MeCN (40 mL) under argon and trimethylsilyl chloride (370 µL, 3.05 mmol) was added. The solution first stirred at 70°C for 5.5 h. Then, H_2O (100 mL) was added and the mixture was extracted with MTBE (2 x 20 mL) and then with CH_2Cl_2 (4 x 20 mL). The aqueous layer was concentrated by three-quarters under reduced pressure and the pH of the solution was adjusted to 1 with concentrated HCl. The solution was left at room temperature until crystals were formed. The brownish crystals were collected, recrystallized from 50% aqueous ethanol and dried *in vacuo* to give compound **2** (0.29 g, 92%). MP 286°C; IR (ATR, cm^{-1}): 3329, 3085, 2838, 2552, 1725, 1628, 1559, 1536, 1219, 1201, 1142, 1098, 936, 905, 760; ^{1}H NMR (DMSO-d_6): *δ* (ppm) = 6.95 (s, 1H, *H*3), 8.19 (s, 1H, *H*6); ^{13}C NMR (DMSO-d_6): *δ* (ppm) = 116.0 (*C*3), 140.3 (*C*5), 147.7 (*C*6), 152.4 (*C*2),

160.8 (*C*OOH), 173.7 (*C*4); ASAP (neg.) mass spectrum *m/z* 154.9975 (calculated for $C_6H_3O_5$ 154.9975). All characterization data matched the literature [21].

References

[1] H. Kalant, *Addiction*, **92**, 267 (1997).

[2] T. Reisine and G. W. Pasternak, *Opioid Analgesics and Antagonists*, p. 521, Goodman & Gilman's. The Pharmacological Basis of Therapeutics, McGraw-Hill, New York, NY, 1996.

[3] J. A. Hawkins, *Opium Addicts and Addictions*, p. 1, V. A. Danville and J. T. Townes, 1937, Reprint: Arno Press, New York, NY, 1981.

[4] P. L. Schiff Jr., *Am. J. Pharm. Educ.*, **66**, 186 (2002).

[5] L. D. Kapoor, *Opium Poppy: Botany, Chemistry, and Pharmacology*, p. 1, The Haworth Press, Binghampton New York, NY, 1995.

[6] J. Bruneton, *Pharmacognosy, Phytochemistry, Medicinal Plants, Technique & Documentation*, p. 749, Lavoisier Publishing, Paris, 1995.

[7] G. E. Trease, and W. C. Evans, *Pharmacognosy*, 12th ed., p. 576, Balliere Tindall, London, 1983.

[8] J. E. Robbers, M. K. Speedie and V. E. Tyler, *Pharmacognosy and Pharmacobiotechnology*, p. 163, Williams and Wilkins, Baltimore MD, 1996.

[9] G. R. Hamilton and T. F. Baskett, *Can. J. Anaesth.*, **47**, 367 (2000).

[10] F. W. Sertürner, *Trommsdorff's Journal der Pharmazie für Aerzte, Apotheker und Chemisten*, **13**, 229 (1805).

[11] S. Agharkar, S. Lindenbaum and T. Higuchi, *J. Pharm. Sci.*, **65**, 747 (1976).

[12] A. T. Serajuddin, *Adv. Drug Deliv. Rev.*, **59**, 603 (2007).

[13] S. Lovell, P. Subramony and B. Kahr, *J. Am. Chem. Soc.*, **121**, 7020 (1999).

[14] P. Pace, E. Nizi, B. Pacini, S. Pesci, V. Matassa, R. De Francesco, S. Altamura and V. Summa, *Bioorg. Med. Chem. Lett.*, **14**, 3257 (2004).

[15] J. B. Epp and T. S. Widlanski, *J. Org. Chem.*, **64**, 293 (1999).

[16] L. J. van den Bos, J. D. C. Codee, J. C. van der Toorn, T. J. Boltje, J. H. van Boom, H. S. Overkleeft and G. A. van der Marel, *Org. Lett.*, **6**, 2165 (2004).

[17] P. L. Gould, *Int. J. Pharm.*, **33**, 201 (1986).

[18] S. M. Berge, L. D. Bighley and D. C. Monkhouse, *J. Pharm. Sci.*, **66**, 1 (1977).

[19] C. Balakrishna, N. Payili, S. Yennam, P. U. Devi and M. Behera, *Bioorganic Med. Chem. Lett.*, **25**, 4753 (2015).

[20] Y. Y. Xie, Z. Lu, X. L. Kong, T. Zhou, S. Bansal and R. Hider, *Eur. J. Med. Chem.*, **115**, 132 (2016).

[21] J. P. Easterly and H. E. Hennis; *U.S. Patent No. 3152148, 1964.*

3.2 Bioinspired Organic Acid Salts of Several Basic Compounds

1. Introduction

Alkaloids in *Papaver somniferum* and *Chelidonium majus* occur almost exclusively in the laticifer system, which has been shown to contain a discrete population of alkaloid-storing vacuoles [1-3]. Like other plant vacuoles, *P. somniferum* latex vacuoles contain significant amounts of organic acids (OAs) including meconic acid, malic acid, and phenolic acids, which lowers the internal pH compared to their cytoplasmatic environment. A proposed mechanism for alkaloid storage is protonation of the alkaloid by the acidic vacuolar compartment resulting in a salt formation, e.g. with OAs or mineral acids [4]. An early indication of the importance of OA salts was the isolation of morphine as meconate salt from opium by Sertürner in the early 19th century [5].

Following the blueprint of nature, it should be shown whether natural compounds and active pharmaceutical ingredients (APIs) (**Fig. 1**) are able to form soluble protic ionic liquids (PILs).

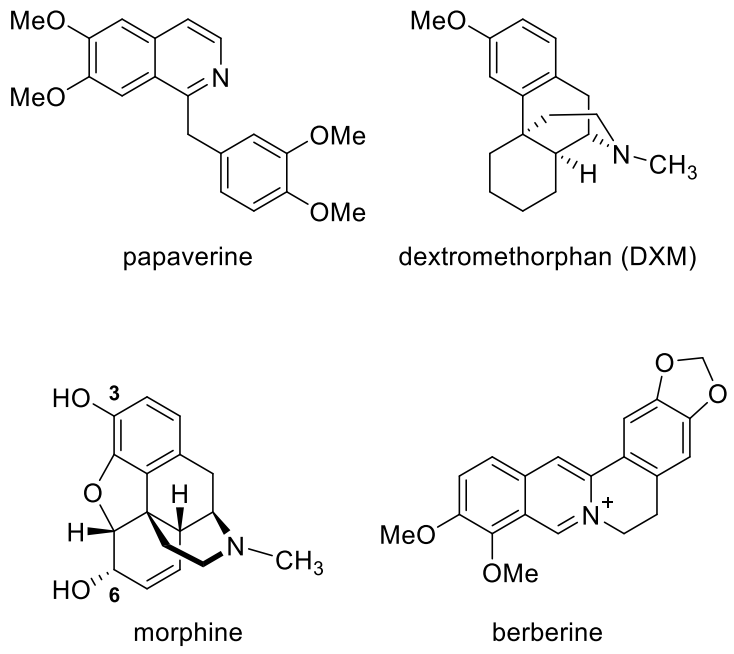

Figure 1: Natural compounds and APIs used in a salt screening program.

Therefore, a salt screening program was carried out with mostly large carboxylates of natural origin (**Fig. 2**), and the obtained salts were characterized both in their solid state and their supramolecular behavior.

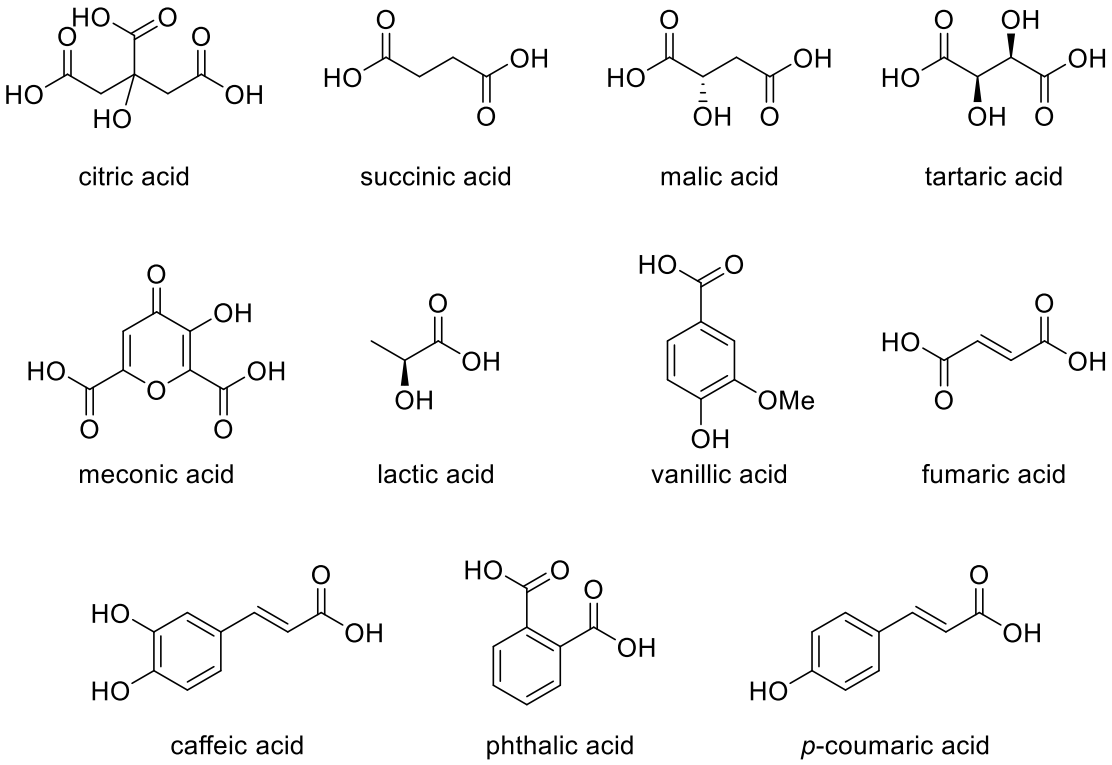

Figure 2: Naturally occurring OAs utilized in a salt screening program.

The pK_a rule of thumb can be a valuable tool for salt selection strategies because it is based on years of experience in salt formation in the pharmaceutical industry. It is assumed, that a pK_a difference (ΔpK_a) between Brønsted-acid and base of higher than 4, results in a completely ionized acid-base complex and thus salt formation [6, 7].

In order to enable complete ionization of the samples, the pK_a values of all bases and acids were first determined. The morphology of the obtained salts was characterized using XRPD and the thermal behavior was studied by means of DSC or simple melting point measurements. If possible, the dissolution rate and its molecular pattern in aqueous solution were examined using potentiometric and photometrical solubility.

2. Experimental Section

2.1 Materials

Papaverine hydrochloride, dextromethorphan hydrobromide monohydrate, and morphine hydrochloride trihydrate were purchased from Fagron GmbH & Co. KG (Barsbüttel, Germany). Berberine chloride was purchased from TCI Chemicals (Eschborn, Germany), Dowex 1X8 chloride strongly basic anion exchange resin, citric acid, succinic acid, malic acid, and tartaric acid from Sigma Aldrich (Schnelldorf, Germany) or TCI Chemicals (Eschborn, Germany). All acids were used without further purification. Meconic acid was synthesized following literature [8]. Ultrapure water was delivered by Merck Milli-Q system (Darmstadt, Germany).

2.2 Methods

2.2.1 Preparation of organic acid salts

PILs, protic OILs and low melting salts were prepared in analogy to previous reports [9]. Briefly, 100 mg papaverine, dextromethorphan, or morphine were suspended in 5 mL methanol. An equimolar amount of the counterion (organic acid) suspended in 5 mL methanol was added and mixed for 15 min at room temperature. Solvents were evaporated under ambient conditions for three days and the obtained salts then dried *in vacuo*.

For the berberine salts, an anion exchange with Dowex 1X8 chloride has been carried out first. 100 mg of the obtained berberine hydroxide was suspended in 5 mL water and an equimolar amount of counterion (organic acid) suspended in 5 mL water was added and mixed for 15 min at room temperature. Solvents were evaporated under reduced pressure and the obtained salts then dried *in vacuo*.

2.2.2 X-ray powder diffractometry

The obtained OA salts were transferred onto a silicon single crystal zero background specimen holder, covering an area with the diameter of approximately 5 mm. Powder diffractometric studies were performed using a Bruker Discover D8 powder diffractometer (Karlsruhe, Germany) and Cu Ka radiation (unsplit Ka_1+Ka_2 doublet,

mean wavelength l = 154.19 pm) at a power of 40 kV and 40 mA, a focussing Goebel mirror and a 2.5° axial Soller slit. The scattered X-ray beam went through a receiving slit (3.3°). Detection was done with a LynxEye-1D-Detector (Bruker AXS) using the full detector range of 192 channels. Measurements were done in reflection geometry in coupled two theta/theta mode with a step size of 0.025° in 2θ and 0.33 s measurement time per step in the range of 5 – 50°(2θ). Data processing was done with the software package DIFFRAC.Suite (V2 2.2.690, BrukerAXS, Karlsruhe, Germany). The diffraction data was subsequently converted into ASCII format and further handled with Origin (OriginLab, Massachusetts, USA).

2.2.3 Differential scanning calorimetry

Differential Scanning Calorimetry (DSC) was performed on a DSC 8000 instrument (Perkin Elmer, Waltham, MA, USA) using a scanning rate of 20 K/min. Sample size was 3 - 5 mg for all substances. For the PILs three heating and three cooling cycles were performed, the second and the third heating cycle were analyzed to allow for removal of residual water during the first heating cycle. Crucibles were weighted before and after measurements.

2.2.4 Melting point measurement

Melting points were measured with an MP70 Melting Point System from Mettler-Toledo GmbH (Gießen, Germany).

2.2.5 Potentiometric determination of the pK_a

The pK_a values of the compounds were determined on the Sirius T3 (Sirius Analytical, Forest Row, UK) in potentiometric mode and according to the manufacturer's instruction. In brief, 1 - 5 mg of API were dissolved in 1.5 mL of 0.15 M KCl solution at pH 2 (adjusted with 0.5 M hydrochloric acid). After complete dissolution, the solution was back-titrated by addition of 0.5 M potassium hydroxide until pH 12 was reached. In the case of the OAs 1 – 5 mg acid were dissolved in 1.5 mL of 0.15 M KCl solution at pH 12 (adjusted with 0.5 M potassium hydroxide solution). After complete

dissolution, the solution was back-titrated by addition of 0.5 M hydrochloric acid until pH 2 was reached.

2.2.6 Photometrical determination of dissolution rate

Dissolution rates were measured with a Sirius T3 instrument (Sirius Analytical, Forest Row, UK) as described in literature [10]. Tablets with defined surfaces were prepared by compression of 5 - 10 mg substance (salt or morphine free base) in a tablet disk (diameter of the tablet disk was 0.3 cm and is provided by the manufacturer of the machine) under a weight of 0.18 tonnes for 3 min with a manual hydraulic tablet press (Paul Weber, Stuttgart, Germany), as described before [10]. The release of drug substance from these tablet disc allows data collection with a standardized surface area (0.07 cm^2), which is required to fit the data for the calculation of the dissolution rate. The dissolution rates were determined photometrically at room temperature in phosphate buffered saline (PBS, 0.17 M) pH 6.8 at a stirring speed of 4800 rpm following the manufacturer's instructions. The linear part of the release profile was used for calculation of the dissolution rate (dissolved substance per time and surface area).

2.2.7 Potentiometrically and photometrically recorded titration experiments for determination of solubility

Intrinsic and apparent solubility were measured on a Sirius T3 instrument (Sirius Analytical, Forest Row, UK) by potentiometric titration (**Fig. 7**) as described before. In brief, typically 5 - 10 mg of DXM or morphine were dissolved in 1.5 mL of 0.15 M KCl solution at pH 2 (adjusted with 0.5 M hydrochloric acid). After complete dissolution, the solution was back-titrated by addition of 0.5 M potassium hydroxide aqueous solution (blue triangles, **Fig. 7**) until first precipitation occurred and as continuously monitored photometrically (λ = 500 nm). Subsequently, the pH was changed incrementally by repeated addition of minute amounts of 0.5 M hydrochloric acid (red triangles, **Fig. 7**) and 0.5 M potassium hydroxide aqueous solution (blue triangles, **Fig. 7**) throughout the experiment. After each titrant addition the delayed pH gradient of the API due to precipitation or dissolution was measured and used to extrapolate the equilibrium phase where the gradient is zero. Data from analysis with acidity errors larger than 1 mM were excluded.

3. Results and Discussion

First, the pK_a values of the compounds were determined by potentiometric titration measurements (**Table 1**).

Table 1: Obtained pK_a values of basic compounds and OAs.

Substance	*pK_a*
Papaverine	6.38
Dextromethorphan	9.71
Morphine	8.20
Citric acid	2.82, 4.24, 5.37
Succinic acid	3.81, 5.08
Malic acid	3.14, 4.45
Tartaric acid	3.33, 3.86
Meconic acid	1.39, 1.71
Lactic acid	3.91
Vanillic acid	4.17
Fumaric acid	2.76, 3.78
Caffeic acid	3.82
Phthalic acid	2.67, 4.74
p-Coumaric acid	4.34

Subsequently, various salt screening programs based on papaverine, dextromethorphan, morphine, and berberine as well as several natural OAs were carried out (**Fig. 3**).

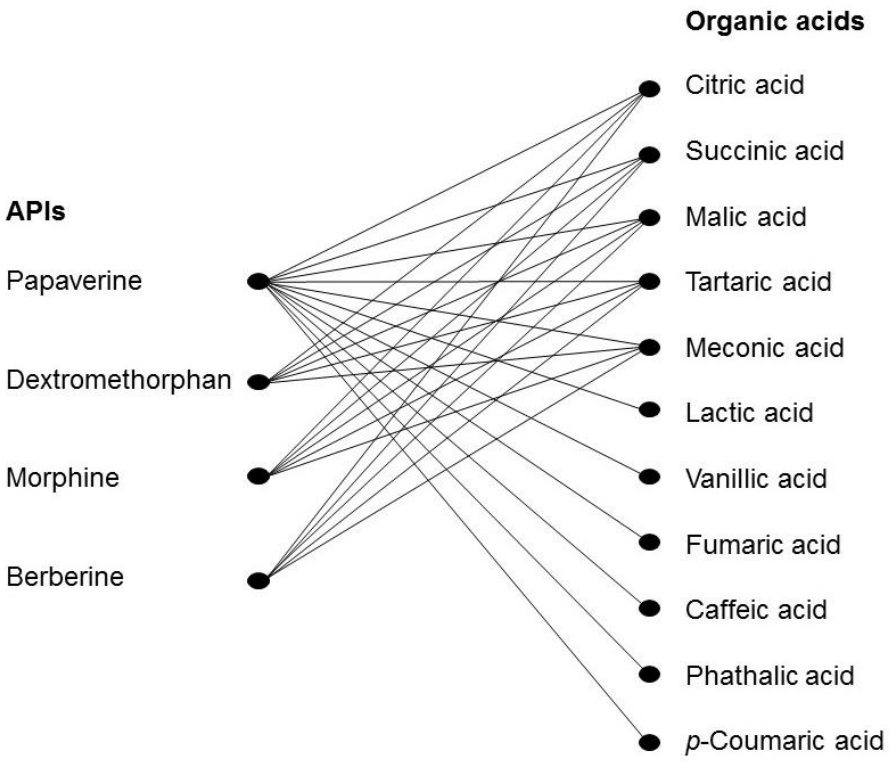

Figure 3: Combinations of APIs and different OAs.

Since the tri- and dicarboxylic acids citric acid, succinic acid, malic acid, and tartaric acid occur in such high concentrations in nature, all APIs have been combined with these acids. In the case of papaverine, an extended salt screening program with aromatic acids and other bulky acids was carried out to prevent the π-π interactions within the papaverine crystals.

3.1 Organic acid-papaverine salts

The morphology of the papaverine salts was assessed using XRPD measurements (**Fig. 4**). Most of them showed a defined diffractogram indicating a crystalline salt. As can be seen from the unstructured diffractograms, the papaverine caffeate and partly the coumarate were amorphous salts. This can be explained by the sterically demanding properties of both acids and the occurrence of π-π interactions within the API and OA, which may reduce the formation of a long-range order between the non-covalent heterodimers from papaverine and the counterions. The difference in the morphology of the caffeate and the coumarate can be explained by the different pK_a

values of the two acids (pK_a caffeic acid: 3.82, pK_a *p*-coumaric acid: 4.34) and by the additional hydroxyl group of the caffeic acid, which increases the interaction between the heterodimers consisting of papaverine and caffeic acid. All other salts were crystalline, which can be attributed to the sterically non-demanding behavior of the OAs and to insufficient pK_a differences (Δ pK_a < 4) between papaverine and the OAs.

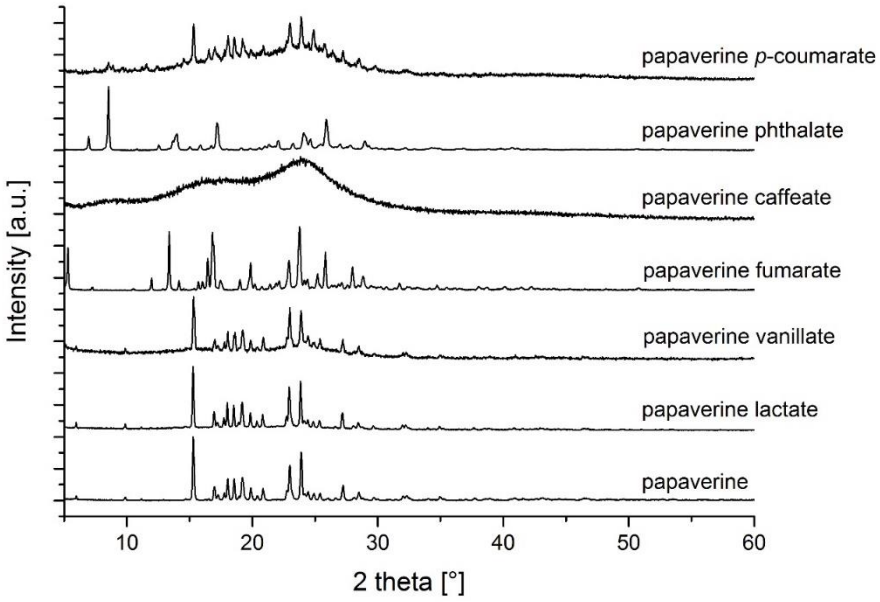

Figure 4: X-ray diffractograms of the papaverine derived OA salts.

The thermal properties of the samples were measured by DSC and melting point measurements (**Table 2**). The amorphous caffeate was characterized by a glass transition temperature (T_g) at 110 °C, whereas the crystalline samples showed a specific melting point between 116 and 180 °C with the vanillate having the highest melting point.

Table 2: MPs and glass transition temperatures of papaverine free base and its salts.

Samples	MP [°C]	T_g [°C]
papaverine	149	
papaverine lactate	143	
papaverine vanillate	180	
papaverine fumarate	179	
papaverine caffeate		110
papaverine phthalate	116	
papaverine coumarate	122	

3.2 Organic acid-dextromethorphan salts

The solid-state forms of the dextromethorphan (DXM) samples were analyzed using XRPD (**Fig. 5**). The unstructured diffractograms of DXM succinate, DXM malate and DXM tartrate are indicative of an amorphous salt. This can be explained by the flexibility of the aliphatic CA counterions, which leads to a sterically demanding and consequently more space-consuming behavior and reduces the formation of a long-range order between the non-covalent heterodimers of DXM and OA (**Fig. 6**) [11].

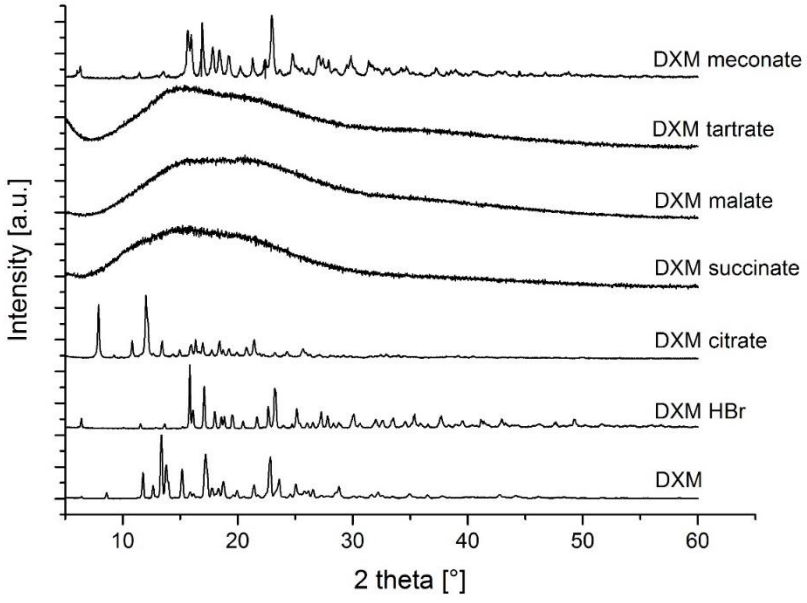

Figure 5: XRPD diffractograms of the DXM free base compared to bromide, citrate, succinate, malate, tartrate and meconate salts.

In contrast, the DXM free base homodimers and heterodimers of DXM bromide, DXM citrate, and DXM meconate were arranged with a certain long-range molecular order due to the reduced flexibility of the counterions (**Fig. 6**) [12, 13].

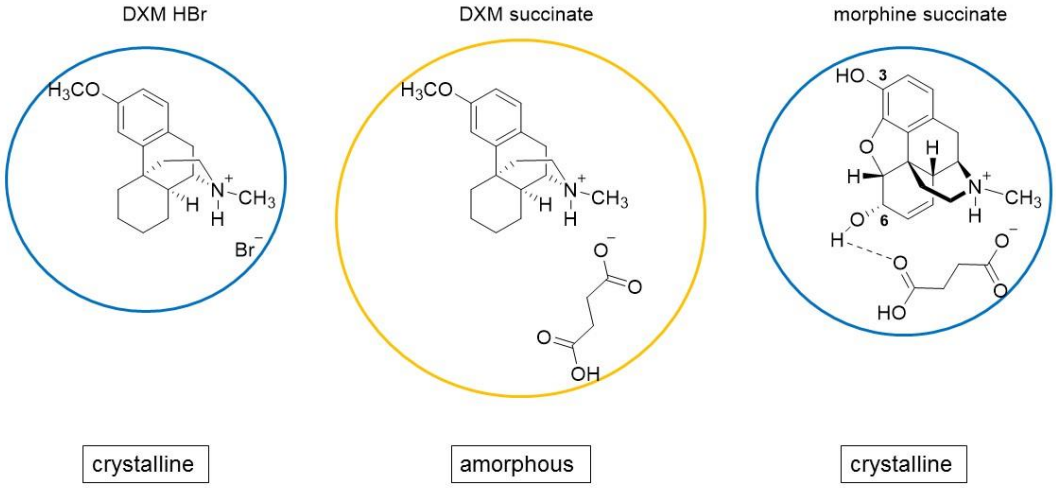

Figure 6: Heterodimers of DXM and morphine salts indicating the sterically demanding behavior of the DXM carboxylate.

The thermal properties of the amorphous samples are as expected and characterized by a T_g ranging between 18 and 63 °C with the succinate having the lowest T_g and the crystalline samples showed a specific melting point between 57 and 116 °C with the meconate having the highest melting point (**Table 3**).

Table 3: MPs and glass transition temperatures of the DXM samples.

Samples	MP [°C]	T_g [°C]
DXM	109	
DXM hydrobromide monohydrate	114	
DXM citrate	57	
DXM succinate		18
DXM malate		47
DXM tartrate		63
DXM meconate	116	

The solubility profiles of the dextromethorphan samples were obtained by potentiometric titration and were determined using an accelerated method of measuring the duration of supersaturation (**Fig. 7**). In general, increasing the supersaturation period with increased apparent solubility is the goal for drugs suffering from poor water solubility.

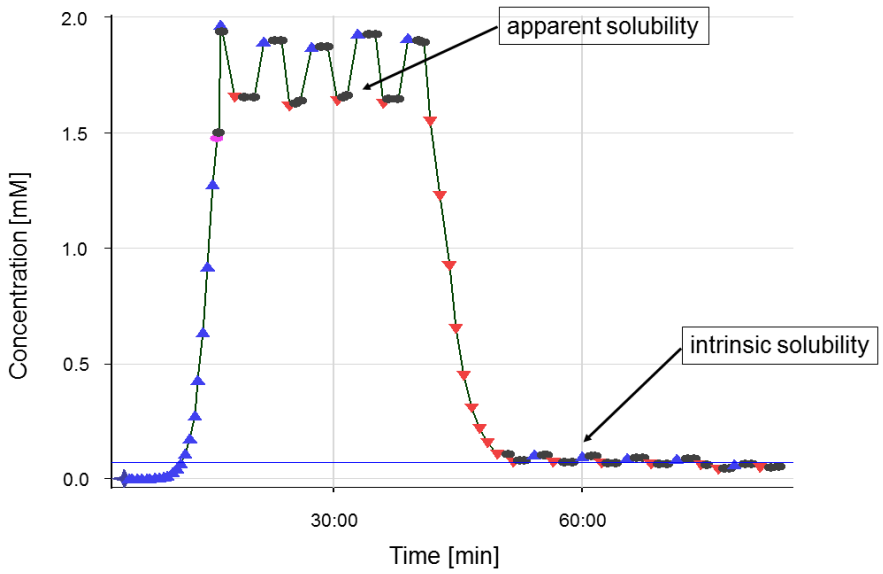

Figure 7: Exemplary representation of a potentiometric solubility measurement.

The peak concentration during the supersaturation phase (apparent solubility) was of a comparable order of magnitude for all samples (**Fig. 8a**), which shows that the counterion has no influence on the improvement in the solubility profile of DXM. For both crystalline and amorphous groups, the intrinsic solubility (equilibrium solubility) was generally one order of magnitude lower than the apparent solubility (**Fig. 8b**).

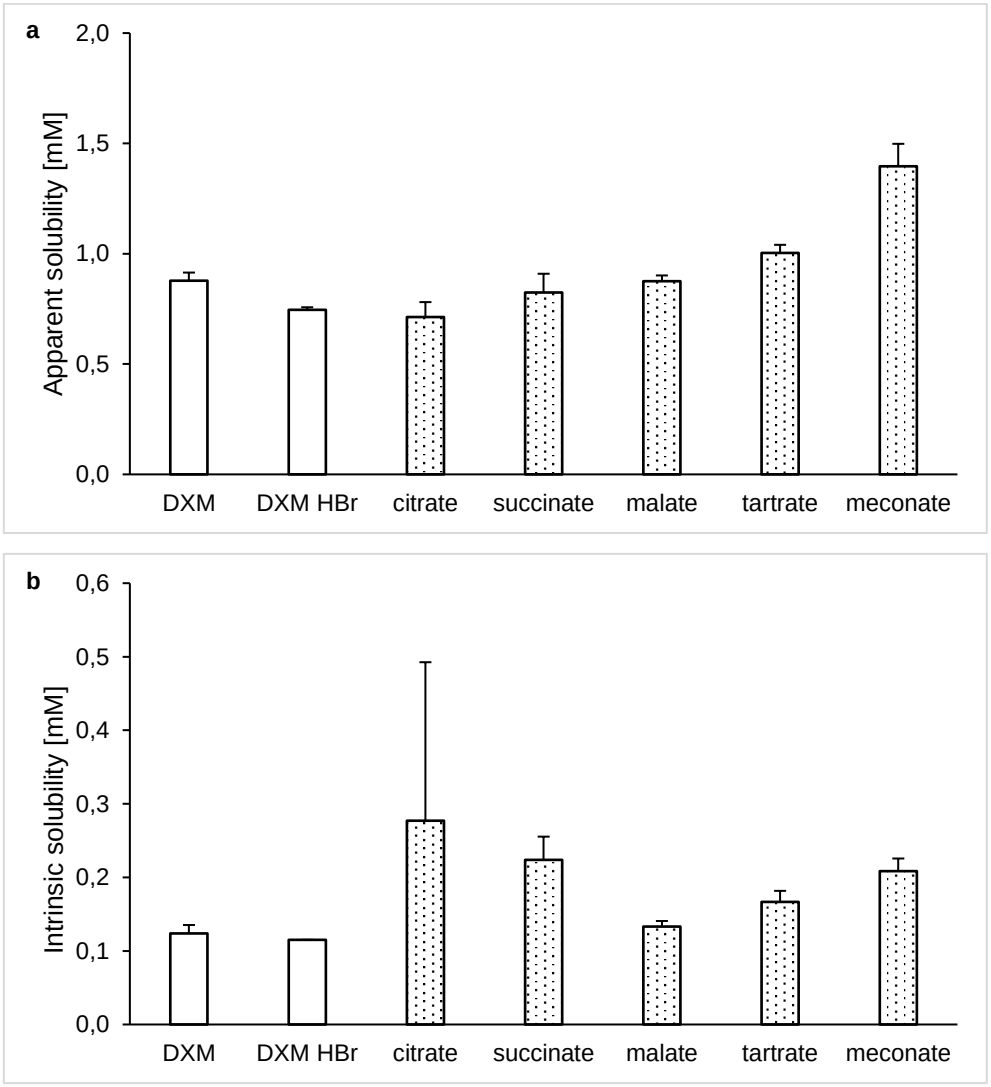

Figure 8: (a) Apparent solubility [mM] and (b) intrinsic solubility [mM] of the salts, free base and HBr salt.

3.3 Organic acid-morphine salts

The X-ray diffractograms indicate that the morphine free base and all morphine salts were crystalline, which is due to the morphine constitution (**Fig**. **9**). In addition to the ionic interaction, in contrast to DXM, hydrogen bonding can occur between the morphine hydroxy group at position 6 and the carboxy or hydroxy group of the counterion, which reduces the flexibility and consequently the steric behavior of the counterions (**Fig. 6**). This reduced flexibility of the counterions enables a certain long-range molecular order within the crystals [12, 13].

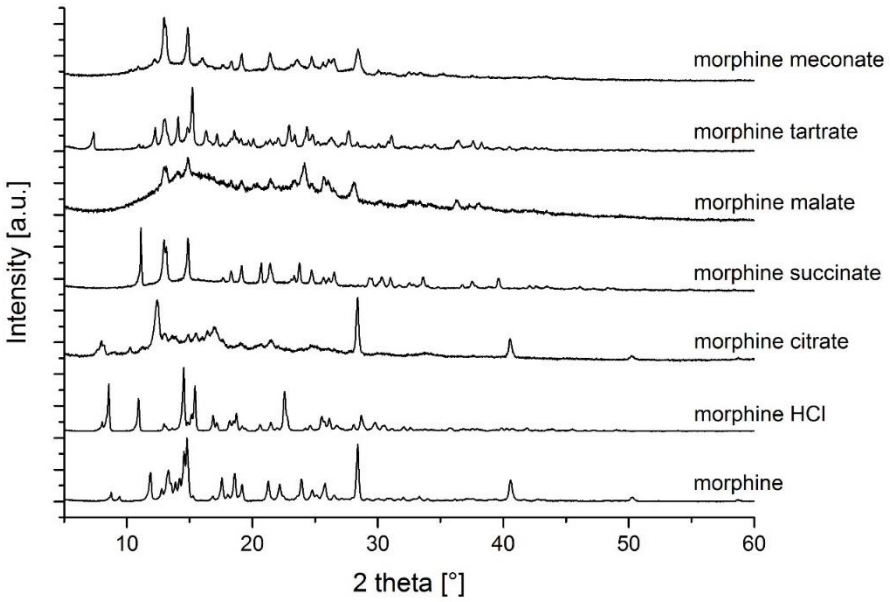

Figure 9: XRPD diffractograms of the morphine free base compared to chloride, citrate, succinate, malate, tartrate and meconate salts.

The melting points of the morphine salts are between 138 and 195 °C, with the malate having the lowest melting point measured. On the other hand, the morphine free base and the morphine hydrochloride trihydrate have melting points of greater than 200 °C, which indicates stronger crystal lattice forces in these samples (**Table 4**). The decrease of the melting point can be explained by the sterically demanding nature of the carboxylate counterions compared to the small chloride counterion, which leads to a weaker crystal lattice in the solid and consequently to lower melting temperatures.

Table 4: MPs of the morphine samples

Samples	MP [°C]
morphine	255
morphine HCl trihydrate	260
morphine citrate	181
morphine succinate	161
morphine malate	138
morphine tartrate	156
morphine meconate	195

The dissolution rate of the drug substance was measured in PBS buffer at pH 6.8. The rates of the citrate, succinate, and malate were 3 - 5 times higher than the dissolution rate of the morphine free base, the chloride, and the tartrate. Instead, the dissolution rate of the meconate could not be determined because the salt pellet did not dissolve (**Fig. 10**). The peak concentration determined by potentiometric titration during the supersaturation phase (apparent solubility) was 3 - 4 times higher for the chloride and the citrate than for the other samples (**Fig. 11a**). In addition, the intrinsic solubility (equilibrium solubility) for the citrate salt was 2 - 3-fold higher than for the other samples and generally one order of magnitude lower than the apparent solubility (**Fig. 11b**).

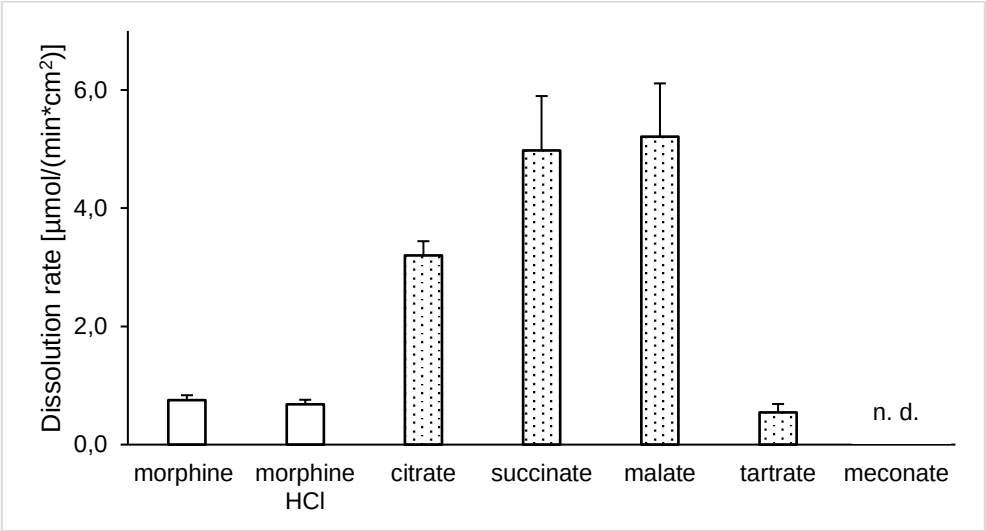

Figure 10: Dissolution rate of the morphine OA salts and morphine free base.

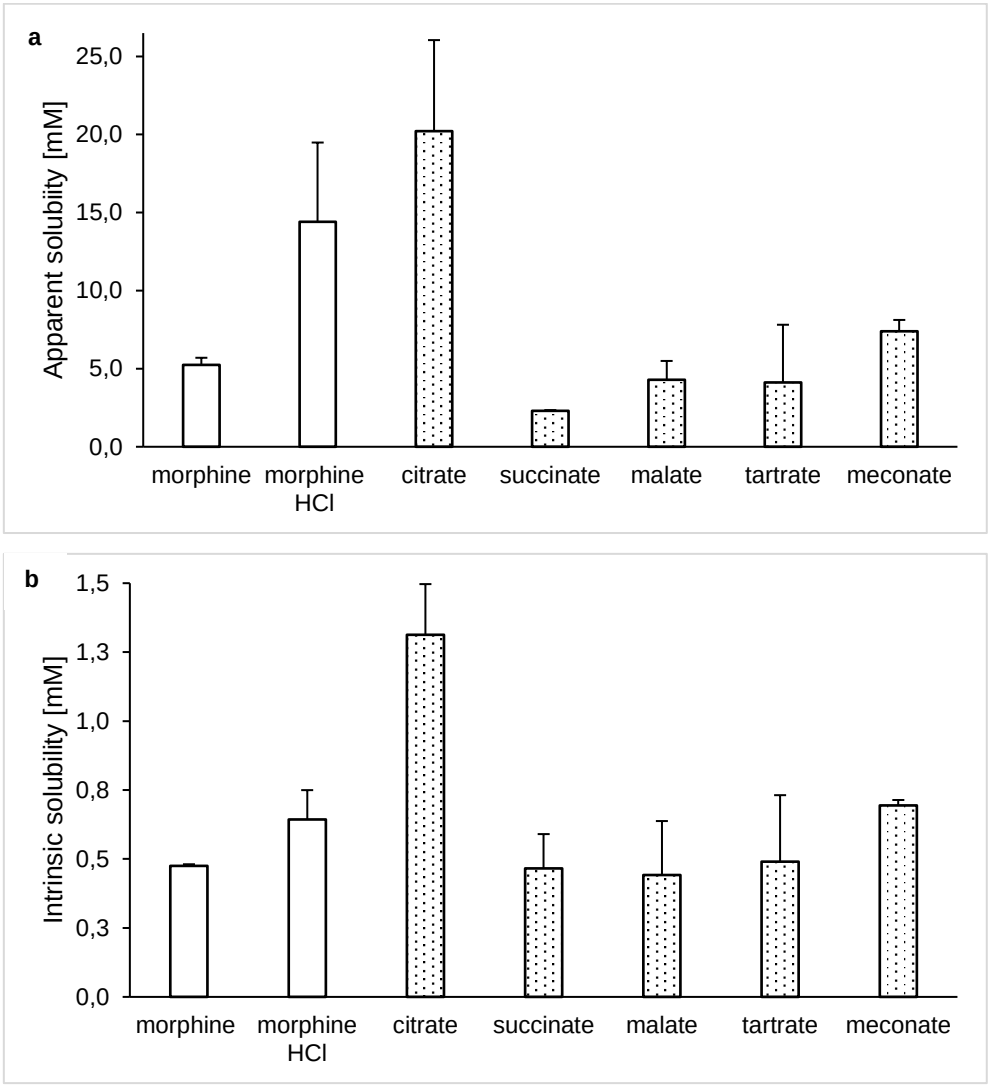

Figure 11: (a) Apparent solubility [mM] and (b) intrinsic solubility [mM] of the salts, free base and HCl salt.

3.4 Organic acid-berberine salts

As can be seen from the diffractograms, all berberine salts were crystalline solids (**Fig. 12**). Due to the rigid constitution of berberine and many possible π-π interactions between the berberine molecules, the counterions could not prevent such interactions, which led to crystals with a certain long-range molecular order [12, 13].

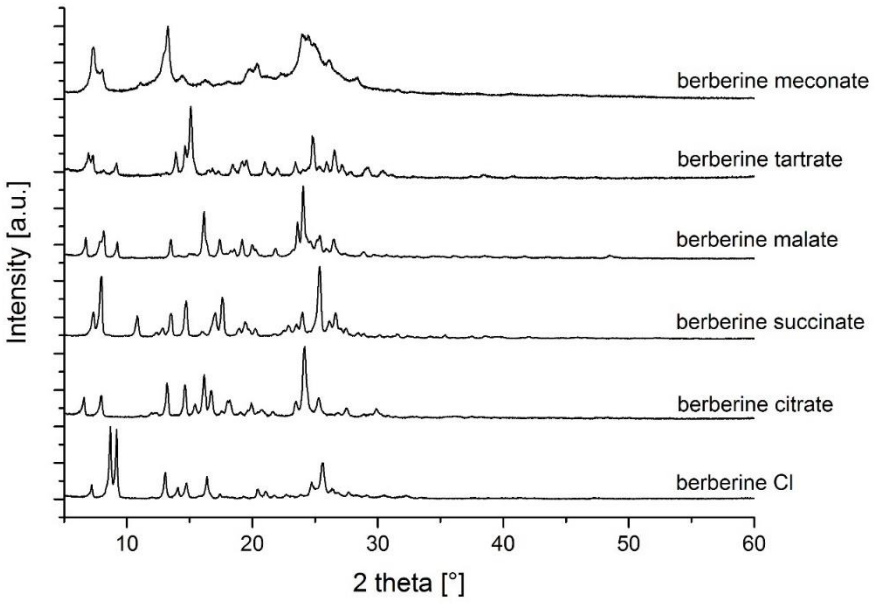

Figure 12: XRPD diffractograms of the berberine chloride, citrate, succinate, malate, tartrate and meconate salts.

In accordance with the X-ray diffractograms, the samples showed specific melting points in a range between 120 and 150 °C with the tartrate having the highest (**Table 5**).

Table 5: MPs of the berberine salts.

Samples	MP [°C]
berberine chloride	145
berberine citrate	140
berberine succinate	138
berberine malate	120
berberine tartrate	150
berberine meconate	140

Because of the permanent positive charge of berberine resulting in a sufficient water solubility, a determination of the peak concentration during the supersaturation phase (apparent solubility), by potentiometric titration was not possible.

4. Conclusion

Naturally occurring OAs are appropriate counterions for basic compounds and can reduce the crystal lattice forces within the salts, resulting in reduced melting point of the crystals or a T_g for amorphous salts. In the case of dextromethorphan, some aliphatic OAs facilitate the formation of amorphous protic ionic liquids (PILs), salts with melting points < 100 °C, which can be explained by the sterically demanding and space consuming behavior of the counterions, preventing a certain long-range molecular order within the solids. In the case of morphine, the OAs reduce the crystal lattice energy within the crystalline salts compared to small-size halides, resulting in decreased melting points of the organic salts. The comparison of the results of the constitutionally similar bases dextromethorphan and morphine indicates that the interaction potential between the non-covalent heterodimers consisting of API and counterion is also relevant for the crystal lattice formation. For example, the additional hydrogen bond between morphine and counterion leads to a stronger interaction and consequently to a reduced space-consuming behavior of the counterion, resulting in a crystalline salt. In addition, in the case of papaverine salt screening, the aromatic OAs caffeic acid and *p*-coumaric acid prevent strong interactions within the API molecules through π-π interactions, which leads to reduced lattice forces in the salt. Taking everything into consideration, the ability of OAs to act as counterions for basic secondary metabolites and to reduce the lattice forces in the obtained salts may explain their unexpectedly high concentration in plant vacuoles. Since papaverine combines the interesting properties, aromaticity and basic character, compared to the other APIs used here, the papaverine salt screening was extended to the tri- and dicarboxylic acids citric acid, succinic acid, malic acid, tartaric acid and meconic acid.

Acknowledgements

Dr. Johannes Wiest is gratefully acknowledged for his theoretical support and advise during the salt screening project.

References

[1] Pham, T. T.; Roberts, M. F. *Phytochem. Analysis* **1991,** *2*, 68-73.

[2] Fairbairn, J. W.; Hakim, F.; Elkheir, Y. *Phytochemistry* **1974,** *13*, 1133-1139.

[3] Matile, P.; Jans, B.; Rickenbacher, R. *Biochemie und Physiologie der Pflanzen* **1970,** *161*, 447-458.

[4] Roberts, M. F.; Homeyer, B. C.; Pham, T. D. T. *Z. Naturforsch.* **1991**, 377-388.

[5] Hamilton, G. R.; Baskett, T. F. *Can J Anaesth* **2000,** *47*, 367-74.

[6] Stahl, P. H.; Wermuth, C. G. *Weinheim, Wiley-VCH* **2011**.

[7] Cruz-Cabeza, A. J. *CrystEngComm* **2012,** *14*, 6362.

[8] Güntzel, P.; Forster, L.; Schollmayer, C.; Holzgrabe, U. *Org. Prep. Proced. Int.* **2019,** *50*, 512-516.

[9] Bica, K.; Rijksen, C.; Nieuwenhuyzen, M.; Rogers, R. D. *Phys. Chem. Chem. Phys.* **2010,** *12*, (8), 2011-2017.

[10] Gravestock, T.; Box, K.; Comer, J.; Frake, E.; Judge, S.; Ruiz, R. *Anal. Methods* **2011,** *3*, (3), 560.

[11] Agharkar, S.; Lindenbaum, S.; Higuchi, T. *J. Pharm. Sci.* **1976,** *65*, 747-749.

[12] Hidber, P. C; Graule, T. J.; Gauckler, L. J. *J. Am. Ceram. Soc.* **1996,** *79*, 1857-1867.

[13] Dengale, S. J.; Grohganz, H.; Rades, T.; Lobmann, K. *Adv. Drug. Deliv. Rev.* **2016,** *100*, 116-25.

3.3 Bioinspired Ion Pairs Transforming Papaverine into a Protic Ionic Liquid and Salts

Paul Güntzel, Klaus Schilling, Simon Hanio, Jonas Schlauersbach, Curd Schollmayer, Lorenz Meinel, and Ulrike Holzgrabe*

Institute of Pharmacy and Food Chemistry, Am Hubland, University of Würzburg, DE-97074 Würzburg, Germany

Reprinted with permission from ACS Omega, 2020, 5, 30, 19202-19209.

Abstract: Microbial, mammalian and plant cells produce and contain SMs, which typically are soluble in water to prevent cell damage by crystallization. The formation of ion pairs, e.g. with CAs or mineral acids, is a natural blueprint to keep basic metabolites in solution. Here, we aim at showing whether the mostly large carboxylates form soluble PILs with the basic natural product papaverine resulting in enhanced aqueous solubility. The obtained PILs were characterized by ^{1}H-^{15}N HMBC NMR and in solid state using XRPD, DSC, and dissolution measurements. Furthermore, their supramolecular pattern in aqueous solution was studied by means of potentiometric and photometrical solubility, NMR aggregation assay, dynamic light scattering, zeta potential and viscosity measurements. Thereby, we identified the naturally occurring CAs citric acid, malic acid and tartaric acid being appropriate counterions for papaverine and facilitate the formation of PILs with their beneficial characteristics, like improved dissolution rate and enhanced apparent solubility.

Keywords: protic ionic liquids; solid state; CAs; peptizers; supramolecular behaviour; suspension

Introduction

Plant vacuoles are storage compartments for SMs such as alkaloids and flavonoids, as well as for small molecules like CAs, amino acids, and sugars. These organic acids (OAs) may have higher concentrations in the vacuole than in the cytosol, whereas for most amino acids, the vacuolar concentrations were similar to the cytosolic concentrations [1, 2]. Some carboxylates such as citrate and malate enter the vacuole by specific transporter proteins; they represent the major CAs in plants and play a major role in cellular processes and are involved in several metabolic pathways as intermediates of energy metabolism. Additionally, they may also serve as counterions for cationic alkaloids to improve their water solubility [3, 4]. An early indicator of the importance of OA salts in nature was given by Sertürner in the 19th century. He isolated morphine as its meconate salt from opium, the dried milky sap from *Papaver somniferum* [5, 6].

Salt formation of poorly water-soluble organic bases with acids may increase apparent solubility in an aqueous environment compared to the free bases. The concept of salt formation is one among other pharmaceutical strategies, like cocrystal formation, complexation, and particle size reduction, to deal with the problem of poor water solubility and a low oral bioavailability of APIs [7]. However, these salt formulations may suffer from poor solution stability within supersaturated states leading to API precipitation hence improper adsorption from the gastrointestinal tract. Therefore, a constant high counterion-to-API ratio is necessary to prevent precipitation of the API which leads to an increased duration of supersaturation and consequently, to a more stable solution. A strategy combining salt formation and a reduction of the interaction between molecules hence decrease of the melting point, which may result in improved dissolution rates, is the formulation of an ionic liquid (IL) [8, 9]. ILs are defined as organic salts with melting points below 100 °C, with attractive properties, including low volatility, low flammability, polarity, and high viscosity [9-12]. They can be subdivided in PILs and AILs. Many AILs have been prepared and characterized to date; most of them were based on halogenated counter-anions such as tetrafluoroborate (BF_4^-), hexafluorophosphate (PF_6^-), and derivatives thereof. Because of toxicological and ecological issues, these halide-containing anions are not suitable for therapeutic applications. An alternative approach to overcome these drawbacks is the development of bio-inspired ionic liquids (Bio-ILs), which are solely composed of

naturally occurring molecules - components having well characterized biodegradable and toxicological properties [13]. Larger counterions reduce lattice forces within crystals which is why bulky natural CAs might be particularly valuable for PILs formation of basic, poorly water-soluble APIs with the ultimate goal of improve apparent solubility and/or dissolution rates [14-16]. PILs are prepared in a simple neutralization reaction of certain Brønsted acids and Brønsted bases in equimolar ratio [17, 18]. A subset of PILs are the protic oligomeric ILs (OILs), which are the result of a reaction of several equivalents of a Brønsted acid with one equivalent of a Brønsted base to form H-bonded acid-oligomer based ILs [19, 20].

The effect of OAs or other dispersants with low molecular weight is mainly based on the charging of the surface of the powder particles, thereby increasing the repulsive double-layer forces. In the Derjaguin-Landau-Verwey-Overbeek (DLVO) theory, the suspension's properties are determined by its attractive and repulsive forces. Attractive van der Waals forces can be counteracted by repulsive forces resulting from either overlapping of the electrical double layers ("electrostatic" stabilization) and/or layering of materials adsorbed on the surface ("steric" stabilization) [21, 22].

Considering numerous beneficial properties of liquid salts, including improved water solubility and dissolution rate, ILs have drawn the attention of pharmaceutical research as potential drug formulations [9, 23, 24]. As a model system we tried to prepare PILs from papaverine using different types of natural OAs, namely citric acid, malic acid and tartaric acid (α-hydroxycarboxylic acids, AHAs), succinic acid (carboxylic acid) and meconic acid (β-hydroxycarboxylic acid, BHA). The PILs were compared with papaverine's free base. Papaverine is marketed as chloride salt and used for the treatment of visceral spasms. In order to understand the pattern of the various PILs, they were characterized by means of ^{1}H-^{15}N HMBC NMR, X-ray powder diffraction (XRPD), differential scanning calorimetry (DSC) and photometrical dissolution rate measurements. The supramolecular behavior of the papaverine citrate solutions was characterized by means of photometrical and potentiometric solubility measurements, as well as the solubility after 0.5 h and subsequent HPLC measurements, NMR aggregation assay, viscosity measurements, dynamic light scattering (DLS) and zeta potential measurements.

Results and Discussion

Structure and physical characteristics

The naturally occurring molecule papaverine, a basic SM, and a collection of natural OAs were combined to improve pharmaceutical parameters of the basic alkaloid by the bioinspired strategy of salt formation (**Fig. 1**). As the first step, we prepared various combinations of papaverine and OAs in different ratios (**Table 1**).

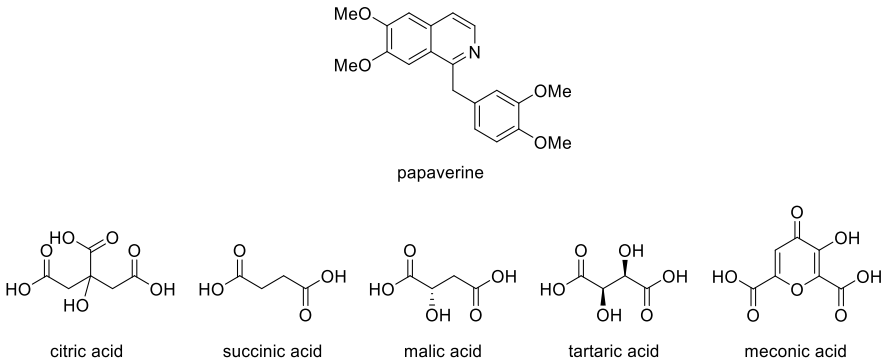

Figure 1: Used naturally occurring molecules.

Table 1**: **List of prepared natural PILs, protic OILs and crystalline salts.

Combination	Molar Ratio	Abbreviation
papaverine:citric acid	1:1, 1:2, 1:3	PA 1:1, PA 1:2, PA 1:3
papaverine:succinic acid	1:1	
papaverine:malic acid	1:1, 1:2, 1:3	
papaverine:tartaric acid	1:1, 1:2, 1:3	
papaverine:meconic acid	1:1	

The obtained salts were characterized in their solid state (XRPD, DSC, dissolution rate) as well as in solution by ^{1}H-^{15}N HMBC NMR measurements as well as ^{1}H NMR, DLS, zeta potential, solubility, and viscosity to study the supramolecular behavior.

2D NMR measurements and solid-state characterization

The ionic nature of the samples was analyzed by ^{1}H-^{15}N HMBC NMR measurements. In all cases (molar ratio 1:1, 1:2, 1:3, papaverine:OA (i.e. citric acid, malic acid and tartaric acid)) the nitrogen signal of the papaverine was substantially shifted upon protonation; the free base (black) resonated at -79.5 ppm, whereas the nitrogen signal of the hydrochloride (red) at -182.5 ppm indicating the formation of a salt (**Fig. 2a**). The ^{15}N signals of the citrate were even more shifted, the nitrogen signal for the 1:1 (black) and 1:3 (red) papaverine citrate occurs at -190 ppm and -192.5 ppm, respectively, indicating a full protonation of the papaverine nitrogen in these mixtures (**Fig. 2b**).

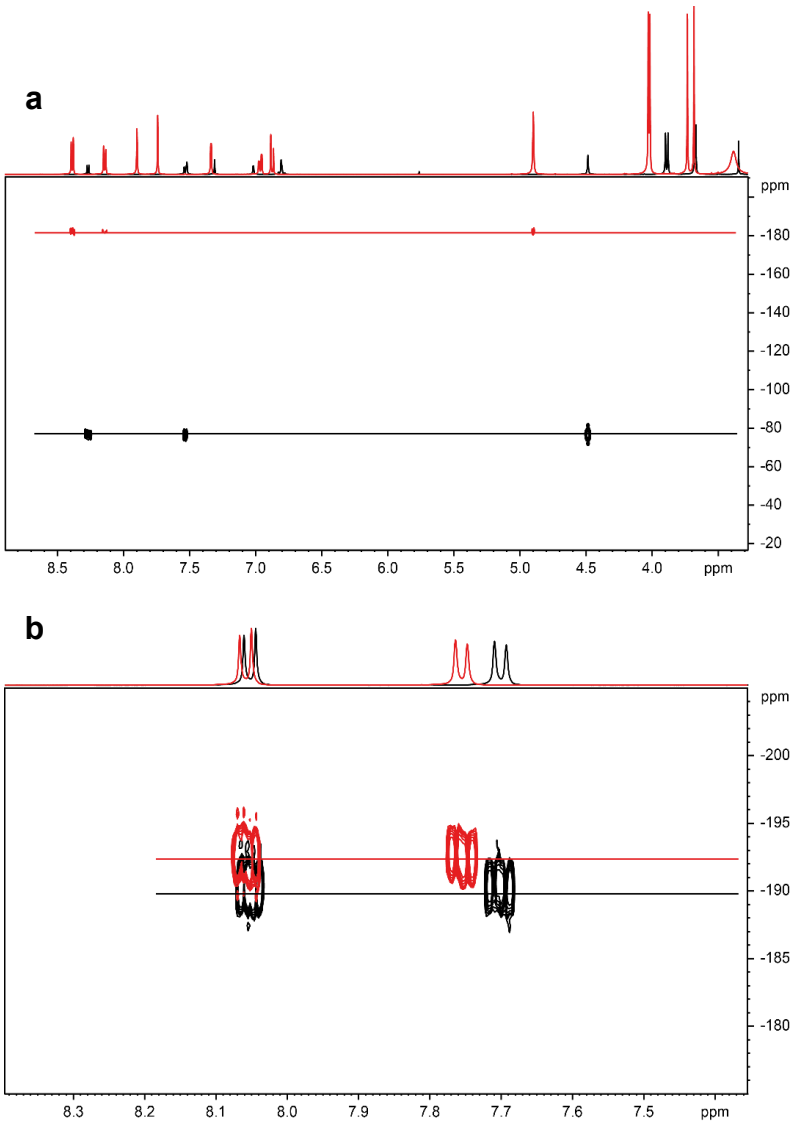

Figure 2: (a) ^{1}H-^{15}N NMR spectra of papaverine free base (black) at -79.5 ppm and papaverine HCl (red) at -182.5 ppm (DMSO-d_6, 5 Hz) and of (b) papaverine:citric acid (molar ratio 1:1, black) at -190 ppm and papaverine:citric acid (molar ratio 1:3, red) at -192.5 ppm (D_2O/KCl, 5 Hz).

The solid-state forms of the samples were analyzed by means of XRPD (**Fig. 3**). As can be seen from the unstructured diffractograms, papaverine citrate, papaverine malate and papaverine tartrate (molar ratio 1:1 (PILs), 1:2, 1:3 (protic OILs)) were amorphous salts with decreased crystal lattice energy [14]. This can be explained by intramolecular hydrogen bonding between the hydroxylic group and the free CA group present in all AHAs, which diminishes intermolecular interactions between the heterodimers, consisting of papaverine and AHAs, and thus prevents a long-range molecular order within the solids. In contrast, the papaverine free base homodimers as well as the heterodimers of papaverine hydrochloride, papaverine succinate and papaverine meconate, respectively, were arranged with a certain long-range molecular order, because no intramolecular hydrogen bonding was possible within the counterions [25, 26].

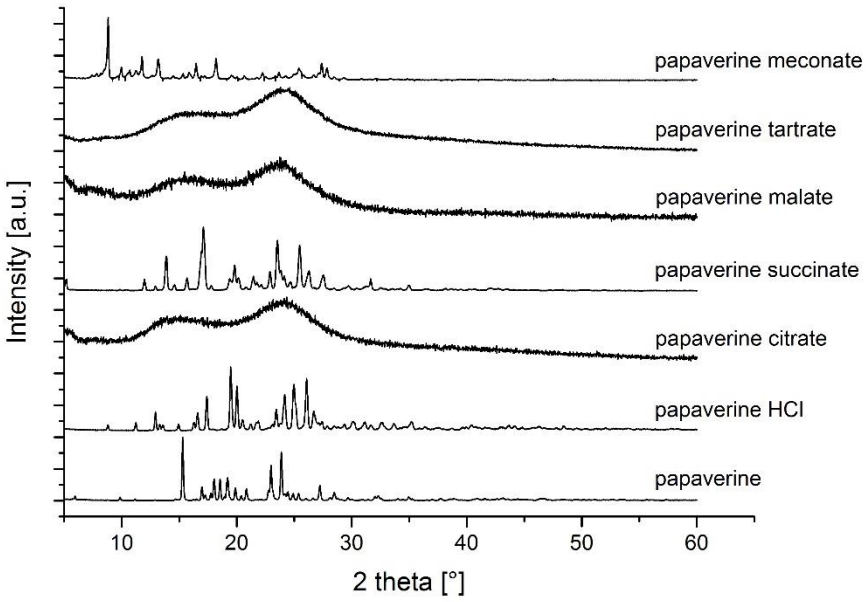

Figure 3: XRPD diffractograms of the papaverine free base compared to the chloride, citrate, succinate, malate, tartrate and meconate salts (molar ratio 1:1).

The thermal properties of the samples were measured by DSC (**Table 2**). As expected, all amorphous samples being the citrate, malate and tartrate were characterized by a glass transition temperature (T_g) ranging between 30 and 50 °C, whereas the

crystalline samples showed a specific melting point between 88 and 220 °C with the hydrochloride having by far the highest melting point.

Table 2**: **DSC measurement results of the samples (molar ratio 1:1).

Samples	MP [°C]	T_g [°C]
papaverine	149	
papaverine hydrochloride	220	
papaverine citrate		30
papaverine succinate	134	
papaverine malate		50
papaverine tartrate		40
papaverine meconate	88	

Dissolution rate, solubility, and supramolecular aggregates

The drug substance dissolution rate was measured in PBS buffer pH 6.8. The dissolution rate of the amorphous salts was more than 3-fold higher than the dissolution rate of crystalline salts (**Fig. 4**). The peak concentration during the supersaturation phase (apparent solubility), determined by potentiometric titration in potassium chloride solution, was higher for all amorphous samples (independent of molar ratio). For both groups, the intrinsic solubility (equilibrium solubility) was generally one order of magnitude lower than the apparent solubility (**Fig. 5**). Interestingly, both water solubilities, apparent and intrinsic, of papaverine increased with an increasing amount of counterion, which is in accordance with the observation for the drug substance selurampanel (BGG) by A. Balk [8]. This indicated an intermolecular interaction and stabilization between papaverine and carboxylates, like citrate, malate or tartrate, which were acting as peptizers.

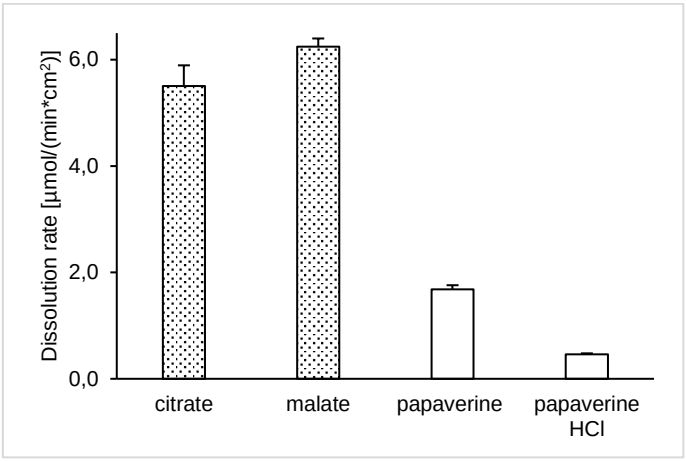

Figure 4: Dissolution rate of the PILs (molar ratio 1:1). Filled bars are amorphous salts, white bars are crystalline.

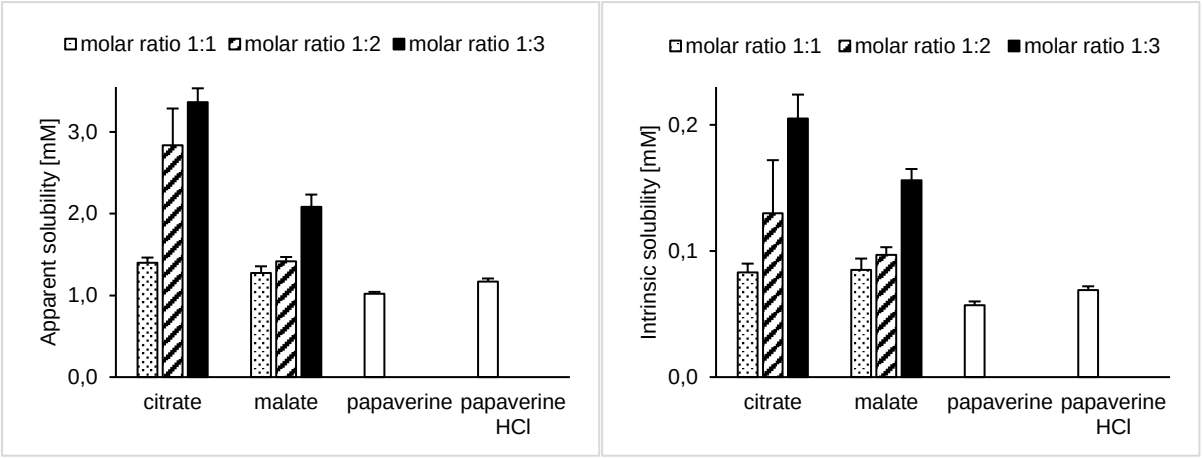

Figure 5: (left) Apparent solubility [mM] and (right) intrinsic solubility [mM] of PILs (different molar ratios), free base and HCl salt.

The supramolecular association of papaverine and the counterion in solution was analyzed by a ^{1}H NMR based aggregation assay (**Fig. 6**) [27, 28]. As reference spectra for the lowest aggregation concentration of papaverine a mixture of papaverine/citric acid (20 mM) and Tween 80 and a solution of papaverine HCl and Tween 80 were prepared. Upon increasing the starting concentration 20 mM to 80 mM of papaverine/citric acid, the signals of the very slightly aggregated papaverine (20 mM) were shifted to the upfield (e.g. 8.2 ppm to 8.15 ppm or 7.93 ppm to 7.75 ppm). The concentration-dependent changes in chemical shifts (Δ ppm) can be explained by local environmental changes in the magnetic field around the molecule because of the accumulation of aromatic systems with their shielding effects. Another indicator of aggregates is the change in the number of signals, as can be seen at 6.8 - 6.9 ppm (20 mM) compared with 6.7 ppm (80 mM). The shape of the signal (i.e. sharp or broad)

is related to the size and tumbling rate of a supramolecular species. A multimeric species would be expected to have a slower tumbling rate and faster relaxation time and thus a broader peak shape. The broadening of a resonance at higher concentrations is also an evidence for the existence of aggregates. In the ^{1}H NMR spectrum of the papaverine HCl salt, the aromatic signals of papaverine were also shifted to the upfield, indicating aggregation. In contrast to the citrate salt, maximal aggregation is obtained at 20 mM for the hydrochloric acid salt. Moreover, in the 40 mM concentration precipitation and subsequent sedimentation occurred, which shows the better water solubility of the citrate salt.

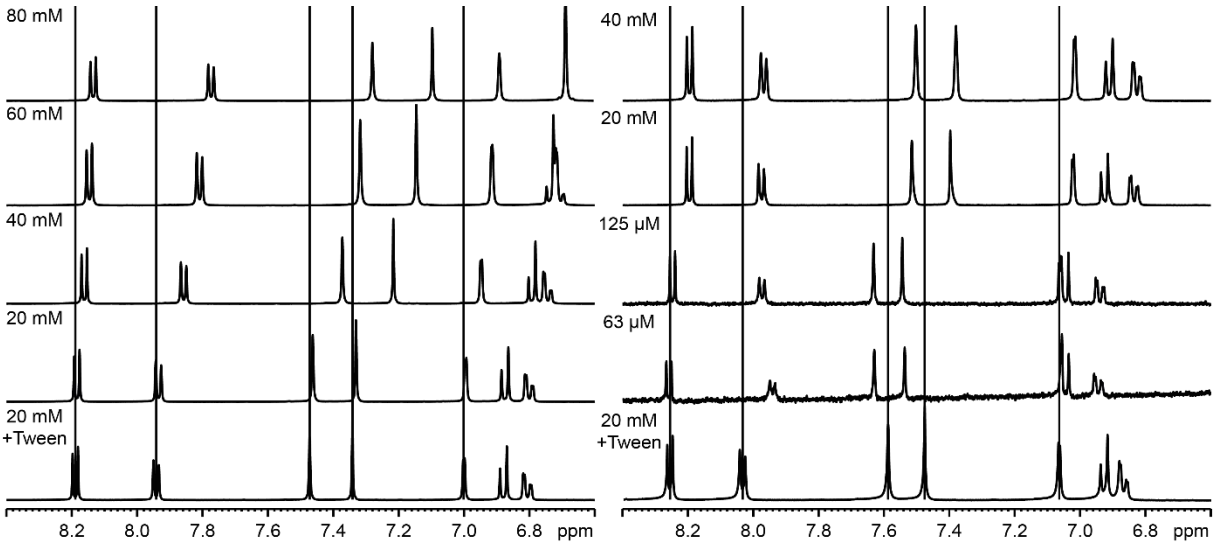

***Figure 6**: (left) ^{1}H NMR of papaverine citrate (molar ratio 1:1) and (right) of the HCl salt in various concentrations.*

The particle size and the polydispersity index (PDI) of supramolecular aggregates of papaverine in water were checked by means of dynamic light scattering (DLS) (**Tab. 3**). The low PDI < 0.1 indicates monodisperse systems, PDI = 0.1 - 0.2 refers a small distribution and PDI > 0.2 polydisperse systems. It was not possible to measure the 80 mM HCl salt solution, because a sedimentation of non-dissolved papaverine was observed.

Citric acid performed as peptizer and stabilized higher concentrations of papaverine (80 mM) with only a small distribution of particle size (PDI about 0.20). Chloride on the other hand was not able to stabilize aqueous papaverine solutions in higher

concentrations (80 mM) and led to polydisperse solutions (PDI = 0.56) at lower concentrations (20 mM).

Table 3: Dynamic light scattering of papaverine:citric acid (molar ratio 1:1, 1:2, 1:3) compared with papaverine HCl in different papaverine concentrations in water.

Samples	20 mM Hydrodynamic Diameter [nm]	PDI	40 mM Hydrodynamic Diameter [nm]	PDI	80 mM Hydrodynamic Diameter [nm]	PDI
P. HCl	**64** ± 69 **297** ± 113	0.56	**38** ± 11 **295** ± 5	0.24	----	--
PA 1:1	**11** ± 1 **254** ± 8	0.22	**1** ± 0 **249** ± 5	0.16	**2** ± 0 **298** ± 49	0.20
PA 1:2	**12** ± 1 **301** ± 17	0.22	**3** ± 2 **293** ± 16	0.17	**3** ± 2 **372** ± 63	0.20
PA 1:3	**3** ± 0 **959** ± 59	0.42	**7** ± 7 **265** ± 17	0.18	**12** ± 10 **263** ± 4	0.17

The influence of the size of the aggregates with regard to the water solubility of papaverine was investigated (**Fig. 7**). Firstly, the starting concentration (300 mM) of dissolved papaverine in water (PA 1:1, PA 1:2, PA 1:3) and the supernatant of the papaverine HCl solution were measured by means of HPLC. Secondly, all solutions were filtered (cellulose acetate filter, pore size 200 nm) to remove all aggregates (> 200 nm) and again, the papaverine concentration was determined by HPLC. The concentration of dissolved papaverine decreased significantly for the PILs, while no change in the solubility of the HCl salt could be observed. This finding supports the hypothesis of citric acid stabilized, larger supramolecular aggregates of papaverine in accordance with the ^{1}H NMR assay. Chloride as a counterion could not act as a stabilizer for large supramolecular aggregates of papaverine which led to smaller particles and hence less dissolved papaverine.

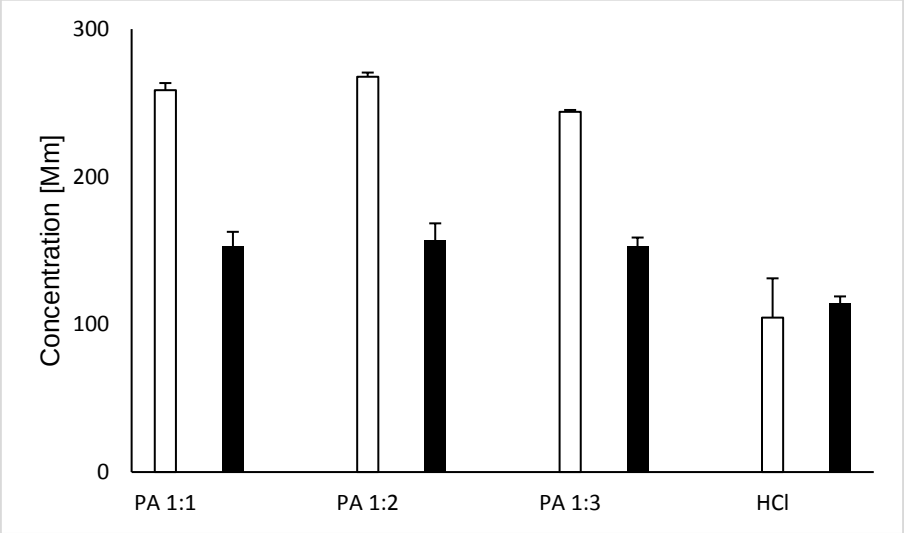

Figure 7: Equilibrium solubility. White bars are unfiltrated solutions, the black bars are filtrated solutions.

Surface charge properties of nanosuspensions were studied by the measurement of the zeta potential, which is a stability indicating parameter in colloidal systems. A minimum zeta potential of ± 30 mV is required for electrostatically stabilized suspensions. For a combined electrostatic and steric stabilization, roughly ± 20 mV are sufficient [29]. The nanosuspensions consisting of papaverine and different concentrations of citric acid were electrostatically stabilized through negatively charged citrate which is adsorbed on papaverine's surface. This leads to a negative surface of the particles, and through unadsorbed negatively charged citrate in solution, an increased ionic strength results [25, 30]. Furthermore, intramolecular hydrogen bonds between the hydroxylic group and the free CA group are present in all citric acid ionic species, which hinder attractive particle interactions, leading to a sterically stabilized suspension [31].

The zeta potential values are commonly calculated by determining the particle's electrophoretic mobility in an electric field and then converting the electrophoretic mobility to the zeta potential [29]. This analysis was performed in potassium chloride solution (0.15 M) and the results can be seen as an indicator of long-term stability of the suspension. For the formulation "PA 1:1" a zeta potential of -22 mV was measured, for "PA 1:2" -63 mV, and for "PA 1:3" -5 mV. The largest value of -63 mV indicates the physically most stable suspension, while lower values indicate physically instable suspensions. The papaverine hydrochloride salt had a zeta potential of +18 mV. The

change of the charge of the aggregates from positive (hydrochloride) to negative (citrate salts) supports the hypothesis of an adsorption of the negative charged citrate onto the papaverine.

Table 4: Dynamic viscosity measurements of papaverine:citric acid (molar ratio 1:1, 1:2, 1:3) compared with papaverine HCl (40 mM papaverine).

Samples	Dynamic viscosity [mPas]
Water	0.88
KCl solution	0.88
papaverine HCl (in KCl)	0.93
PA 1:1 (in water)	0.94
PA 1:2 (in water)	0.95
PA 1:3 (in water)	0.97

The suspension's viscosity increased with increasing concentration of the counterion (**Tab. 4**). The presence of large amounts of unadsorbed negatively charged citrate remaining in solution led to an increased ionic strength and consequently to a decreased Debye length between papaverine aggregates and unadsorbed citrate [25]. The citrate papaverine suspensions offered an increased viscosity compared to the papaverine hydrochloride suspension. This is explained by the nature of the sterically sophisticated citrate in contrast to the small size of chloride as a counterion.

Conclusion

Taking everything into consideration, OAs acting as counterions for basic SMs and facilitate the formation of PILs and protic OILs. The beneficial properties of these salts consisting of APIs and naturally occurring OAs, like enhanced dissolution rate, increased apparent solubility, and stabilized suspensions offer a promising strategy to optimize pharmaceutical parameters. Also, the low acquisition costs and the safety of most naturally occurring OAs are promising for novel pharmaceutical salts and clinical translation thereof. In the future we will perform further salt screening programs with natural OAs in order to demonstrate the applicability of the bioinspired approach and

the obtained PILs herein will be analyzed in terms of enhanced solubility studies *in vitro* and *in vivo* as well as the membrane transport.

Experimental Section

Materials

Papaverine was purchased from Fagron GmbH & Co. KG (Barsbüttel, Germany). Citric acid, succinic acid, malic acid, and tartaric acid were purchased from Sigma Aldrich (Schnelldorf, Germany) or TCI Chemicals (Eschborn, Germany) and were used without further purification. Meconic acid was synthesized following the literature [32]. Ultrapure water was delivered by Merck Milli-Q system (Darmstadt, Germany).

Methods

Preparation of PILs, protic OILs and low melting salts

PILs, protic OILs and low melting papaverine salts were prepared in analogy to previous reports [33]. Briefly, 100 mg papaverine was suspended in 5 mL methanol and an equimolar amount (2-fold or 3-fold excess, respectively) of the counterion (organic acid) suspended in 5 mL methanol was added and mixed for 15 min at room temperature. Solvents were evaporated under ambient conditions for three days and subsequently dried *in vacuo*.

Nuclear magnetic resonance measurement

NMR measurement were performed on a Bruker Avance III 400 MHz spectrometer (Karlsruhe, Germany) operating at 400.13 MHz with a PA BBI inverse probe head, and data processing with the TopSpin 3.5pl7 software.

For ^{1}H NMR, the acquisition parameters were applied as follows: 16 scans, at a temperature of 300 K, flip angle of 30°, spectral width of 20.55 ppm, and transmitter offset of 6.175 ppm. The acquisition time was set to 3.985 s followed by relaxation delay of 1.0 s with collection of 64K data points at a sample spinning frequency of 20 Hz. Processing parameters were set to an exponential line broadening window function of 0.3 Hz, an automatic baseline correction, and manual phasing. After a setting time of 5 minutes at 300 K, the spectra were recorded in D_2O.

The 2D ^{1}H-^{15}N HMBC spectra were recorded at 300 K with 128 increments in t1. The long-range coupling constant was set to 5 Hz. The data were processed using a sine window function in both dimensions zero-filling in F1 dimension and linear prediction in the t1 dimension prior to Fourier transformation. Automatic baseline correction in both dimensions was performed.

X-ray powder diffractometry

PILs, protic OILs and crystalline papaverine salts were transferred onto a silicon single crystal zero background specimen holder, covering an area with the diameter of approximately 5 mm. Powder diffractometric studies were done using a Bruker Discover D8 powder diffractometer (Karlsruhe, Germany) and Cu Ka radiation (unsplit Ka_1+Ka_2 doublet, mean wavelength l = 154.19 pm) at a power of 40 kV and 40 mA, a focussing Goebel mirror and a 2.5° axial Soller slit. The scattered X-ray beam went through a receiving slit (3.3°). Detection was done with a LynxEye-1D-Detector (Bruker AXS) using the full detector range of 192 channels. Measurements were done in reflection geometry in coupled two theta/theta mode with a step size of 0.025° in 2θ and 0.33 s measurement time per step in the range of 5 – 50°(2θ). Data collection was done with the software package DIFFRAC.Suite (V2 2.2.690, BrukerAXS, Karlsruhe, Germany). The diffraction data was subsequently converted into ASCII format and further handled with Origin (OriginLab, Massachusetts, USA).

Photometrical determination of dissolution rate

Dissolution rates were measured with a Sirius T3 instrument (Sirius Analytical, Forest Row, UK) as described earlier [34]. Tablets with defined surfaces were prepared by compression of 5 - 10 mg substance (salt or papaverine free base) in a tablet disk (diameter of the tablet disk was 0.3 cm and is provided by the manufacturer of the machine) under a weight of 0.18 tonnes for 3 min with a manual hydraulic tablet press (Paul Weber, Stuttgart, Germany), as described before [34]. The release of drug substance from these tablet disc allows data collection with a standardized surface area (0.07 cm^2), which is required to fit the data for the calculation of the dissolution rate [34]. The dissolution rates were determined photometrically at room temperature in phosphate buffered saline (PBS, 0.17 M) pH 6.8 at a stirring speed of 4800 rpm following the manufacturer's instructions. The linear part of the release profile was used for calculation of the dissolution rate (dissolved substance per time and surface area).

Potentiometrically and photometrically recorded titration experiments for determination of solubility

Intrinsic and apparent solubility were measured on a Sirius T3 instrument (Sirius Analytical, Forest Row, UK) by potentiometric titration as described before [35, 36]. In brief, typically 5 - 10 mg of API were dissolved in 1.5 mL of 0.15 M KCl solution at pH 2 (adjusted with 0.5 M hydrochloric acid). After complete dissolution, the solution was back-titrated by addition of 0.5 M potassium hydroxide until first precipitation occurred and as continuously monitored photometrically (λ = 500 nm). Subsequently, the pH was changed incrementally by repeated addition of minute amounts of acid and base throughout the experiment. After each titrant addition the delayed pH gradient of the API due to precipitation or dissolution was measured and used to extrapolate the equilibrium phase where the gradient is zero. Data from analysis with acidity errors larger than 1 mM were excluded.

Differential scanning calorimetry

Differential Scanning Calorimetry (DSC) was performed on a DSC 8000 instrument (Perkin Elmer, Waltham, MA, USA) using a scanning rate of 20 K/min. Sample size was 3 - 5 mg for all substances. For the PILs three heating and three cooling cycles were performed, the second and the third heating cycle were analyzed to allow for removal of residual water during the first heating cycle. Crucibles were weighted before and after measurements.

Dynamic light scattering sample preparation and analysis

The average particle size of different concentrations of papaverine citrate and papaverine hydrochloric acid salt (20 mM, 40 mM, 80 mM) in water was measured by DLS. Measurements were performed with unfiltered samples in disposable UV-cuvettes (1.5 mL) from Brand (Wertheim, Germany) using a Delsa^{TM} Nano HC particle analyzer from Beckman Coulter (Brea, CA, USA) with backscattering at an angle of 165°. Measurements were performed in triplicate with an accumulation of 70 scans at 298 K, and the data were analyzed by the CONTIN algorithm. The average particle sizes were evaluated with a refractive index of 1.333 for all samples and the experimentally measured dynamic viscosities of the specific solutions were also used (see also determination of dynamic viscosity).

Zeta potential measurement

Zeta potential measurements of the papaverine salts (40 mM) in potassium chloride solution (0.15 M) were performed in DI-water with its conductivity adjusted to 50 µS/cm^2, in order to determine the surface charge and to estimate the long-term stability properties. The analysis was performed by using a Delsa^{TM} Nano HC particle analyzer from Beckman Coulter (Brea, CA, USA) at 298 K with a flow cell (60 V, base frequency 115 - 140 Hz, scattering angle 15°). The electrophoretic mobility was converted to the zeta potential by the Helmholtz-Smoluchowski equation. All measurements were performed in triplicate.

Liquid chromatography

All HPLC analyses were performed with an Agilent 1100 modular chromatographic system equipped with an online vacuum degasser, a binary pump, an autosampler, a thermostatted column compartment and a variable wavelength detector (Agilent, Waldbronn, Germany). The system was operated, and the data were processed using the Agilent ChemStation® Rev. B.03.02. software.

A Hypersil GOLD C18 column (150 x 4.6 mm i.d., with a particle size of 5 µm and a pore size of 100 Å) (ThermoFisher Scientific, Waltham, MA, USA) was used as stationary phase. Mobile phase A consisted of an aqueous 10 mM dipotassium hydrogenphosphate buffer adjusted to pH 7.4 with orthophosphoric acid, while mobile phase B was methanol. The gradient worked at a flow rate of 1.0 mL/min and utilized a linear gradient from 10 to 90% B from 0 to 25 min. 90% B are then hold isocratically for 5 min and the system is reequilibrated by a gradient back to 10% within 2 min followed by a 3 min isocratic step. The total run time was 35 min and the injection volume was 10 µL. The UV detection was performed at 254 nm and the runs were recorded at ambient temperature.

Determination of dynamic viscosity

The density was determined using an Anton Paar (Graz, Austria) Density Meter DMA 4100 M at 298 K. The dynamic viscosity was measured on an Anton Paar (Graz, Austria) rolling-ball viscometer LOVIS 2000 M using capillary LOVIS 1.8 equipped with a steel ball (Mat. No. 73109, diameter 1.5 mm, steel 1.4125, density 7.66 g/cm^3). The temperature was constantly kept at 298 K and the inclination angle was 70° for all measurements.

Acknowledgment

Our thanks go out to Johannes Wiest for his support and advise during the whole project.

Author Information

***Corresponding Author**: Ulrike Holzgrabe - *Institute of Pharmacy and Food Chemistry, Am Hubland, University of Würzburg, DE-97074 Würzburg, Germany*

E-Mail address: *ulrike.holzgrabe@uni-wuerzburg.de*

References

[1] Farre, E. M.; Tiessen, A.; Roessner, U.; Geigenberger, P.; Trethewey, R. N.; Willmitzer, L. Analysis of the compartmentation of glycolytic intermediates, nucleotides, sugars, organic acids, amino acids, and sugar alcohols in potato tubers using a nonaqueous fractionation method. *Plant Physiol.* **2001,** *127*, (2), 685-700.

[2] Martinoia, E.; Massonneau, A.; Frangne, N. Transport processes of solutes across the vacuolar membrane of higher plants. *Plant Cell Physiol.* **2000,** *41*, (11), 1175-1186.

[3] Frei, B.; Eisenach, C.; Martinoia, E.; Hussein, S.; Chen, X. Z.; Arrivault, S.; Neuhaus, H. E. Purification and functional characterization of the vacuolar malate transporter tDT from Arabidopsis. *J. Biol. Chem.* **2018,** *293*, (11), 4180-4190.

[4] Neuhaus, H. E. Transport of primary metabolites across the plant vacuolar membrane. *FEBS Lett.* **2007,** *581*, 2223-2226.

[5] Hamilton, G. R.; Baskett, T. F. In the arms of Morpheus the development of morphine for postoperative pain relief. *Can J Anaesth* **2000,** *47*, (4), 367-374.

[6] Sertürner, F. W. Trommsdorff's Journal der Pharmazie für Aerzte, Apotheker und Chemisten, 13, 1805.

[7] Domingos, S.; Andre, V.; Quaresma, S.; Martins, I. C.; Minas da Piedade, M. F.; Duarte, M. T. New forms of old drugs: improving without changing. *J. Pharm. Pharmacol.* **2015,** *67*, (6), 830-846.

[8] Balk, A.; Widmer, T.; Wiest, J.; Bruhn, H.; Rybak, J. C.; Matthes, P.; Muller-Buschbaum, K.; Sakalis, A.; Luhmann, T.; Berghausen, J.; Holzgrabe, U.; Galli, B.; Meinel, L. Ionic liquid versus prodrug strategy to address formulation challenges. *Pharm. Res.* **2015,** *32*, (6), 2154-2167.

[9] Marrucho, I. M.; Branco, L. C.; Rebelo, L. P. Ionic liquids in pharmaceutical applications. *Annu. Rev. Chem. Biomol. Eng.* **2014,** *5*, 527-546.

[10] Welton, T. Room-Temperature Ionic Liquids. Solvents for Synthesis and Catalysis. *Chem. Rev.* **1999,** *99*, (8), 2071-2084.

[11] Welton, T. Room-Temperature Ionic Liquids. Solvents for Synthesis and Catalysis. *Chem. Rev.* **1999,** *99*, (8), 2071-2084.

[12] Easton, M. E.; Choudhary, H.; Rogers, R. D. Azolate Anions in Ionic Liquids: Promising and Under-Utilized Components of the Ionic Liquid Toolbox. *Chem. Eur. J.* **2019,** *25*, (9), 2127-2140.

[13] Fukaya, Y.; Sekikawa, K.; Ohno, H. Bio ionic liquids: room temperature ionic liquids composed wholly of biomaterials. *Green Chem.* **2007,** *9*, 1155-1157.

[14] Agharkar, S.; Lindenbaum, S.; Higuchi, T. Enhancement of Solubility of Drug Salts by Hydrophilic Counterions: Properties of Organic Salts of an Antimalarial Drug. *J. Pharm. Sci.* **1976,** *65*, (5), 747-749.

[15] Balk, A.; Holzgrabe, U.; Meinel, L. 'Pro et contra' ionic liquid drugs - Challenges and opportunities for pharmaceutical translation. *Eur. J. Pharm. Biopharm.* **2015,** *94*, 291-304.

[16] Stoimenovski, J.; Dean, P. M.; Izgorodina, E. I.; MacFarlane, D. R. Protic pharmaceutical ionic liquids and solids: aspects of protonics. *Faraday Discuss.* **2012,** *154*, 335-52; discussion 439-64, 465-471.

[17] Stoimenovski, J.; Dean, P. M.; Izgorodina, E. I.; MacFarlane, D. R. Protic pharmaceutical ionic liquids and solids: aspects of protonics. *Faraday Discuss.* **2012,** *154*, 335-52; discussion 439-64, 465-471.

[18] Greaves, T. L.; Drummond, C. J. Protic Ionic Liquids: Evolving Structure-Property Relationships and Expanding Applications. *Chem. Rev.* **2015,** *115*, (20), 11379-11448.

[19] Johansson, K. M.; Izgorodina, E. I.; Forsyth, M.; MacFarlane, D. R.; Seddon, K. R. Protic ionic liquids based on the dimeric and oligomeric anions: [(AcO)xH(x-1)]. *Phys. Chem. Chem. Phys.* **2008,** *10*, (20), 2972-2978.

[20] Bica, K.; Rogers, R. D. Confused ionic liquid ions--a "liquification" and dosage strategy for pharmaceutically active salts. *Chem. Commun.* **2010,** *46*, (8), 1215-1217.

[21] Samin, S.; Hod, M.; Melamed, E.; Gottlieb, M.; Tsori, Y. Experimental Demonstration of the Stabilization of Colloids by Addition of Salt. *Phys. Rev. Appl.* **2014,** *2*, (2).

[22] Israelachvili, J. Intermolecular and Surface forces, 3rd ed. Academic Press, London, U.K., 2011.

[23] Egorova, K. S.; Gordeev, E. G.; Ananikov, V. P. Biological Activity of Ionic Liquids and Their Application in Pharmaceutics and Medicine. *Chem. Rev.* **2017,** *117*, (10), 7132-7189.

[24] Shamshina, J. L.; Barber, P. S.; Rogers, R. D. Ionic liquids in drug delivery. *Expert Opin Drug Deliv* **2013,** *10*, (10), 1367-1381.

[25] Hidber, P. C. G., T. J.; Gauckler, L. J. Citric acid - A dispersant for aqueous alumina suspensions. *J. Am. Ceram. Soc.* **1996,** *79*, (7), 1857-1867.

[26] Dengale, S. J.; Grohganz, H.; Rades, T.; Lobmann, K. Recent advances in co-amorphous drug formulations. *Adv Drug Deliv. Rev.* **2016,** *100*, 116-125.

[27] LaPlante, S. R.; Carson, R.; Gillard, J.; Aubry, N.; Coulombe, R.; Bordeleau, S.; Bonneau, P.; Little, M.; O'Meara, J.; Beaulieu, P. L. Compound aggregation in drug discovery: implementing a practical NMR assay for medicinal chemists. *J. Med. Chem.* **2013,** *56*, (12), 5142-5150.

[28] Wiest, J.; Saedtler, M.; Bottcher, B.; Grune, M.; Reggane, M.; Galli, B.; Holzgrabe, U.; Meinel, L. Geometrical and Structural Dynamics of Imatinib within Biorelevant Colloids. *Mol. Pharm.* **2018,** *15*, (10), 4470-4480.

[29] Jacobs, C.; Müller, R. H. Production and characterization of a budesonide nanosuspension for pulmonary administration. *Pharm. Res.* **2002,** *19*, (2), 189–194.

[30] Araujo, F. A.; Kelmann, R. G.; Araujo, B. V.; Finatto, R. B.; Teixeira, H. F.; Koester, L. S. Development and characterization of parenteral nanoemulsions containing thalidomide. *Eur. J. Pharm. Sci.* **2011,** *42*, (3), 238-245.

[31] Leong, Y.-K. Role of Molecular Architecture of Citric and Related Polyacids on the Yield Stress of α-Alumina Slurries: Inter- and Intramolecular Forces. *J. Am. Ceram. Soc.* **2010,** *93*, (9), 2598-2605.

[32] Güntzel, P.; Forster, L.; Schollmayer, C.; Holzgrabe, U. A Convenient Preparation of Carboxy-γ-pyrone Derivatives: Meconic Acid and Comenic Acid. *Org. Prep. Proced. Int.* **2019,** *50*, (5), 512-516.

[33] Bica, K.; Rijksen, C.; Nieuwenhuyzen, M.; Rogers, R. D. In search of pure liquid salt forms of aspirin: ionic liquid approaches with acetylsalicylic acid and salicylic acid. *Phys. Chem. Chem. Phys.* **2010,** *12*, (8), 2011-2017.

[34] Gravestock, T.; Box, K.; Comer, J.; Frake, E.; Judge, S.; Ruiz, R. The "GI dissolution" method: a low volume, in vitro apparatus for assessing the dissolution/precipitation behaviour of an active pharmaceutical ingredient under biorelevant conditions. *Anal. Methods* **2011,** *3*, (3), 560.

[35] Hsieh, Y. L.; Ilevbare, G. A.; Van Eerdenbrugh, B.; Box, K. J.; Sanchez-Felix, M. V.; Taylor, L. S. pH-Induced precipitation behavior of weakly basic compounds: determination of extent and duration of supersaturation using potentiometric titration and correlation to solid state properties. *Pharm. Res.* **2012,** *29*, (10), 2738-2753.

[36] Stuart, M.; Box, K. Chasing equilibrium: measuring the intrinsic solubility of weak acids and bases. *Anal. Chem.* **2005,** *77*, (4), 983-990.

3.4 Single Crystals of Active Agents in Multiple Myeloma and Water Solubility Improvement by Use of Deep Eutectic Solvents

Paul Güntzel[a], Marco Block[a], Klaus Schilling[a], Andreas Hartung[a], Andreas Stoy[b], Daniela Brünnert[c], Manik Chatterjee[C], Krzysztof Radacki[b], Holger Braunschweig[b], Lorenz Meinel[a] and Ulrike Holzgrabe[a,*]

[a]*Institute of Pharmacy and Food Chemistry, Am Hubland, University of Würzburg, DE-97074 Würzburg, Germany*

[b]*Institute of Inorganic Chemistry, Am Hubland, University of Würzburg, DE-97074 Würzburg, Germany*

[c]*Department of Internal Medicine II, Translational Oncology, University Hospital of Würzburg, DE-97080, Germany*

*Corresponding author. Tel.: +49 931 3185461

E-Mail address: Ulrike.holzgrabe@uni-wuerzburg.de – **to be submitted after patent filing**

Abstract: Isoquinolone-type inhibitors of the heat shock protein 70 (HSP 70) are a promising strategy for the therapy of the malignant B-cell tumor multiple myeloma (MM), a common hematological cancer. Unfortunately, these potent agents suffer from poor water solubility, which diminishes the application for *in vitro* and consequently *in vivo* studies. Here, we characterized the solids using X-ray powder diffraction (XRPD), infrared (IR) spectroscopy and single crystal X-ray structure analysis, to obtain more information about the intermolecular interactions within the crystals. The combination of hydrogen bonding and π-π-stacking could be identified as reason for the strong crystal lattice and consequently for the poor water solubility of the isoquinolone-type HSP70 inhibitors. A deep eutectic solvent (DES) approach was used to enhance the water solubility of HSP70 inhibitors, analyzed by a shake flask experiment, and enables *in vitro* bioactivity studies in murine MM cell line (MOPC.315 BM luc+). Furthermore, facilitate choline-based DES *in vitro* bioactivity studies and improved the inhibitor's water solubility in an order of magnitude.

Keywords: HSP70 inhibitors; single crystal; solid state; deep eutectic solvent; solubility; shake flask; MOPC

Introduction

The malignant B-cell tumor multiple myeloma (MM) is characterized by osteolytic bone lesions and is after non-Hodgkin's lymphoma the second most common haematological cancer [1]. Current therapies include autologus hematopoietic stem cell transplantation as well as the use of proteasome inhibitors like bortezomib, carfilzomib or ixazomib either alone or in combination with an immunmodulatory agent (IMiD) like lenalidomide and a corticosteroid like dexametasone. Alternatively, the histone deacetylase inhibitor panobinostat is combined with bortezomib and dexamethasone [2]. With the therapeutic advancement in the last decades, the median survival could be increased to approx. 6.5 years [3]. Still, after initial therapeutic success of any therapy, patients ultimately suffer from relapse emerging the development of novel substances.

A promising new strategy for the treatment in the MM is a dual depletion of heat shock protein90 (HSP90) and the heat shock factor-1/heat shock protein70 (HSF-1/HSP70) system. Researchers have already developed different potent HSP90 inhibitors (**Fig. 1**), like geldanamycin derivatives 17-AAG (**1a**), 17-DMAG (**1b**) and isoxazol NVP-AUY922 (**2**), but clinical cell studies revealed an upregulation of HSP70 upon HSP90 inhibition, which diminished the efficiacy of the HSP90 inhibition approach [4-6].

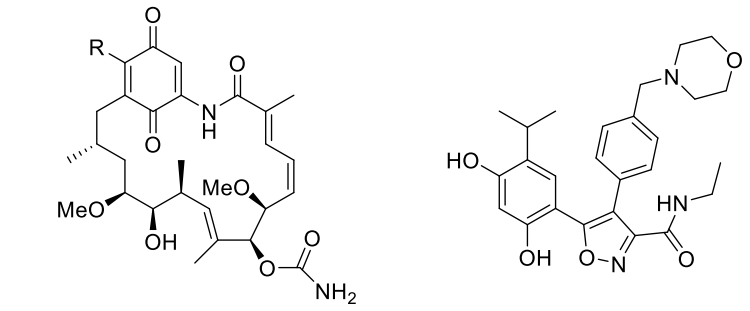

Geldanamycin: R = OCH_3
1a: R = $NHCH_2CH_2CH=CH_2$
1b: R = $NHCH_2CH_2N(CH_3)_2$

2

Figure 1: HSP90 inhibitors 17-AAG (1a), 17-DMAG (1b) and NVP-AUY922 (2).

Hence, a simultaneously application of HSP90 and HSP70 inhibitors seems to be promising. For this reason, potent inhibitors of the HSP70 protein (**3**-**8**) were already developed in our group (**Fig. 2**) [7]. However, these isoquinolone-type HSP70 inhibitors

suffer from poor water solubility and very high melting points > 220 °C, even though, the compounds meet the requirements of the Lipinski's rule of five [8].

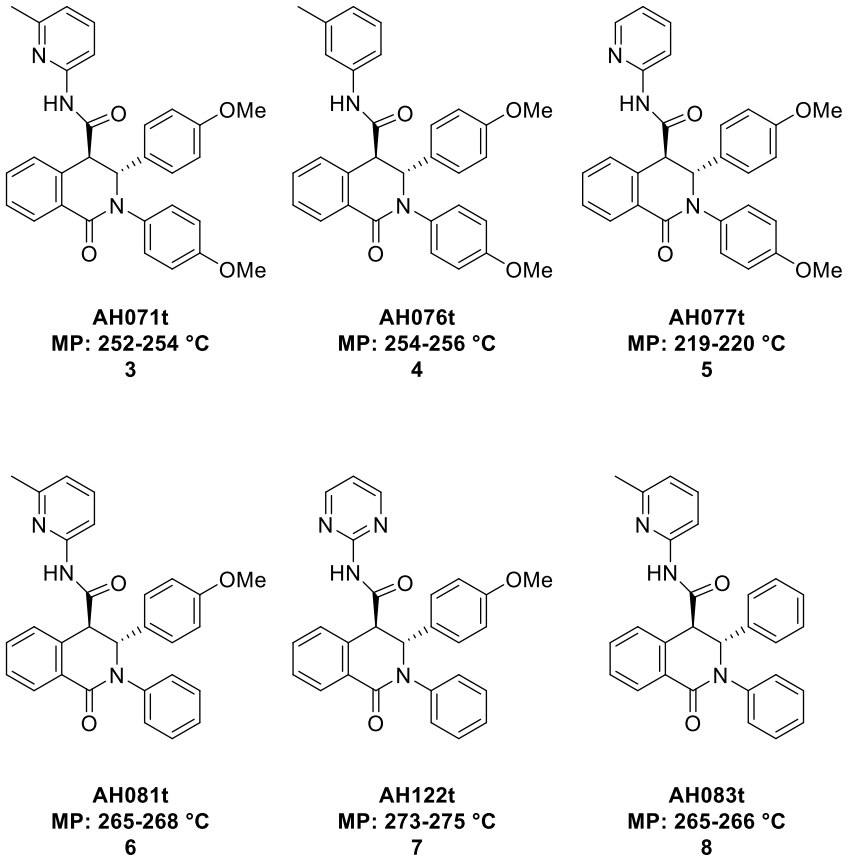

Figure 2: Isoquinolone-type HSP70 inhibitors [7].

Deep eutectic solvents (DES), a subset of solid dispersions (SDs), are an extension of the ionic liquid model (ILs, salts with a melting point < 100 °C) and can replace conventional organic acids (OAs) for salt formation [9-11]. DES are eutectic mixtures of two or more distinct components, e.g. HBDs and HBAs which typically interact via strong hydrogen bonding [12, 13]. In analogy to the IL model, DES can prevent strong lattice forces within the solid as well as prevent compound's recrystallization by hydrotropic solubilization and stabilization [14-16].

The aim of this study was to obtain more information about intermolecular interactions between the compound's molecules (**3**-**8**) by solid-state techniques like X-ray powder diffraction (XRPD) and infrared (IR) spectroscopic measurements as well as single crystal X-ray analysis. A ^{1}H NMR aggregation assay was carried out to analyze the

supramolecular behavior of compound **7** and a DES approach was used to improve its water solubility, followed by *in vitro* bioactivity studies.

Experimental Section

Materials

The isoquinolone-type HSP70 inhibitors **3**, **4**, **5**, **6**, **7** and **8** were synthesized according to the literature [7]. All solvents, dimethyl sulfoxide (DMSO-d_6, 99.9% D), Roswell Park Memorial Institute-1640-medium (RPMI-1640 medium), penicillin, streptomycin, L-glutamine and sodium pyruvate were purchased from Sigma-Aldrich (Schnelldorf, Germany). Fetal bovine serum (FBS) was purchased from Gibco (Paisley, UK). Tween 80 was purchased from Caelo (Hilden, Germany). HPLC grade water was obtained by a Millipore system from Merck (Darmstadt, Germany). Standard 5 mm NMR tubes (400 MHz) and coaxial insert tubes were purchased from Norell (Landsville, PA, USA).

Methods

Preparation of single crystals

5 mg of pure compound were dissolved in chloroform/ethanol (1:1), filtrated and the obtained clear solution was stored in a capped (cap was perforated) preparation vial under exclusion of light. After solvent evaporation under ambient conditions, crystals remain on the bottom of the vials.

Single crystal X-ray structure analysis

The crystal data of **3**, **4**, **5**, **6**, **7** and **8** were collected on a four-circle XtaLAB-Synergy-Dualflex-HyPix diffractometer with an HyPix Hybrid Pixel Array detector and with multi-layer mirror monochromated Cu_{Ka} radiation from a PhotonJet (Cu) X-ray Source micro-focus sealed X-ray tube. The structure was solved using intrinsic phasing method (ShelXT) [17], refined with the ShelXLprogram [18] and expanded using Fourier techniques. All non-hydrogen atoms were refined anisotropically. Hydrogen atoms were included in structure factor calculations. All hydrogen atoms were assigned to idealized geometric positions.

Infrared spectroscopy (IR)

The IR measurements of the pure crystalline HSP70 inhibitors **3**, **4**, **5**, **6**, **7** and **8** were conducted using Jasco FT/IR-6100 spectrometer from Jasco (Gross-Umstadt, Germany) with diamond attenuated total reflection unit.

Preparation of DES

Eutectic preparation was carried out using fast solvent evaporation under reduced pressure, according to a reported method [19]. The calculated amounts of HBD (citric acid, xylitol), HBA (choline chloride, serine amide hydrochloride, proline) and polymer (PVP; 5% or 10%) were dissolved in ethanol (3 mL). The weighted amount of compound was dissolved in dichloromethane and mixed with the ethanolic solution of the excipients in a rotary evaporation flask. The resulting solution was evaporated under reduced pressure.

X-ray powder diffractometry (XRPD)

Amorphous DES and pure crystalline HSP70 inhibitors **3**, **4**, **5**, **6**, **7** and **8** were transferred onto a silicon single crystal zero background specimen holder, covering an area with the diameter of approximately 5 mm. Powder diffractometric studies were done using a Bruker Discover D8 powder diffractometer (Karlsruhe, Germany) and Cu Ka radiation (unsplit Ka_1+Ka_2 doublet, mean wavelength l = 154.19 pm) at a power of 40 kV and 40 mA, a focussing Goebel mirror and a 2.5° axial Soller slit. The scattered X-ray beam went through a receiving slit (3.3°). Detection was done with a LynxEye-1D-Detector (Bruker AXS) using the full detector range of 192 channels. Measurements were done in reflection geometry in coupled two theta/theta mode with a step size of 0.025° in 2θ and 0.33 s measurement time per step in the range of 5 – 50°(2θ). Data collection was done with the software package DIFFRAC.Suite (V2 2.2.690, BrukerAXS 2009 – 2011, Karlsruhe, Germany). The diffraction data was subsequently converted into ASCII format and further handled with Origin (OriginLab, Massachusetts, USA).

Nuclear magnetic resonance measurement (NMR)

NMR measurements of the pure crystalline compound **7** were performed using a Bruker Avance III 400 MHz spectrometer (Karlsruhe, Germany) operating at 400.13 MHz with a PA BBI inverse probe head, and data processing with the TopSpin 3.5pl7 software.

^{1}H NMR the acquisition parameters: 16 scans, at a temperature of 300 K, flip angle of 30°, spectral width of 20.55 ppm, and transmitter offset of 6.175 ppm. The acquisition time was set to 3.985 s followed by relaxation delay of 1.0 s with collection of 64K data points at a sample spinning frequency of 20 Hz. Processing parameters were set to an exponential line broadening window function of 0.3 Hz, an automatic baseline correction, and manual phasing. After a setting time of 5 minutes at 300 K, the spectra were recorded in DMSO.

Solubility measurements after DES preparation

DES (containing compound **7** (5 mg, 11 µmol)) were dissolved in PBS 7.4 (ad 1 mL), stored at room temperature and aliquots were taken after 0, 0.5, 2, 4, 8, 12 and 24 h. All solubility/stability measurements were performed in triplicate and the concentration of dissolved compound **7** determined using HPLC.

Liquid chromatography (HPLC)

HPLC analyses were performed with an Agilent 1100 modular chromatographic system equipped with an online vacuum degasser, a binary pump, an autosampler, a thermostatted column compartment and a variable wavelength detector (Agilent, Waldbronn, Germany). The system was operated, and the data are processed using the Agilent ChemStation® Rev. B.03.02. software.

A Hypersil GOLD C18 column (150 x 4.6 mm i.d., with a particle size of 5 µm and a pore size of 100 Å) (ThermoFisher Scientific, Waltham, MA, USA) was used as stationary phase to determine the concentrations of dissolved compound **7** in DES aqueous solutions. Mobile phase A consisted of an aqueous 10 mM dipotassium hydrogenphosphate buffer adjusted to pH 7.4 with orthophosphoric acid, while mobile phase B was methanol. The gradient worked at a flow rate of 1.0 mL/min and utilized a linear gradient from 10 to 90% B from 0 to 25 min. 90% B were then hold isocratically for 5 min and the system is reequilibrated by a gradient back to 10% within 2 min

followed by a 3 min isocratic step. The total run time was 35 min and the injection volume was 10 µL. The UV detection was performed at 254 nm and the runs were recorded at ambient temperature.

Cell tests

The murine MM cell line MOPC.315 BM luc$^+$ (MOPC) were used [20]. Cells were cultured at 37 °C in a humified incubator using RPMI-1640 medium enriched with 20% FBS, 100 U/mL Penicillin, 100 µg/mL Streptomycin, 2 mM L-Glutamine and 1 mM Sodium-pyruvate. For MOPC cells, medium was supplemented with additional 25 µM β-mercaptoethanol. Cell culture was freshly grown every 3 months.

Viability assessment

For viability assessment, 7,000 MOPC.315 BM luc$^+$ cells were seeded per well of a 96 well plate and cells were treated with various concentrations of compound 7 or the respective solvent control. After 3 days, cells were washed with PBS, pelleted and resuspended in 200 µL of cold annexin V binding buffer (10 mM HEPES/NaOH, 140 mM NaCl, 2.5 mM $CaCl_2$, pH7.4) containing 1 µL of annexin V solution and 1 µg/mL propidium iodide. Thereby, annexin V was prepared as described before, and coupled to PromoFluor 647 or fluorescein isothiocyanate (FITC) (PromoCell, Heidelberg, Germany) [21, 22]. Cells were incubated for 15 min followed by flow cytometry viability analysis. Flow cytometry was performed using a FACSCalibur (BD Biosciences, Heidelberg, Germany).

Results and Discussion

Structure and Physical Characteristics

The series of potent isoquinolone-type HSP70 inhibitors suffer from poor water solubility and offer high melting points > 220 °C [7]. The solid-state forms of the compounds were analyzed by means of XRPD (**Fig. 4**). As can be seen from the structured diffractograms all solids are crystalline. Compounds **3**, **4** and **5** show similar diffractograms with a dominant peak at 8°, because they are substances of the same group of isoquinolones with substituted phenyl residues in position 2 and 3 (**Fig. 3**). Correspondingly, substances **6** and **7** with just one substituted phenyl residue in

position 3 and substance **8** with unsubstituted phenyl residues are characterized by a dominant peak at 10°.

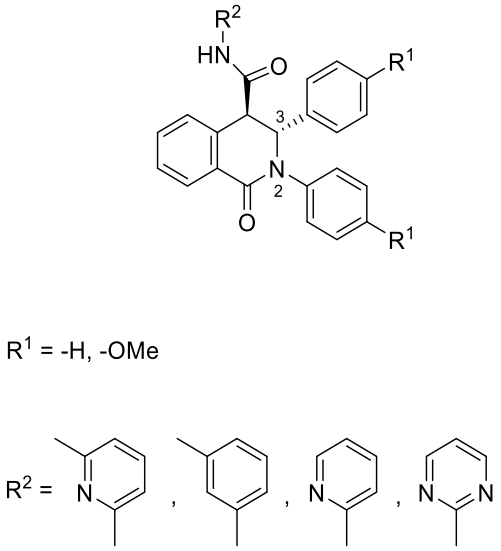

Figure 3: Different substituted isoquinolones.

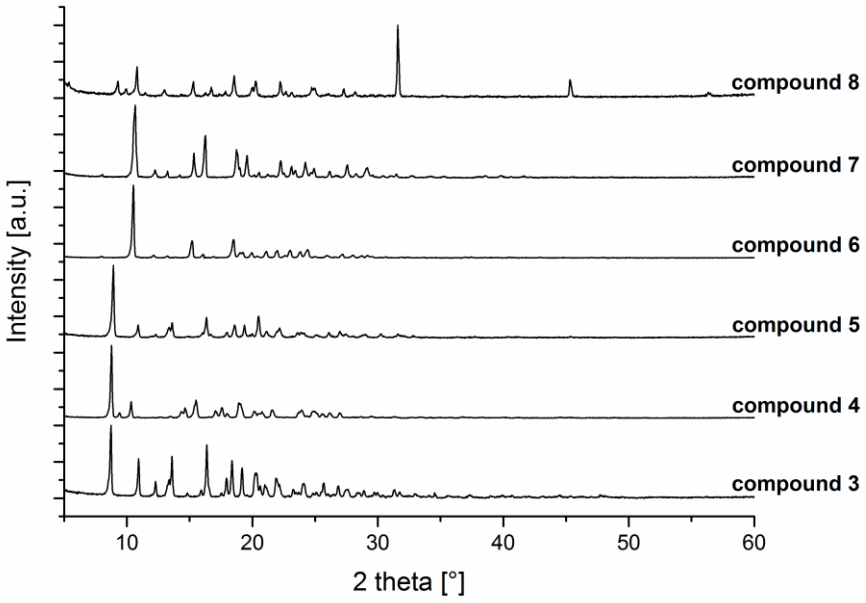

Figure 4: XRPD of the isoquinolone-type HSP70 inhibitors.

The IR spectrum can provide information about intermolecular interactions between the molecules within the crystal. The amide N-H stretching modes occurred within a

narrow wavenumber range (3250 cm^{-1} – 3300 cm^{-1}; **Table 1**) for all compounds (**Fig. 5**). Because “free” amide N-H bonds with a high stretching frequency occur at around 3500 cm^{-1}, this shift to lower wavenumbers indicated a hydrogen bond between the amide proton resulting in a decreased stretching frequency of the N-H bond [23].

Table 1: N-H stretching modes of HSP70 inhibitors.

Compound	***N-H stretching mode (cm^{-1})***
3	3274
4	3249
5	3282
6	3249
7	3258
8	3280

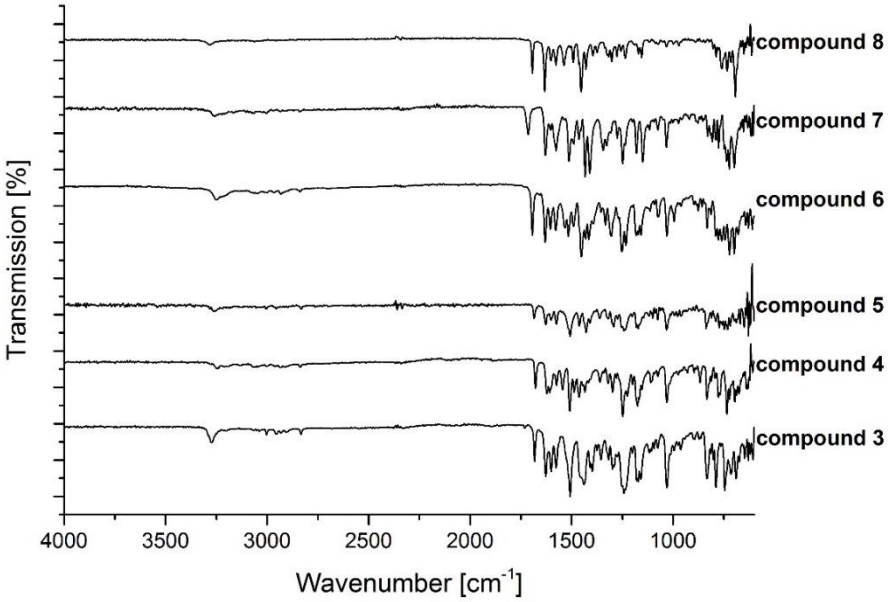

Figure 5: Infrared spectra of the isoquinolone-type HSP70 inhibitors.

The single crystal X-ray structure analysis offered a hydrogen bond between the amide proton and the carbonyl function of the isoquinolone ground structure (**Fig. 10a**) and a

high ordered packing of the molecules within the crystal (**Fig. 6-11**) for all compounds, in accordance to the XRPD and IR results.

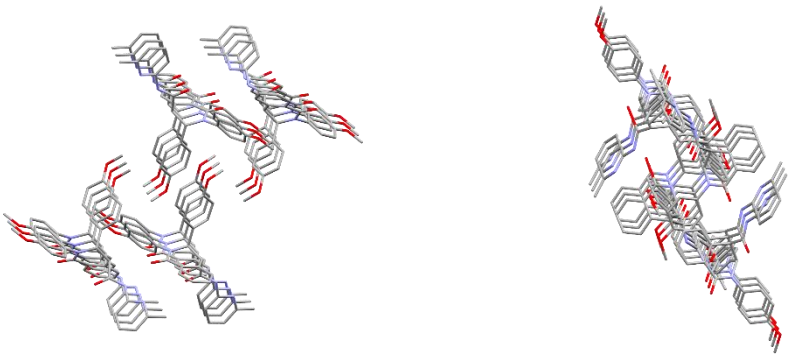

Figure 6: Single crystal structure analysis - high ordered crystal lattice of compound 3.

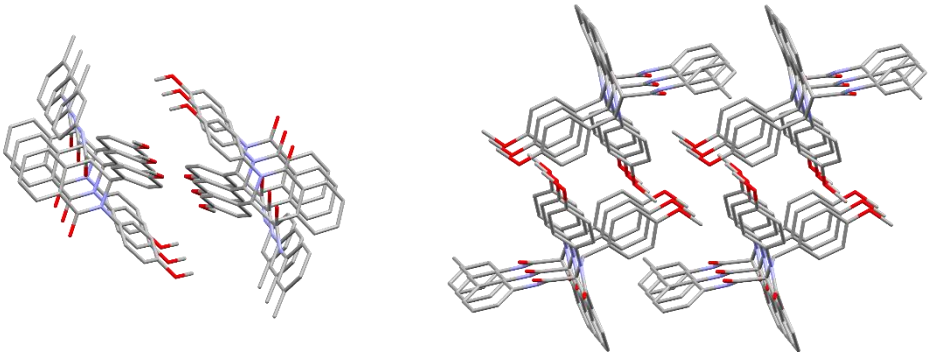

Figure 7: Single crystal structure analysis - high ordered crystal lattice of compound 4.

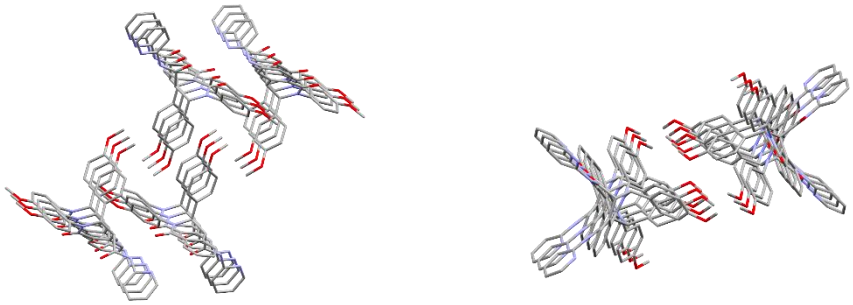

Figure 8: Single crystal structure analysis - high ordered crystal lattice of compound 5.

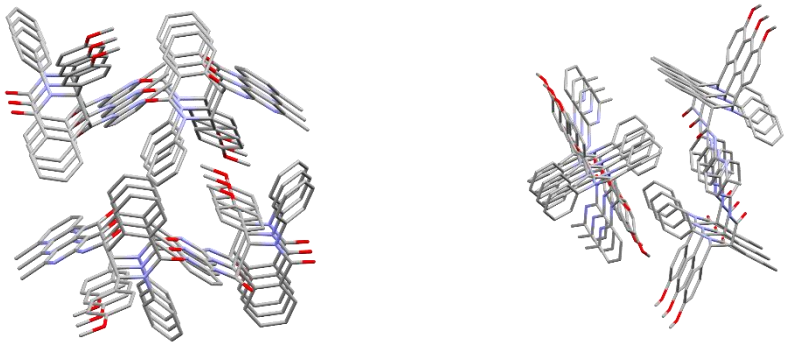

Figure 9: Single crystal structure analysis - high ordered crystal lattice of compound 6.

a

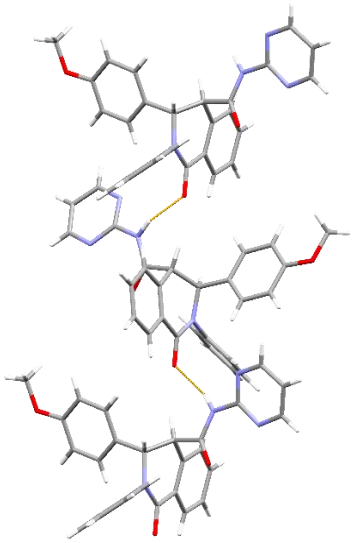

b

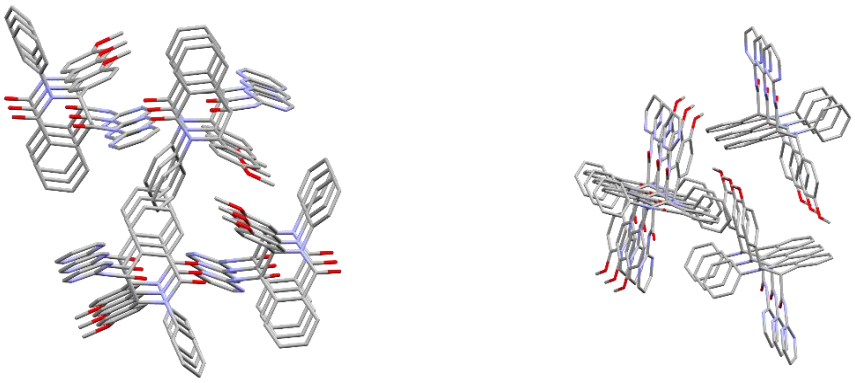

Figure 10: Single crystal structure analysis – (a) H-bonds (yellow) between molecules of compound 7 and (b) high ordered crystal lattice of compound 7.

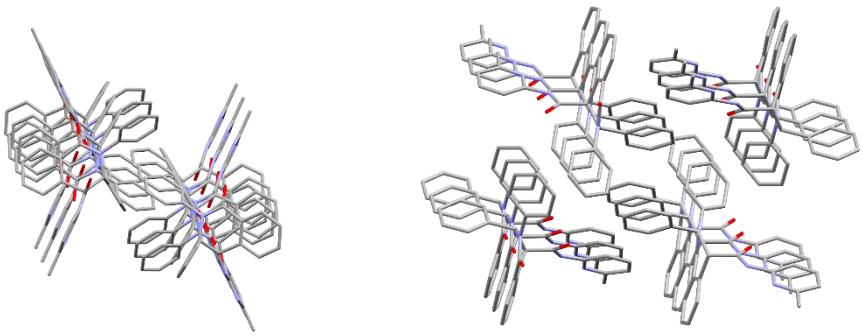

Figure 11: Single crystal structure analysis - high ordered crystal lattice of compound 8.

Supramolecular behavior and DES approach of compound 7

The supramolecular association behavior of **7** in solution was analyzed by a ^{1}H NMR based aggregation assay [24, 25]. As reference spectrum a solution of very low concentration of compound **7** (2 mM) and Tween 80 was prepared. For multimeric species a concentration-dependent change in the chemical shifts (Δ ppm) would be expected, explained by local environmental changes in the magnetic field around the molecule because of accumulation of the aromatic systems with their shielding effects. No down field shift of the signals was observed upon increasing the starting concentration from 250 µM to 2 mM, indicating that no aggregation of the compound could be observed (**Fig. 12**). Furthermore, the shape of the signal (i.e. sharp or broad) is related to the size and the tumbling rate of a supramolecular species. Aggregation leads to slower tumbling rates and faster relaxation times and thus to broader peak shapes [24]. This fact, that no signal broadening was observed, supported the notion of no aggregation in solution.

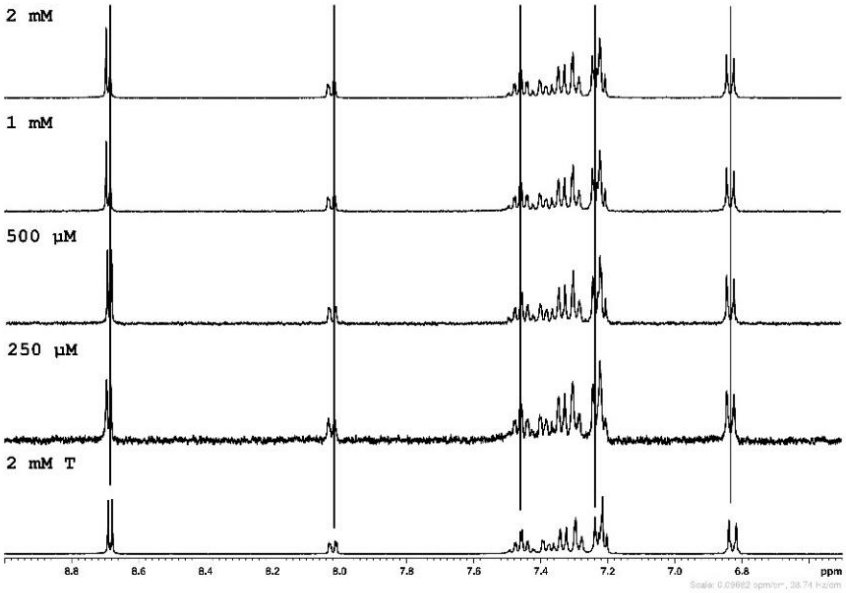

Figure 12: ^{1}H NMR in DMSO-d_6 of compound 7 in various concentrations.

Because of the lack of water solubility of the HSP70 inhibitors, DES were employed as vehicle to enable a sufficient solubility in aqueous solutions. Following the theory, that excipients of the DES prevent recrystallization of dissolved compound **7**, result in hydrotropic solubilization [15, 16]. Therefore, three different halide salt, organic or amino acid, sugar and PVP based DES were generated to obtain a suitable formulation for the *in vitro* studies (**Table 2**).

Table 2: Different DES formulations for compound 7.

HBA	***HBD***	***Polymer***
choline chloride (2 mmol)	citric acid (2 mmol)	PVP (5%)
choline chloride (2 mmol)	xylitol (2 mmol)	PVP (5%)
serine amide hydrochloride (2 mmol), proline (2 mmol)	xylitol (2 mmol)	PVP (10%)

The amorphous X-ray diffractograms of the different DES-based formulations revealed the disruption of the crystal lattice of **7** in DES compared with the crystalline pure compound (**Fig. 13**).

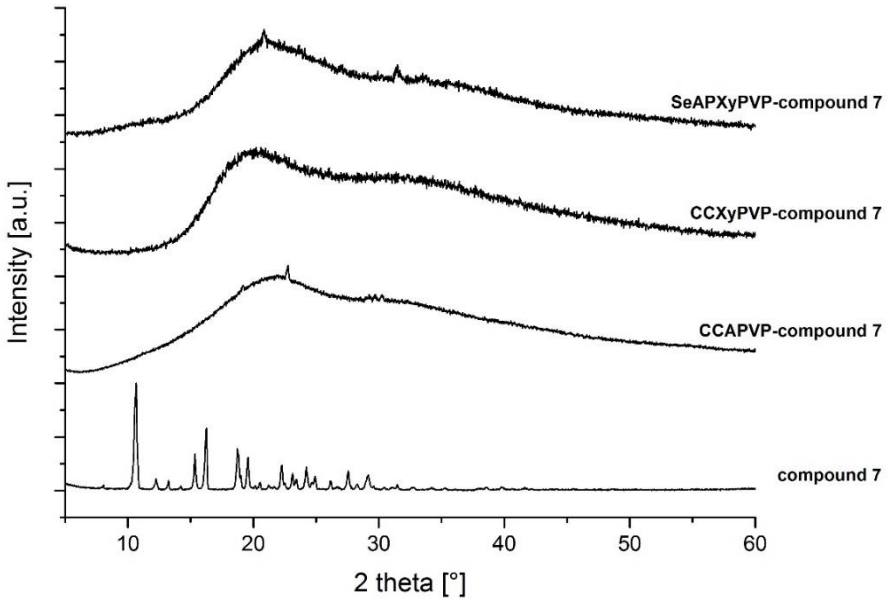

Figure 13: XRPD of pure compound and different DES based formulations.

The stability and *in vitro* bioactivity studies were carried out with DES consisting of compound **7**, choline chloride, citric acid and PVP (5% w/w). A shake flask experiment revealed increased water solubility of **7** (**Fig. 14**). The initial concentration of **7** (9 mM) was 4500 times higher compared to the pure compound (2 µM). Even after 24 h a stable concentration of 1 mM could be reached.

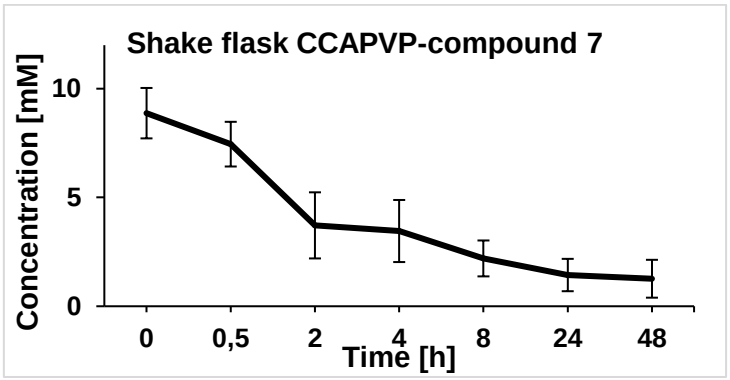

Figure 14: Shake flask experiment of CCAPVP-compound 7.

In vitro viability cell tests were carried out to analyze the influence of the DES on MOPC and to compare the efficacy of the compound dissolved in DMSO (control) and in the

DES (**Fig. 15**). Both, the control (0.77 µM) and the DES with compound **7** (0.84 µM) show EC50 values in the same range of concentration; the DES without compound had no effect to MOPC.

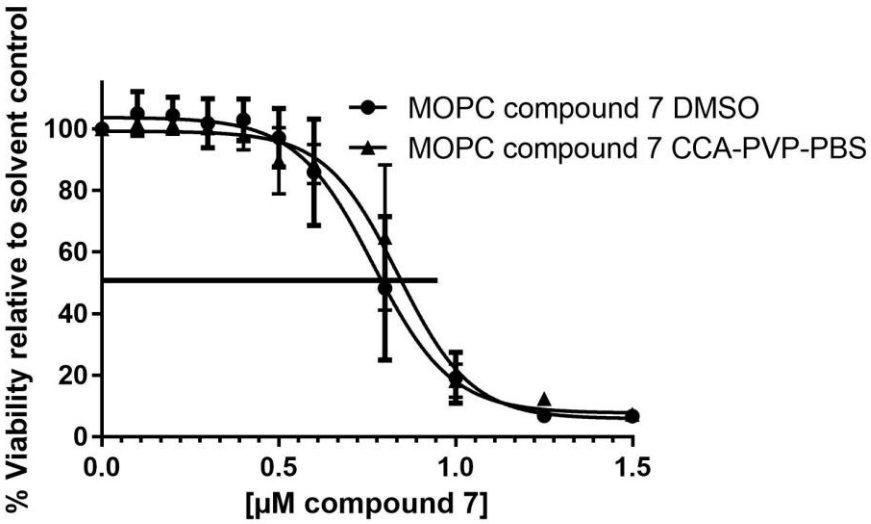

Figure 15: Viability cell tests of compound 7 dissolved in DMSO compared to the CCAPVP-compound 7.

Conclusion

Taking together, DES consisting of naturally occurring compounds and **7** can be a helpful tool to prevent strong lattice forces within crystals. DES formulations showed an improved water solubility of poor soluble compounds. Furthermore, such formulations enable *in vitro* cell activity studies. However, for *in vivo* studies the non-toxic behavior of the excipients must be checked, first.

Acknowledgment

Our thanks go out to Johannes Wiest for his support and advice during characterization of the DES.

References

[1] Paramore, A.; Frantz, S. *Nat. Rev. Drug Discov.* **2003,** *2*, 611-612.

[2] Kumar, S. K.; Rajkumar, V.; Kyle, R. A.; van Duin, M.; Sonneveld, P.; Mateos, M. V.; Gay, F.; Anderson, K. C. *Nat. Rev. Dis. Primers* **2017,** *3*, 17046.

[3] Usmani, S. Z.; Hoering, A.; Cavo, M.; Miguel, J. S.; Goldschimdt, H.; Hajek, R.; Turesson, I.; Lahuerta, J. J.; Attal, M.; Barlogie, B.; Lee, J. H.; Kumar, S.; Lenhoff, S.; Morgan, G.; Rajkumar, S. V.; Durie, B. G. M.; Moreau, P. *Blood Cancer J.* **2018,** *8*, 123.

[4] Powers, M. V.; Clarke, P. A.; Workman, P. *Cancer Cell* **2008,** *14*, 250-262.

[5] Neckers, L.; Workman, P. *Clin. Cancer Res.* **2012,** *18*, 64-76.

[6] Workman, P. *Cancer Lett.* **2004,** *206*, 149-157.

[7] Chatterjee, M.; Hartung, A.; Holzgrabe, U.; Mueller, E.; Peinz, U.; Sotriffer, C.; Zilian, D. *Patent US9975853B2* **2018**.

[8] Lipinski, C. A.; Lombardo, F.; Dominy, B. W.; Feeney, P. J. *Adv. Drug Deliv. Rev.* **2001,** *46*, 3-26.

[9] Wasserscheid, P.; Keim, W. *Angew. Chem.* **2000,** *112*, 3926-3945.

[10] Cherukuvada, S.; Nangia, A. *Chem. Commun.* **2014,** *50*, 906-923.

[11] Dengale, S. J.; Grohganz, H.; Rades, T.; Lobmann, K. *Adv. Drug Deliv. Rev.* **2016,** *100*, 116-125.

[12] Abbott, A. P.; Capper, G.; Davies, D. L.; Rasheed, R. K.; Tambyrajah, V. *Chem. Commun.* **2003**, 70-71.

[13] Harris, R. C. *Ph.d. Thesis, University of Leicester* **2009**.

[14] Agharkar, S.; Lindenbaum, S.; Higuchi, T. *J. Pharm. Sci.* **1976,** *65*, 747-749.

[15] Booth, J. J.; Abbott, S.; Shimizu, S. *J. Phys. Chem. B* **2012,** *116*, 14915-14921.

[16] Claudio, A. F.; Neves, M. C.; Shimizu, K.; Canongia Lopes, J. N.; Freire, M. G.; Coutinho, J. A. *Green Chem.* **2015,** *17*, 3948-3963.

[17] Sheldrick, G. M. *Acta Cryst.* **2015,** *71*, 3-8.

[18] Sheldrick, G. M. *Acta Cryst.* **2008,** *64*, 112-122.

[19] Ali, A. M.; Ali, A. A.; Maghrabi, I. A. *Acta Pharm* **2015,** *65*, 133-146.

[20] Riedel, S. S.; Mottok, A.; Brede, C.; Bauerlein, C. A.; Jordan Garrote, A. L.; Ritz, M.; Mattenheimer, K.; Rosenwald, A.; Einsele, H.; Bogen, B.; Beilhack, A. *PLoS One* **2012,** *7*, e52398.

[21] Logue, S. E.; Elgendy, M.; Martin, S. J. *Nat. Protoc.* **2009,** *4*, 1383-1395.

[22] Steinbrunn, T.; Chatterjee, M.; Bargou, R. C.; Stuhmer, T. *PLoS One* **2014,** *9*, e97443.

[23] Pimentel, G. C.; Sederholm, C. H. *J. Chem. Phys.* **1956,** *24*, 639-641.

[24] LaPlante, S. R.; Carson, R.; Gillard, J.; Aubry, N.; Coulombe, R.; Bordeleau, S.; Bonneau, P.; Little, M.; O'Meara, J.; Beaulieu, P. L. *J. Med. Chem.* **2013,** *56*, 5142-5150.

[25] Wiest, J.; Saedtler, M.; Bottcher, B.; Grune, M.; Reggane, M.; Galli, B.; Holzgrabe, U.; Meinel, L. *Mol. Pharm.* **2018,** *15*, 4470-4480.

3.5 Determination of the Enantiospecific Activity of Isoquinolone-type HSP70 Inhibitors

1. Introduction

As already published for a number of HSP70 inhibitor derivatives and mentioned in chapter 3.4, the enantiospecific activity of these inhibitors against the human multiple myeloma (MM) cell line INA-6 could only be assigned to the (*R*,*R*)-enantiomer [1, 2]. Hence the enantiomers of **7** have to be separated by means of preparative HPLC, according to the literature [1]. The enantiospecific activity was then determined by bioactivity measurements.

2. Experimental Section

2.1 Materials

The isoquinolone-type HSP70 inhibitor **7** was synthesized as a racemate according to the reference [2]. All solvents, dimethyl sulfoxide (DMSO-d_6, 99.9% D), Roswell Park Memorial Institute-1640-medium (RPMI-1640 medium), penicillin, streptomycin, L-glutamine, and sodium pyruvate were purchased from Sigma-Aldrich (Schnelldorf, Germany). 20% Fetal bovine serum (FBS) was purchased from Gibco (Paisley, UK). Tween 80 was purchased from Caelo (Hilden, Germany). HPLC grade water was obtained by a Millipore system from Merck (Darmstadt, Germany). Standard 5 mm NMR tubes (400 MHz) and coaxial insert tubes were purchased from Norell (Landsville, PA, USA).

2.2 Methods

2.2.1 Preparative chiral liquid chromatography – enantiomeric separation

Preparative HPLC was performed using an Agilent 1100 modular chromatographic system equipped with a binary pump (PrepPump G1361 A), an autosampler (PrepALS G2260A), a multi-wavelength detector (MWD G1365B) and a fraction collector (PrepFC G1364B) (Agilent, Waldbronn, Germany). The system was operated, and the data are processed using the Agilent ChemStation® Rev. B.03.02. software.

A Lux Cellulose-1 chiral column (250 x 21.2 mm i.d., with a particle size of 5 µm) (Phenomenex, Aschaffenburg, Germany) was used as stationary phase to separate the enantiomers of compound **7** and the system worked at a flow rate of 20 mL/min and utilized an isocratic flow (H_2O:CH_3CN = 60:40). The total run time was 35 min and the injection volume was 900 µL (22 mM). The UV detection was performed at 254 nm and the runs were recorded at ambient temperature.

2.2.2 Electronic circular dichroism spectroscopy (ECD)

The ECD measurements of enantiomers **7** (2.2 mM in methanol) were performed under nitrogen using a Jasco J-715 spectrometer at room temperature, equipped with a standard cell (0.1 cm). The ECD data were processed using SpecDis.

2.2.3 Cell tests

The human MM cell line INA-6, a kind gift of Martin Gramatzki (University Medical Center Schleswig-Holstein, Kiel, Germany) and the murine MM cell line MOPC.315 BM luc^+ (MOPC) were used [3]. Cells were cultured at 37 °C in a humified incubator using RPMI-1640 medium enriched with 20% FBS, 100 U/mL Penicillin, 100 µg/mL Streptomycin, 2 mM L-Glutamine, and 1 mM Sodium-pyruvate. For INA-6 cells, medium was supplemented with additional 2 ng/mL IL-6 and for MOPC cells, with additional 25 µM β-mercaptoethanol. Cell cultures were freshly grown every 3 months.

2.2.4 Viability assessment

For viability assessment, 7,000 MOPC.315 BM luc^+ or 7,500 INA-6 cells were seeded per well of a 96 well plate and cells were treated with various concentrations of enantiomers **7** or the respective solvent control. After 3 days, cells were washed with PBS, pelleted and resuspended in 200 µL of cold annexin V binding buffer (10 mM HEPES/NaOH, 140 mM NaCl, 2.5 mM $CaCl_2$, pH 7.4) containing 1 µL of annexin V solution and 1 µg/mL propidium iodide. Thereby, annexin V was prepared as described in literature, and coupled to PromoFluor 647 or fluorescein isothiocyanate (FITC) (PromoCell, Heidelberg, Germany) [4, 5]. Cells were incubated for 15 min followed by

flow cytometry viability analysis. Flow cytometry was performed using a FACSCalibur (BD Biosciences, Heidelberg, Germany).

3. Results and Discussion

In order to analyze the enantiospecific activity, first a separation of the enantiomers of **7** (**Fig. 1**) was carried out by means of preparative HPLC using a chiral column.

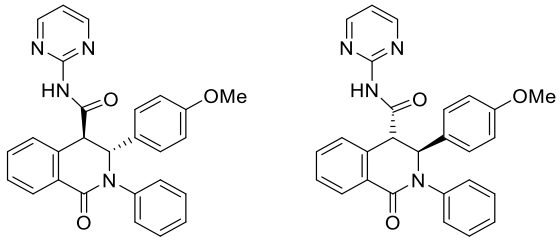

Figure 1: Enantiomers of compound 7 [2].

Since the enantiomers should be obtained in high purity, an isocratic flow (H_2O:CH_3CN = 60:40) was used, which led to a retention difference of enantiomer A and enantiomer B of 6 minutes (**Fig. 2**).

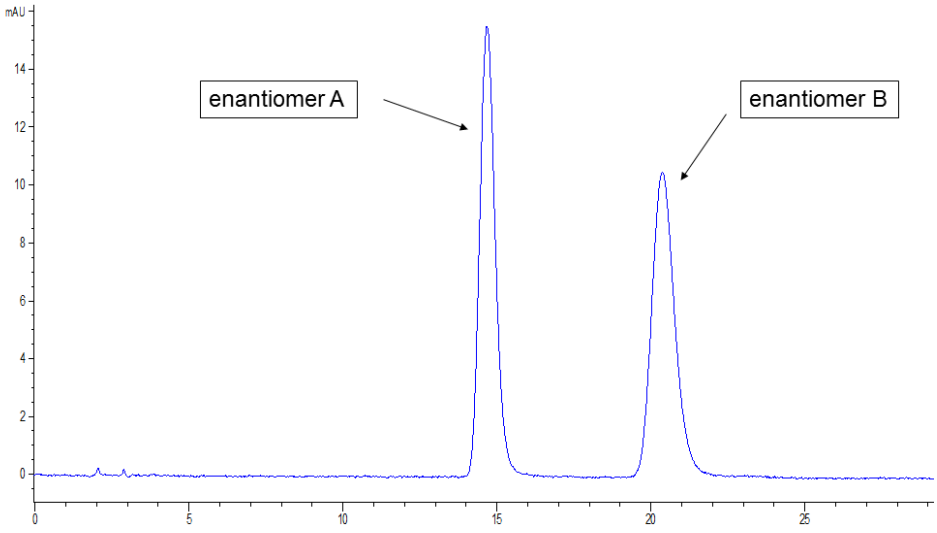

Figure 2: HPLC chromatogram of the separated racemate of compound 7.

The absolute configurations of the separated enantiomers ((*R*,*R*) and (*S*,*S*)) were then determined using ECD measurements and quantum chemical calculations. The difference between the absorption of left (A^l) and right (A^r) circularly polarized lights is defined as circular dichroism (CD) and is given as the ellipticity θ [6].

$$CD\ (\lambda) = A^l - A^r \qquad\qquad \theta\ (\lambda) = 3300 \cdot CD$$

While the absorption behavior for non-chiral compounds and racemates is not different and the ellipticity is zero in these cases, the difference in absorption for enantiomers is exactly the opposite of one another, so that the curves are mirror images of one another. ECD spectra were recorded and the configuration of the stereocenters was assigned by comparison with calculated quantum chemical spectra of the enantiomers (**Fig. 3**).

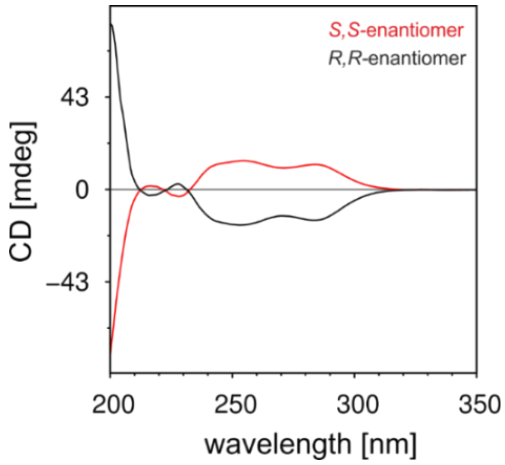

Figure 3: ECD spectrum of both enantiomers of compound 7.

The enantiomers showed enantioselective behavior in the viability. While the (*S*,*S*)-enantiomer (enantiomer B) has no activity against MM cells, an EC_{50} value of 0.70 µM was determined for the (*R*,*R*)-enantiomer (enantiomer A) (**Fig. 4**). These results are in accordance with previous findings [1, 2].

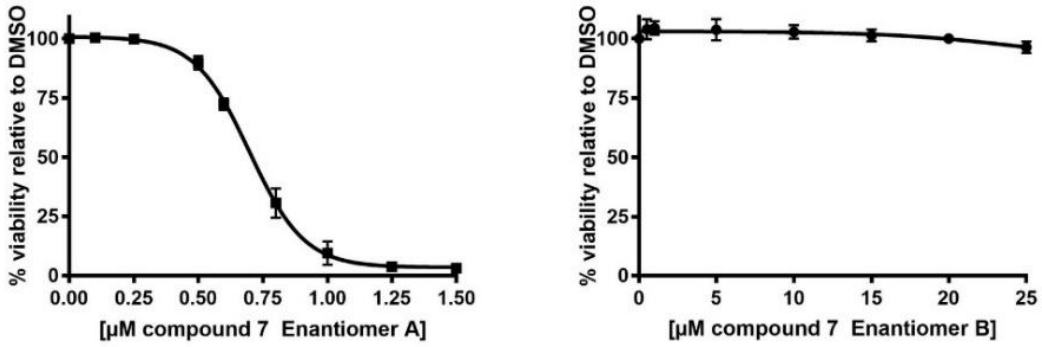

Figure 4: Activity study of both enantiomers of compound 7 on MM cells.

4. Conclusion

As determined in the present work as well as in previous studies, the activity of the recently developed HSP70 inhibitors can only be assigned to the (*R*,*R*)-enantiomer [1, 2]. Since these active agents are very promising in MM, further bioactivity studies of compound **7** are recently being carried out *in vitro* and *in vivo*.

Acknowledgment

Thanks to Prof. Dr. Dr. h. c. mult. Gerhard Bingmann and Dr. Shaimaa Seaf (Institute of Organic Chemistry, University of Würzburg, Germany) for the implementation of the ECD measurements and to Dr. Daniela Brünnert (Department of Internal Medicine II, Translational Oncology, University Hospital of Würzburg, Germany) for carrying out the activity studies.

References

[1] Hartung, A. *Ph.d. Thesis, University of Würzburg* **2013**.

[2] Chatterjee, M.; Hartung, A.; Holzgrabe, U.; Mueller, E.; Peinz, U.; Sotriffer, C.; Zilian, D. *Patent US9975853B2* **2018**.

[3] Riedel, S. S.; Mottok, A.; Brede, C.; Bauerlein, C. A.; Jordan Garrote, A. L.; Ritz, M.; Mattenheimer, K.; Rosenwald, A.; Einsele, H.; Bogen, B.; Beilhack, A. *PLoS One* **2012,** *7*, e52398.

[4] Logue, S. E.; Elgendy, M.; Martin, S. J. *Nat. Protoc.* **2009,** *4*, 1383-1395.

[5] Steinbrunn, T.; Chatterjee, M.; Bargou, R. C.; Stuhmer, T. *PLoS One* **2014,** *9*, e97443.

[6] Berova, N.; Di Bari, L.; Pescitelli, G. *Chem. Soc. Rev.* **2007,** *36*, 914-931.

4 Final discussion

The project of this thesis was aimed to assess the suitability of naturally occurring organic acids (OAs) as appropriate counterions for alkaloids and basic active pharmaceutical ingredients (APIs). The resulting protic ionic liquids (PILs) and oligomeric ionic liquids (OILs) might be of relevance in the development of novel drug formulations due to their improved physicochemical properties such as an increased dissolution rate and improved water solubility. Therefore, different salt screening programs of various OAs and several basic or cationic compounds were carried out and the obtained salts were first characterized in their solid state. Most of the used OAs were inexpensively available from commercial suppliers. However, meconic acid, a carboxy-γ-pyrone OA occurring in opium, the milky sap of *Papaver somniferum*, was only available for unreasonable prices. Hence, a novel synthetic approach towards meconic acid was envisioned firstly. The subsequent salt screenings of the basic and cationic compounds papaverine, morphine, berberine, and dextromethorphan and natural OAs with different characteristics revealed the formation of PILs for various combinations of a basic compound and OA.

In order to validate the potential of OAs in the solubility enhancement of potential drugs, the concept of solid dispersions (SDs) was applied to HSP70 inhibitors of the isoquinolone type. These compounds suffer from poor water solubility because of their constitution, which leads to hydrogen bonding and π-π interactions between compounds' molecules resulting in a highly ordered and strong crystal lattice within the crystals. Since *in vitro* activity studies of the HSP70 inhibitors were aimed, a deep eutectic solvent (DES) approach was used to improve the aqueous solubility of these compounds. Since the isoquinolones were synthesized as a racemate, it was aimed to determine the enantiospecific activity of the HSP70 inhibitors. Therefore, both enantiomers were separated by means of preparative HPLC and the enantiospecific activity of the enantiomers was assigned by ECD measurements and *in vitro* activity studies.

4.1 Synthesis of meconic acid

Since meconic acid was not affordable in the amounts needed, it should be obtained by synthesis. However, hydroxymethylation of readily available kojic acid followed by oxidation with palladium on carbon as described by Lovell et al. [1] failed and therefore a novel synthetic pathway was developed. Starting from kojic acid, a second primary alcohol was introduced followed by the protection of the enol group with benzyl bromide. Then, a very mild oxidation of both primary alcohol groups with TEMPO and BAIB according to Epp et al. and a subsequent deprotection of the enolic group with Me_3SiCl and sodium iodide gave meconic acid [2].

4.2 Salt screenings of basic compounds and several naturally occurring organic acids

In nature, plants use secondary metabolites (SMs) in a variety of ways, e.g. as defence against predators or for coloring to attract insects. Since many of these phytochemicals are also toxic to the plants themselves, nature has developed strategies to protect the plants. For this purpose, the SMs are stored in the central vacuoles of the cells and kept away from the cytoplasm in which metabolic processes take place. In their neutral form, the mostly basic SMs are very poorly water-soluble. To overcome this apparent insolubility, SMs are stored and kept in solution by salt formation with suitable counterions [3]. In general, two types of salts can be distinguished, firstly the inorganic salts with halides or sulphates as anions and secondly the organic salts with carboxylates, e.g. citrate or tartrate as anions.

In order to improve the aqueous solubility of poorly water-soluble APIs, the pharmaceutical industry also uses the principle of salt formation, mostly with halides. These crystalline salts have the advantage of high stability during storage and use but show poor dissolution behavior. To overcome this drawback, the formation of ionic liquids, defined as salts with reduced lattice energy and a melting point < 100 °C, seems to be a promising strategy due to their highly aqueous solubility and dissolution rate. A subunit of ILs are the protic ILs (PILs) which are generated by a simple neutralization reaction of Brønsted acids and Brønsted bases [4]. Based on nature's blueprint, bioinspired-PILs and protic oligomeric ILs (OILs) as well as OA salts were established by means of a salt screening program. This program included the alkaloids

papaverine, morphine, berberine, and dextromethorphan (DXM) and various natural OAs, namely citric acid, succinic acid, malic acid, tartaric acid, lactic acid, fumaric acid, vanillic acid, caffeic acid, phthalic acid, *p*-coumaric acid, and meconic acid.

The obtained salts were first physically characterized. For this purpose, melting points, morphology, and dissolution rates were determined. The supramolecular behavior of the identified PILs in aqueous solution was then examined using potentiometric and photometrical solubility, NMR aggregation assay, dynamic light scattering, zeta potential, and viscosity measurements. For papaverine, the α-hydroxycarboxylic acids (AHAs) citric acid, malic acid, and tartaric acid were identified as suitable counterions for the formation of amorphous PILs. These PILs showed improved dissolution rates and aqueous solubilities compared to the crystalline salts derived from papaverine and succinic acid or meconic acid, respectively. For DXM, on the other hand, aliphatic dicarboxylic acids (succinic acid, malic acid, and tartaric acid) were suitable counterions for PILs. Due to their flexibility and the few possibilities for interaction with DXM, they presumably prevent a long-range order and thus a crystal lattice within the solid. Although morphine and DXM have similar constitutions, no PILs could be identified in the case of morphine. A possible explanation for this can be the additional hydroxyl group in morphine, which enables more interactions between cation and anion. These interactions, in turn limits the flexibility of the anions and thus lead to the formation of a long-range order in the solid. The isoquinoline berberine does not allow the formation of PILs neither, since π-π interactions between the cations and the rigid nature of berberine indicate that the formation of a crystal lattice cannot be disturbed by the anions.

4.3 Papaverine salt screening

The improved dissolution rate of the papaverine PILs can be explained by reduced lattice forces and the lack of long-range order within the amorphous solids while the enhanced apparent solubility of papaverine is enabled by the carboxylates. These act as peptizers and stabilize the occurring papaverine aggregates. The effect of the low molecular weight peptizers is mainly based on their ability to adsorb on the particle's surface. This leads to a change of the positive surface charge, and the non-adsorbed negatively charged carboxylates in solution. An increased ionic strength results in a decreased Debye length between negatively charged papaverine aggregates and

“free” carboxylates and consequently in increased repulsive double-layer forces. These repulsive forces counteract the attractive van der Waals forces, resulting in an electrostatically stabilized colloidal dispersion, which can be explained by the DLVO theory. Furthermore, the sterically demanding carboxylates adsorbed on particle’s surface create a steric barrier inhibiting the complete mutual approach of the individual particles, resulting in an increased viscosity of the colloidal dispersion.

Crystals are characterized by positional order of molecules and a long-range orientation within the solid. The amorphous solids, however, have no long-range order and therefore different but beneficial physicochemical properties, including improved dissolution rate and solubility, compared to their respective crystalline forms. Despite these advantages for the formulation of poorly water-soluble drugs, the amorphous form of an individual drug, consisting of homodimers, suffers from thermodynamic instability. This instability leads to recrystallization during preparation, storage, and administration and consequently lower bioavailability. The formation of amorphous PILs, consisting of drug and α-hydroxycarboxylic acids (AHAs), can overcome these drawbacks, because of the formation of heterodimers. Intramolecular hydrogen bonding between the AHAs diminishes intermolecular interactions between the heterodimers and thus prevents a long-range order as well as precipitation, stabilizing amorphous forms in solid state. Furthermore, AHAs can act as peptizers and stabilize the dispersion of drug molecules during administration in line with the DLVO theory. The presented bioinspired PILs may be regarded as a starting point for further pharmaceutical and clinical research, because of their stability during preparation, storage and administration, and their beneficial characteristics, including the low acquisition costs and the safety of most naturally occurring OAs.

4.4 Single crystals of isoquinolone-type HSP70 inhibitors and DES approach to improve the water solubility

Isoquinolone-type HSP70 inhibitors used in the treatment of multiple myeloma (MM) suffer from poor water solubility and show melting points of higher than 220 °C [5]. Especially the low water solubility severely hampers the use of these compounds in further *in vitro* and *in vivo* studies and hence it was assessed whether the developed strategy of solid dispersions might improve their performance and enable easier

formulation. Firstly, single crystals of the inhibitors were formed, and the crystal structure was analyzed by means of single crystal X-ray analysis. The intermolecular interactions within the crystals of these active agents were determined by means of XRPD, IR, and NMR measurements. The obtained X-ray spectra show highly ordered crystals with hydrogen bonding and π-π stacking within the compound molecules. This observation explains the high melting points and the very poor water solubility of these isoquinolones.

In order to improve the water solubility of the lead compound, an approach for a deep eutectic solvent (DES) was chosen. Naturally occurring compounds were used as auxiliary substances and can improve the apparent water solubility of the inhibitor by interrupting the molecular interactions and consequentially by disrupting the crystal lattice [6, 7]. The initial 4500-fold increase in water solubility of the DES compared to the pure compound, can be explained by hydrotropic solubilization and stabilization of the isoquinolone by the excipients, decelerating recrystallization of the compound. Since DES can be “tailored” to different APIs by varying the auxiliary substances, they can be seen as an alternative to the universal but toxic organic cosolvent DMSO and are therefore a promising strategy for *in vitro* cell studies. These results showcase the potential of the developed strategy for solubility enhancement rendering formation of DES a highly interesting approach in drug formulation.

4.5 Enantiospecific activity of isoquinolone-type HSP70 inhibitors

Since the isoquinolone-type HSP70 inhibitors are synthesized as racemates, the enantiomers must be separated first by means of preparative HPLC using a chiral column. The determination of the enantiospecific activity was carried out by EDC measurements as well as bioactivity studies.

As already described in the literature [5, 8], the enantiospecific activity of this type of inhibitors against the human MM cell line INA-6 could only be assigned to the (*R*,*R)*-enantiomer.

4.6 Conclusion

Taken together, naturally occurring organic acids (OAs) are suitable counterions for Brønsted bases, which lead to the formation of PILs and protic OILs with properties beneficial for the use in *in vitro* studies and development of pharmaceutical formulation. These properties include increased water solubility as well as enhanced dissolution rate [9, 10]. Since most natural carboxylic acids are well characterized, inexpensive and show harmless toxicity behavior, their use as counterions for poorly water-soluble APIs seems to be a promising strategy to optimate or manipulate the drug's properties, such as its absorption, pharmacodynamics or pharmacokinetics [11].

The large amount of naturally occurring OAs with different properties, including mono-, di- and tricarboxylic acids, AHAs, BHAs, benzoic acid derivatives, and hydroxycinnamic acid derivatives, as well as the specific API constitution enable "tailor-made" formation of PILs and OILs. Simple variation of the respective anions and cations generates formulations of different physical and chemical properties. In addition, the concentration of counterion is important for the stability of a colloidal dispersion and consequently for the solubility of the drug. The simple manufacturing processes of PILs through a simple neutralization reaction as well as the low acquisition costs of most natural acids are very promising for the pharmaceutical research and industry.

The isoquinolone-type HSP70 inhibitors suffer from poor water solubility and high melting points, which diminishes their use in further *in vitro* and *in vivo* studies and consequently their potential use in treatment of MM [5]. Single crystal X-ray analysis of various HSP70 inhibitors revealed highly ordered crystal lattices and intermolecular interactions, such as hydrogen bonding and π-π stacking within the crystals.

In order to prevent such intermolecular interactions, a DES approach was used, which was based on naturally occurring excipients and led to improved water solubility and a delayed recrystallization process of the inhibitors. Since DES offer easy-to-use manufacturing processes, such as simple melting and evaporating processes, as well as low acquisition costs of the components, this strategy seems to be very promising for the use in *in vitro* cell studies.

FINAL DISCUSSION

In conclusion, formation of PILs and DES can be considered as powerful tools in pharmaceutical drug formulation due to their generally broad application as well as harmless toxicity profiles.

References

[1] Lovell, S.; Subramony, P.; Kahr, B. *J. Am. Chem. Soc.* **1999,** *121*, 7020-7025.

[2] Epp, J. B.; Widlanski, T. S. *J. Org. Chem.* **1999,** *64*, 293-295.

[3] Choi, Y. H.; van Spronsen, J.; Dai, Y.; Verberne, M.; Hollmann, F.; Arends, I. W.; Witkamp, G. J.; Verpoorte, R. *Plant Physiol.* **2011,** *156*, 1701-1705.

[4] Greaves, T. L.; Drummond, C. J. *Chem. Rev.* **2015,** *115*, 11379-448.

[5] Chatterjee, M.; Hartung, A.; Holzgrabe, U.; Mueller, E.; Peinz, U.; Sotriffer, C.; Zilian, D. *Patent US9975853B2* **2018**.

[6] Faggian, M.; Sut, S.; Perissutti, B.; Baldan, V.; Grabnar, I.; Dall'Acqua, S. *Molecules* **2016,** *21*.

[7] Dengale, S. J.; Grohganz, H.; Rades, T.; Lobmann, K. *Adv. Drug Deliv. Rev.* **2016,** *100*, 116-125.

[8] Hartung, A. *Ph.d. Thesis, University of Würzburg* **2013**.

[9] Marrucho, I. M.; Branco, L. C.; Rebelo, L. P. *Annu. Rev. Chem. Biomol. Eng.* **2014,** *5*, 527-546.

[10] Johansson, K. M.; Izorodina, E. I.; Forsyth, M.; MacFarlane, D. R.; Seddon, K. R. *Phys. Chem. Chem. Phys.* **2008,** *10*, 2972-2978.

[11] Stoimenovski, J.; Dean, P. M.; Izgorodina, E. I.; MacFarlane, D. R. *Faraday Discuss.* **2012,** *154*, 335-352; discussion 439-464, 465-471.

5 Summary

Formation of protic ionic liquids (PILs) derived from a given drug and a low molecular weight organic acid (OA) opens a novel gateway in improving solubility and dissolution kinetics for drug formulation. Especially the wide range of potential OAs with different physicochemical properties enables “tailor-made” formulations precisely chosen for the respective drug. Since OAs are more demanding counterions than halides, they might prevent strong lattice forces within the crystals resulting in low melting temperature salts, e.g. ionic liquids (ILs). Furthermore, OAs with low molecular weight may act as dispersants and can charge the surface of the powder particles, thereby increasing the repulsive double-layer forces and consequently the suspensions stability. The easy-to-handle manufacturing processes of the salts (simple neutralization reaction between a Brønsted acid and a Brønsted base), the low acquisition costs and the low toxicity of most naturally occurring OAs render them attractive counterions for basic APIs.

The deep eutectic solvent (DES) strategy has been successfully applied to synthetic poorly water-soluble HSP70 inhibitors. It was shown that the water solubility of the isoquinolone compounds can be increased by formation of DES utilizing naturally occurring excipients. Since the excipients prevent the intermolecular interactions within the inhibitor molecules and consequently the formation of a highly ordered crystal lattice within the solids, the water solubility of the compound increased by three orders of magnitude. Because DES are obtained through simple melting or evaporating processes and can replace organic cosolvents, e.g. DMSO, they appear to be a promising alternative for improving the physicochemical properties of drugs.

6 Zusammenfassung

Die Bildung von protischen Ionic Liquids (PILs) ausgehend von einem Arzneistoff und einer niedermolekularen organischen Säure (OA) eröffnet einen neuen Ansatz zur Verbesserung der Wasserlöslichkeit und Lösungskinetik für die Arzneimittelformulierung. Insbesondere die Fülle an OAs mit ihren unterschiedlichen physikochemischen Eigenschaften ermöglicht Formulierungen, die auf eine bestimmte Verbindung zugeschnitten sind. Im Gegensatz zu Halogeniden sind Carboxylate voluminöse Gegenionen, weshalb sie die Ausbildung eines starken Kristallgitters unterbinden können, was zur Bildung von niedertemperatur-schmelzenden Salzen, wie z. B. Ionischen Flüssigkeiten, führt. Des Weiteren können organische Säuren mit geringem Molekulargewicht als Dispergatoren wirken, welche durch Adsorption an die Partikeloberfläche eine Ladung induzieren, was die abstoßenden Doppelschichtkräfte erhöht und somit die Suspension stabilisiert. Die einfachen Herstellungsprozesse der Salze durch eine Neutralisationsreaktion zwischen einer Brønsted-Säure und Brønsted-Base sowie die geringen Anschaffungskosten und die geringe Toxizität der meisten natürlich vorkommenden organischen Säuren machen diese zu attraktiven Gegenionen für basische Wirkstoffe um deren Löslichkeitsprofil zu verbessern.

Ein Deep Eutectic Solvent (DES) Ansatz wurde anschließend erfolgreich auf synthetische wenig lösliche HSP70-Inhibitoren angewandt. Es wurde gezeigt, dass die Wasserlöslichkeit dieser Isochinolone durch die Bildung von DES (basierend auf natürlich-vorkommenden Hilfsstoffen) verbessert werden kann. Da die Hilfsstoffe die intermolekularen Wechselwirkungen zwischen den Inhibitor-Molekülen verhindern und somit die Ausbildung eines Kristallgitters unterbinden, wurde die Wasserlöslichkeit des Inhibitors um das 4500-fache erhöht. Da DES durch einfache Schmelz- oder Verdampfungsprozesse erhalten werden, sind sie als kostengünstige Alternative zu organischen Lösemitteln, z. B. DMSO, zu betrachten, um die physikochemischen Eigenschaften von Arzneimitteln zu verbessern.

7 Appendix

7.1 List of Publications

Research papers

- Güntzel, P.; Schilling, K.; Hanio, S.; Schlauersbach, J.; Schollmayer, C.; Meinel, L.; Holzgrabe, U. *Bioinspired Ion Pairs Transforming Papaverine into a Protic Ionic Liquid and Salts*, ACS Omega **2020,** *5*, 19202-19209.
- Güntzel, P.; Forster, L.; Schollmayer, C.; Holzgrabe, U. *A Convenient Preparation of Carboxy-γ-pyrone Derivatives: Meconic Acid and Comenic Acid*, Org. Prep. Proced. Int. **2019,** *50*, (5), 512-516.
- Güntzel, P.; Nagel, C.; Weigelt, J.; Betts, J. W.; Pattrick, C. A.; Southam, H. M.; La Ragione, R. M.; Poole, R. K.; Schatzschneider, U. *Biological activity of manganese(I) tricarbonyl complexes on multidrug-resistant Gram-negative bacteria: From functional studies to in vivo activity in Galleria mellonella*, Metallomics **2019**, *11*, 2033-2042.
- Berninger, M.; Erk, C.; Fuß, A.; Skaf, J.; Al-Momani, E.; Israel, I.; Raschig, M.; Güntzel, P.; Samnick, S.; Holzgrabe, U. *Fluorine Walk: The Impact of Fluorine in Quinolone Amides on their Activity Against African Sleeping Sickness*, Eur. J. Med. Chem. **2018**, *152*, 377-391.
- Güntzel, P.; Block, M.; Schilling, K.; Hartung, A.; Stoy, A.; Brünnert, D.; Chatterjee, M.; Radacki, K.; Braunschweig, H.; Meinel, L.; Holzgrabe, U. *Single Crystals of Active Agents in Multiple Myeloma and Water Solubility Improvement by Use of Deep Eutectic Solvents [to be submitted after patent filing]*

7.2 Documentation of authorship

This section contains a list of the individual contribution for each author to the publications reprinted in this thesis. Unpublished manuscripts are handled accordingly.

P1	**Güntzel, P.; Forster, L.; Schollmayer, C.; Holzgrabe, U.** A Convenient Preparation of Carboxy-γ-pyrone Derivatives: Meconic Acid and Comenic Acid, Org. Prep. Proced. Int. 2019, 50 (5), 512-516.				
Author		**1**	**2**	**3**	**4**
Study design		X			X
Experimental work: Synthesis		X	X		
Experimental work: NMR analysis		X		X	
Manuscript planning		X			X
Manuscript writing		X			
Correction of manuscript		X			X
Supervision of Paul Güntzel					X

P2	**Güntzel, P.; Schilling, K.; Hanio, S.; Schlauersbach, J.; Schollmayer, C.; Meinel, L.; Holzgrabe, U.** Bioinspired Ion Pairs Transforming Papaverine into a Protic Ionic Liquid and Salts, ACS Omega. 2020, 5, 19202-19209.							
Author		**1**	**2**	**3**	**4**	**5**	**6**	**7**
Study design		X					X	X
Experimental work: Salt formation		X						
Experimental work: XRPD analysis		X						
Experimental work: DSC analysis		X						
Experimental work: determination of dissolution rate		X						
Experimental work: determination of solubility		X						
Experimental work: Zeta potential analysis		X						
Experimental work: HPLC analysis		X	X					
Experimental work: viscosity measurements				X				
Experimental work: DLS analysis		X			X			
Experimental work: NMR analysis		X				X		
Manuscript planning		X					X	X
Manuscript writing		X						
Correction of manuscript		X					X	X
Supervision of Paul Güntzel							X	X

P3	**Güntzel, P.; Block, M.; Schilling, K.; Hartung, A.; Stoy, A.; Brünnert, D.; Chatterjee, M.; Radacki, K.; Braunschweig, H.; Meinel, L.; Holzgrabe, U.** Single Crystals of Active Agents in Multiple Myeloma and Water Solubility Improvement by Use of Deep Eutectic Solvents, **to be submitted after patent filling**.

Author	**1**	**2**	**3**	**4**	**5**	**6**	**7**	**8**	**9**	**10**	**11**
Study design	X			X							X
Experimental work: Single crystal formation	X	X									
Experimental work: XRPD analysis	X										
Experimental work: IR analysis	X										
Experimental work: Single crystal X-ray analysis					X			X	X		
Experimental work: NMR analysis	X										
Experimental work: HPLC analysis	X		X								
Experimental work: DES preparation	X										
Experimental work: cell studies						X	X				
Manuscript planning	X										X
Manuscript writing	X										
Correction of manuscript	X									X	X
Supervision of Paul Güntzel										X	X